Forest Cover, Stand Volume and Biomass Assessment in Dudwa National Park using Satellite Remote Sensing Data (Optical and EnviSat ASAR)

Thesis submitted to the Andhra University, Visakhapatnam

in partial fulfillment of the requirements for the award of
Master of Technology in Remote Sensing & Geographic Information System

Submitted by

Ningthoujam Ramesh Kumar

Supervised by

Dr. P.K. Joshi
Forestry and Ecology Division, IIRS, Dehradun

iirs

Indian Institute of Remote Sensing
(National Remote Sensing Agency)
Dept. of Space, Govt. of India
Dehradun-248 001 INDIA

March, 2007

भारतीय सुदूर सम्वेदन संस्थान
Indian Institute of Remote Sensing
(नेशनल रिमोट सेन्सिंग एजेन्सी)
(NATIONAL REMOTE SENSING AGENCY)
(अन्तरिक्ष विभाग, भारत सरकार)
(DEPT. OF SPACE, GOVT. OF INDIA)
4, कालीदास मार्ग, पोस्ट बाक्स नं॰ 135, देहरादून–248001 (भारत)
4, KALIDAS ROAD, P.B. No. 135, DEHRA DUN–248001 (INDIA)

दूरभाष / Telephone : (0135)
तार / Grams : (0135) रिमोटिपी
REMOTIP!
फैक्स / Fax : 0135-2741987
0135-2748041

CERTIFICATE

This is to certify that the Thesis entitled "***Forest Cover, Stand Volume and Biomass Assessment in Dudwa National Park using Satellite Remote Sensing Data (Optical and EnviSat ASAR)***"is the original contribution of **Mr. Ningthoujam Ramesh Kumar** towards partial fulfillment of the requirements for the award of *Master of Technology in Remote Sensing & Geographic Information System* degree on **Application of Remote Sensing and Geographic Information Systems for Mapping and Monitoring of Natural Resources**. This is a bonafide work carried out by him at Forestry and Ecology Division, Indian Institute of Remote Sensing (National Remote Sensing Agency), Dept. of Space, Govt. of India, Dehradun-248001, under the supervision and guidance of **Dr. P.K. Joshi**, (currently as Associate Professor, TERI University, New Delhi).

(Dr. P.K. Joshi)
(Supervisor)
Forestry and Ecology Division

(Dr. V.K. Dadhwal)
(Dean, IIRS)

ABSTRACT

The Dudwa Tiger Reserve stands out as the primary Protected Area Complex of the terai with one of its components having the status of a National Park. The Dudwa Tiger Reserve comprises of the Dudwa National Park and the Kishanpur Wild life Sanctuary. The terai with its characteristics complex of sal forests, tall grasslands and swamps maintained by periodic flooding, is one among the threatened ecosystems in India. The vegetation is primarily North Indian Moist Deciduous type contributing to the biomass and volume stock of the National Park. Biomass is a key variable in short and long- term changes in the terrestrial pools and fluxes. This study makes an attempt to estimate and compare the forest stand volume and biomass assessment using Landsat ETM and EnviSat Advanced Synthetic Aperture Radar (ASAR) data in the terai forest of Dudwa National Park.

The remotely sensed data, with its high correlations between spectral bands and vegetative parameters, make it the primary source for large area aboveground growing stock volume and biomass estimation, especially in areas of different access.

This study demonstrates the ability to differentiate different forest type/ density classification with an overall accuracy: 91.62 percent and Khat coefficient: 0.90 using optical data whereas, overall accuracy: 73.54 percent and Khat coefficient: 0.71 using ASAR data.

The correlation between radar backscattering coefficient (σ^{o}_{HH}, σ^{o}_{HV}) of different polarizations and timber volume and woody biomass was found to be insignificant. Though, cross polarization backscattering coefficient was better correlated with both these two bio-physical parameters than the like polarizations as relationship is concerned. The result demonstrates the poor relationship between backscattering coefficient, forest volume and biomass. Microwave data with high incidence angle and longer wavelength could have given better results.

Acknowledgements

This report is the outcome of the blessings from my guardians, academic mentors, seniors and colleagues during my work at Indian Institute of Remote Sensing, Dehradun.

I take this opportunity to sincerely thank Dr. V.K. Dadhwal, Dean, IIRS, for providing the necessary support facilities at IIRS during the course work.

I am also thankful to Dr. S.P.S. Kushwaha, Head, Forestry and Ecology Division, IIRS, for moral support, encouragement, timely suggestions and guidance during the research work.

Words are inadequate to convey my gratitude to my Supervisor, Dr. P.K. Joshi, Scientist, Forestry and Ecology Division, IIRS, (currently as Associate Professor, TERI University, New Delhi) for his timely comments, guidance, invaluable suggestions, moral support, fruitful discussions and encouragement throughout the research work.

I am highly indebted to all the Faculty of FED viz., Dr. Sarnam Singh, Dr. M.C. Porwal, Dr. I. J. Singh, Dr. D. N. Pant and Shri. K.K. Das for help provided to me.

I am extremely grateful to Dr. A.K. Mishra, Course Coordinator and Faculty, Marine Science Division, IIRS for motivation, support and guidance throughout this period.

My sincere thanks are due to my M. Tech. colleagues at IIRS, Mr. Rahul of Marine Science Division, Mr. Shekher of Geoscience Division and Ms. Roy of HUSAD who supported me by sparing their valuable time for me. Similarly, I thank FED Researchers; Mr. Mohit Kalra, Dr. Ranjeet Kumar, Mr. Arun Kumar, Mr. Subrata Nandy, Mr. Subrato Paul, Mr. Gaurav Srivastav, Mr. Nikhil Lele, Mr. Himanshu Ranade, Ms. Suchi Mukhopadhayay, Mrs. Pushpa Das and Ms. Sushma Gairola for support during the research period.

I am also grateful to Mr. Bhaskar Bahuguna and Mr. Avdhesh Deoni of Computer Maintenance Cell for the help provided by them.

I sincerely thank all the Bharat Soka Gakai- Dehradun Members for their support and guidance. I am also thankful to my landlord Mr. and Mrs. Kripal Singh Verma and their children, Ms. Anushka, Master Surya and Ms. Sunita for their help, constant support, encouragement and pleasant stay at Dehradun during my course period.

Last but not the least, I am highly indebted to my parents, especially my grandmother and sister for taking care, constant encouragement and support without which I could not have completed the course. I would also like to express my gratitude to my beloved late brother, Mr. Roni Kumar Ningthoujam for his guidance and moral support.

30th March, 2007 Ningthoujam Ramesh Kumar

Dehradun

Dedicated To My Beloved Grand Ma

Naorem Tampak Leima Devi

TABLE OF CONTENTS

LIST OF FIGURES

LIST OF TABLES

CHAPTER-1

INTRODUCTION

1. General

Forests are one of the most important components of the terrestrial ecosystems. They are the storehouse of biological diversity. The human interventions in the natural forest reduce the number of trees per unit area and canopy closure. It affects regeneration, leads to uneven age- class distribution and invasion of alien weeds. The production capacity of the forests could not keep pace with the exponential growth rate of human and livestock populations. In 1995, there were 3454 M ha of forest (including natural forests and forest plantations) worldwide (FAO, 1999). Between 1990 and 1995, the total area of forests decreased by 56.3 M ha, the result of a loss of 65.1 M ha in developing countries and an increase of 8.8 M ha in developed countries (FAO, 1999). The density stratification in such kinds of forests leads to a most challenging task. India's total geographical area about 328 M ha. According to one estimate, India has lost 3.4 M ha of forest lands to dams, new croplands, roads and industries between 1951 and 1972. This means annual rate of deforestation is about 0.15 M ha.

According to the Forest Resources Assessment 2000, world forest covers 3.9 billion ha and spreads on about 30 percent of the land. The net change in forest area was 9.4 M ha per year (rate of deforestation is 14.6 M ha and expansion 5.2 M ha). On global basis, 52 percent of the total forest of the total forests (2800 M ha) are tropical but in India tropical forests account for 86 percent (64.4 M ha) of the total. Out of 64.4 M ha tropical forest in India, dry deciduous forests and moist deciduous forest account for a total of 65 percent (Champion and Seth, 1968). Presently, the recorded forest area in India is 76.54 M ha (FSI, 2001).

1.1 Forest Cover

Within biomes, a forest type is a group of forest ecosystems of generally similar composition that can be readily differentiated from other such groups by their tree and

under canopy species composition, productivity and/or crown closure (FAO definition). Whereas, Forest cover consists of a plant community made up of trees and other woody vegetation, growing more or less closely together. Forest density expressing the growing stock situation constitutes the major stand physiognomic parameter of Indian forest. In India, reliable database on the forest cover, its structure and function are discrete. Forest stock maps are the basic data used by the forest divisions in preparation of forest management plans on 1: 15,000. Forest types with stock density, the site quality and age group of the crop are the main feature shown in the management plan. The conventional method of making stock maps on the basis of ground survey is time consuming. It is therefore, difficult to complete the revision in time. As a result most of the stock maps do not reflect current status of growing stock in the forests.

The canopy closure, number of trees per unit area and basal area are often taken as parameters to measure density. The percent crown closure is a measure of area occupation rather than stand density. However, it is an important structural parameter used to stratify forest. The ecological conditions like, light penetration through the canopy, surface albedo, and rainfall interception are dependent on crown density.

1.2 Stand Volume

Tree volume is defined as amount of wood in a tree (may be gross or net) and stand volume as the amount of wood in a particular forest type. The spectral response of vegetation is reported to provide information on the structure and composition of forest stands. Stand volume estimates were converted to aboveground tree biomass using biomass expansion factors (Lehtonen *et al.*, 2004). The correlation between C- band signal and bole volume are negligible due to the saturation at small bole volumes as a result of the backscatter energy originated from the upper crown layer (Israelson *et al*., 1994). There exists a relationship between radar backscatter and growing stock volume (m^3/ ha) (Le Toan *et al*., 1992, Dobson *et al*., 1992, Rauste *et al*., 1994). Unfortunately, saturation of the backsctter signal occurs at growing stock volume levels of 64 and 143 m^2/ha for C- and L- band respectively (Fransson and Israelsson, 1999).

1.3 Woody Biomass

The forest biomass product has a strong research component and should be viewed as evolutionary. Biomass is defined as total amount of organic matters existing in a unit area at one instance, and described by a weight of organic matters in dry condition. Biomass is the dry weight or total quantity of living organisms of one plant species (species biomass) or of all the species in the community (community biomass). The unit of biomass is, therefore, g/ m^2, kg/ m^2 or ton/ ha. Vegetation biomass includes leaf, stem, root, fruit and flower. Biomass is one of the most important biophysical parameters which define the carbon budget in a terrestrial ecosystem. Basically, biomass is a parameter defined at the ground level, and is measured only at the ground by cutting trees or grasses and by measuring their dry weight. Biomass, in general, includes the aboveground and belowground living mass, such as trees, shrubs, vines, roots, and the dead mass of fine and coarse litter associated with the soil. Traditional techniques based on field measurement are the most accurate ways for collecting biomass data.

According to the Intergovernmental Panel on Climate Change Good Practice Guidance (IPCC, 2003), remote sensing methods are especially suitable for independent verifying the national Land Use. Land-Use Change and Forestry (LULUCF), carbon pool estimates, especially the aboveground biomass. Different approaches for aboveground biomass estimation are adopted, based on (1) field measurement, traditional techniques are the most accurate ways for a collecting biomass data but, they cannot provide the spatial distribution of biomass in large areas (Brown *et al.*, 1989; Brown and Iverson 1992; Honza´k *et al.*, 1996; Schroeder *et al.*, 1997; Houghton *et al.*, 2001; Brown, 2002), (2) remote sensing data with its high correlations between spectral bands and vegetation parameters, make it the primary source for large area aboveground biomass estimation, especially in difficult areas, which has increasingly attracted scientific interest (Tiwari, 1994; Roy and Ravan, 1996; Nelson *et al.*, 2000a;b; Tomppo *et al.*, 2002; Foody *et al.*, 2003; Santos *et al.*, 2003; Zheng *et al.*, 2004; Lu, 2005), and (3) GIS based methods using ancillary data (slope, elevation, soil, precipitation) etc. having indirect relationships are not recommended for aboveground biomass estimation (Brown and Gaston 1995).

1.4 Remote Sensing

For the collection of information related to forestry bio- physical parameters, a combination of forest resources inventory with remote sensing techniques are two approaches for estimation of large forest areas (Krankina *et al.*, 2004). Remotely sensed data have become the primary source for biomass estimation. Either optical sensor data or radar data are more suitable for forest sites with relatively simple forest stand structure than the sites with complex biophysical environments. Remote Sensing systems with its systematic, synoptic and repetitive coverage make potentially outstanding tools to support tropical forest management (Lillesand and Keifer, 1999). Remote sensing techniques have revolutionized the process of data gathering and map making offering the possibilities of conducting resources surveys over large areas rapidly, cost effectively and accurately. Such surveys can provide various levels of information to suit the desired intensity and quality of management planning requirement (Lillesand and Keifer, 1999).

Use of aerial photographs in working plans for stock mapping in India was started during seventies (Maslekar, 1974; Tomar, 1976; Tiwari, 1978). However, aerial photographs could not become popular due to difficulty in their procurement. Satellite remote sensing has played an important role in generating information about forest cover, vegetation type and the landuse changes (Houghton and Woodwell, 1981; Botkin *et al.*, 1984; Malingreau, 1991; Roy, 1993). Standardization of ground sampling methods, understanding of spectral and temporal responses of vegetation, coupled with the recent advancements in the digital image processing techniques have brought about a profound acceptance of the application of satellite remote sensing data in forest inventory and mapping. The National Forest Cover Mapping programme undertaken by Forest Survey of India is primarily based on visual interpretation wherein forests are classified into three major density classes viz., dense forest (> 40%), open forest (40–10%) and scrub forest (< 10%) on 1:250,000 scale. The methodology is subjective and varies with the aptitude of the interpreter. Recent attempts to classify forests using satellite based digital data have resulted in classification based on phenology or leaf duration (evergreen, semi evergreen, moist deciduous, dry deciduous and mangroves), gregariousness of species

(like *Tectona grandis*, *Shorea robusta*, *Dipterocarpus* sp., *Pinus* sp. etc.) or dominance of forests by large canopies (Roy *et al.*, 1985; Roy and Ravan, 1994). Forest structural classification based on broad canopy density classes has been reported using Indian Remote Sensing Satellite Data IRA-1A LISS II (Roy *et al.*, 1990). NDVI provides good information on canopy closure in evergreen/coniferous areas. It has been reported to vary with foliage activity in dry/moist deciduous forest areas (Roy and Ravan, 1994). Consequently results may vary according to differing phenological situations in dry and moist deciduous forest areas.

In recent years remote sensing techniques have become prevalent in estimating aboveground biomass (Nelson *et al.*, 1988; Franklin and Hiernaux, 1991; Leblon *et al.*, 1993; Nelson *et al.*, 2000a; Steininger, 2000; Zheng *et al.*, 2004; Lu, 2005). Most previous research on aboveground biomass estimation is for coniferous forests (Ardo, 1992; Wu and Strahler, 1994; Trotter *et al.*, 1997; Zheng *et al.*, 2004) because of its relatively simple forest stand structure and tree species composition. In moist tropical forests, the study of aboveground biomass estimation becomes problematic because of its complex stand structure and abundant variety in species composition (Lucas *et al.*, 1998; Nelson *et al.*, 2000a; Steininger, 2000; Foody *et al.*, 2001; 2003; Lu *et al.*, 2005). The complexity of vegetation structures results in highly variable standing stocks of aboveground biomass and an even more variable rate of aboveground biomass accumulation following a deforestation event. Therefore, remote sensing-based aboveground biomass estimation has increasingly attracted scientific interest (Nelson *et al.*, 1988; Sader *et al.*, 1989; Franklin and Hiernaux, 1991; Steininger, 2000; Foody *et al.*, 2003; Santos *et al.*, 2003; Zheng *et al.*, 2004; Lu, 2005).

Remote sensing techniques have many advantages in aboveground biomass estimation over traditional field measurement methods and provide the potential to estimate aboveground biomass at different scales. The user's need, the characteristics of remotely sensed data, the scale of the study area, and the availability of economic support have important influences on the design of an aboveground biomass estimation procedure.

1.4.1 Optical Remote Sensing

Landsat data have been used to report in estimation of biomass accumulation rates among secondary growths (Alves and Skole, 1996). In low biomass forests, the NDVI has been used to derive LAI and biomass value and can be used as a reliable predictor of landscape level patterns of productivity in woody species, especially if appropriate scales for temporal and spatial integration are employed, Kuplich *et al.*, 2005. In brief, optical remote sensing are not capable of measuring forest biomass accurately prior to (i) prevalence of persistent clouds and smoke in atmosphere (Henderson *et al.*, 1998) (ii) insufficient sensitivity to forest structure and above ground biomass (Blanchard and Chang, 1993; Kuplich *et al.*, 2005) and (iii) inadequate temporal frequency hindering the natural resources and environment assessment (Kuplich *et al.*, 2005).

There have been two potential methods to estimate biomass from satellite data:

1. *Vegetation classification based method*: In this approach biomass is estimated based on vegetation type classification and on the unit biomass value predetermined for each vegetation type which is basically obtained from the ground observation. Multiplication between the area extent of each vegetation type and the predetermined unit biomass for each type would give the estimate of total biomass. Information on vegetation age or height and vegetation density would increase estimation accuracy.

2. *Direct observation of fresh biomass*: Many investigations have indicated that there is a correlation between microwave backscattering coefficients derived from SAR data or reflectance in case of optical data and biomass (fresh biomass) in leaves and stems of vegetation. However, correlation is usually vegetation types specific.

Satellite observation data cannot provide direct measurement of biomass but can provide indirect estimation based on insitu field data and on models. Biomass estimation by satellite observation is still in the research phase and the biomass product in this project has a strong research component. In general, the Above Ground Biomass can be directly estimated using remotely sensed data with different approaches, such as multiple regression analysis, K nearest-neighbour, and neural network (Roy and Ravan, 1996; Nelson *et al.*, 2000a; Steininger, 2000; Foody *et al.*, 2003; Zheng *et al.*, 2004), and indirectly estimated from canopy parameters, such as crown diameter, which are first

derived from remotely sensed data using multiple regression analysis or different canopy reflectance models (Wu and Strahler, 1994; Woodcock *et al.*, 1997; Phua and Saito, 2003; Popescu *et al.*, 2003). De Jong *et al.*, 2003, used digital airborne imaging spectrometer (DAIS) data to estimate biomass using stepwise linear regression analysis in southern France.

The most frequently used medium spatial-resolution data may be the time-series Landsat data, which have become the primary source in many applications, including aboveground biomass estimation at local and regional scales (Sader *et al.*, 1989; Roy and Ravan, 1996; Fazakas *et al.*, 1999; Nelson *et al.*, 2000a; Steininger, 2000; Mickler *et al.*, 2002; Foody *et al.*, 2003; Phua and Saito, 2003; Calva˜o and Palmeirim, 2004; Zheng *et al.*, 2004; Lu, 2005). Lefsky *et al.*, 2001, evaluated the utility of several remotely sensed data for estimating stand structure attributes—age, basal area, biomass, and diameter at breast height (DBH). Foody *et al.*, 2001, found that neural networks were useful for the aboveground biomass estimation using Landsat TM data in a Bornean tropical rain forest. In Finland and Sweden, Landsat TM data were used to estimate tree volume and Above Ground Biomass using the K nearest-neighbour estimation method (Halme and Tomppo, 2001; Franco-Lopez *et al.*, 2001; Tomppo *et al.*, 2002). Nelson *et al.*, 2000a, analysed secondary forest age and aboveground biomass estimation using Landsat TM data and found that aboveground biomass cannot be reliably estimated without the inclusion of secondary forest age. Steininger, 2000, explored the ability to estimate aboveground biomass of tropical secondary forests using Landsat TM data and found that data saturation was a problem for aboveground biomass estimation in advanced successional forests. The complex forest stand structure, the impact of shadows caused by canopy and topography, and the complex environments influence aboveground biomass estimation performance (Steininger, 2000; Lu, 2005). The close relationship between middle infrared (MIR) reflectance and aboveground biomass implies that MIR reflectance may be more sensitive to change in forest properties than the reflectance in visible and near-infrared wavelengths (Boyd *et al.*, 1999). The AVHRR NDVI data were used to estimate biomass density and assess burned areas, burned biomass, and atmospheric emissions in Africa (Barbosa *et al.*, 1999), and to estimate boreal and temperate forest woody biomass

in six countries (Canada, Finland, Norway, Russia, USA, and Sweden) (Dong *et al.*, 2003). Potter, 1999, used the National Aeronautics and Space Administration–Carnegie Ames Stanford Approach model to estimate aboveground biomass on country-by-country changes in global forest cover for the years 1990–1995. The SPOT VEGETATION data with 1 km X 1km spatial resolution has also been used to estimate aboveground biomass in Canada (Fraser and Li, 2002).

As MODIS data are readily available, the large number of spectral bands may be beneficial to the improvement of aboveground biomass estimation accuracy at the continental or global scale. Baccini *et al.*, 2004, used MODIS data in combination with precipitation, temperature, and elevation for mapping above ground biomass in national forest lands in California, USA. Overall, aboveground biomass estimation using coarse spatial-resolution data is still very limited because of the common occurrence of mixed pixels and the huge difference between the size of field-measurement data and pixel size in the image, resulting in difficulty in the integration of sample data and remote sensing-derived variables. A synthetic analysis of multiscale data with a combination of different modeling approaches may be needed for accurate aboveground biomass estimation in a large area. Ha¨me *et al.*, 1997, estimated coniferous forest biomass through a combination of Landsat TM and AVHRR data. Tomppo *et al.*, 2002, combined TM and IRS-1C Wide Field Sensors (WiFS) data to estimate tree stem volume and aboveground biomass in Finland and Sweden. The Landsat TM data were used as an intermediate step between field data and WiFS data. The nonparametric K nearest-neighbor method was used to analyse relationships between Landsat TM and field data, and nonlinear regression analysis was used to develop models for predicting volume and biomass for WiFS pixels. Wylie *et al.*, 2002, tested grass biomass estimation through scaling Landsat TM to coarse spatial-resolution satellite data (AVHRR) over the Great Plains of North America.

1.4.2 Microwave remote sensing for tropical forest ecosystems

The capabilities of imaging radars for investigating terrestrial ecosystems could best be organized into four broad categories: (1) classification and detection of change in land cover; (2) estimation of woody plant biomass; (3) monitoring the extent and timing

of inundation; and (4) monitoring other temporally dynamic processes, such as freeze/thaw status and soil moisture in fire-disturbed boreal forests.

Due to this unique feature of radar data compared with optical sensor data, the radar data have been used extensively in many fields, including forest-cover identification and mapping, discrimination of forest compartments and forest types, and estimation of forest stand parameters. Previous research has shown the potential of radar data in estimating aboveground biomass (Hussin *et al*., 1991; Ranson and Sun, 1994; Dobson *et al*., 1995; Rignot *et al*., 1994; Saatchi and Moghaddam, 1995; Harrell *et al*., 1997; Luckman *et al*., 1997; 1998; Imhoff *et al*., 2000; Kuplich *et al*., 2000; Castel *et al*., 2002; Sun *et al*., 2002; Santos *et al*., 2003; Treuhaft *et al*., 2004). Kasischke *et al*., 1997, reviewed radar data for ecological applications, including aboveground biomass estimation. Lucas *et al*., 2004, and Kasischke *et al*., 2004, reviewed SAR data for aboveground biomass estimation in tropical forests and temperate and boreal forests, respectively.

Different radar data have their own characteristics in relating to forest stand parameters (Leckie, 1998). However, low or negligible correlations were found between

SAR C-band backscatter and aboveground biomass Le Toan *et al*., 1992. Beaudoin *et al*., 1994, found that the HH return was related to both trunk and crown biomass, and the VV and HV returns were linked to crown biomass. The addition of C-band HV or HH polarization data in the regression equations significantly improved aboveground biomass estimation performance. The saturation problem is also common in radar data. The saturation levels depend on the wavelengths (i.e. different bands, such as C, L, P), polarization (such as HV and VV), and the characteristics of vegetation stand structure and ground conditions.

1.4.2.1 Interaction of Microwave and Vegetated Landscapes

Microwave backscatter is highly dependent on the orientation and size distribution of the scattering elements present within the region being imaged. Because of their high moisture content, individual components of forest canopies and other

vegetative covers (e.g., leaves, branches, trunks) represent discrete scattering and absorbing elements to the microwave power transmitted by imaging radars. Variations in the microwave dielectric constant of vegetation elements or ground surface play a central role in determining the magnitude and phase of the microwave energy, which is scattered from a vegetated surface and recorded and processed into a SAR image. Factors influencing the dielectric constant of vegetated surfaces include temperature of the scattering medium, relative moisture content of vegetation, soil, and snow cover, and the presence of water on vegetation.

Microwave scattering from land surfaces is strongly dependent on the size and orientation of the different elements comprising the vegetation. At longer radar wavelengths (P- and L-bands), microwave scattering and absorption results from interactions with the tree boles and larger branches found within forests, as well as the ground surface. At these wavelengths, the smaller woody stems and the foliage act mainly as attenuators. At shorter radar wavelengths, (C- and X-bands), microwave scattering and absorption results from interactions from smaller branches and leaves and needles in the canopy. The presence of a water-saturated or flooded surface leads to increased double-bounce scattering that enhances the strength of the ground-vegetation interaction term. Finally, the polarization combination of the received backscatter is dependent on the polarization of the transmitted microwave power and on the horizontal and/or vertical orientation of the scattering elements present in the vegetation.

Modeling clearly shows the differential dependence of microwave backscatter on the overall structure of vegetation canopies and on the variations in the characteristics of the ground layer. These models treat a forest stand either as a set of continuous horizontal layers (Richards *et al.*, 1987; Durden *et al.*, 1989; Ulaby *et al.*, 1990; Chauhan *et al.*, 1991) or as a discontinuous layer with individual trees acting as distinct scattering centers (McDonald and Ulaby, 1993). Both model classes are similar in that they calculate the same major scattering terms: (1) volume scattering from the tree canopy (the branches and leaves/needles); (2) direct ground scattering; (3) ground-to-trunk scattering; (4) ground-to-crown scattering; and (5) ground-to-crown-to-ground scattering. Most models

use formulations, which assume the tree trunks and branches can be modeled as lossy dielectric cylinders, and the leaves or needles as dielectric discs or cylinders, respectively.

A three-dimensional microwave backscatter model for forest canopies, which allows explicit spatial arrangement of scatterers have been exercised and validated using SAR and scatterometer data collected over a wide range of vegetation canopies (Sun and Simonett, 1988; Chauhan *et al.*, 1991; Durden *et al.*, 1989; Lang *et al.*, 1994; McDonald *et al.*, 1990; Moghaddan *et al.*, 1994; Way *et al.*, 1994; Ranson and Sun, 1994b; Wang *et al.*, 1993a, 1993b). Because of their complexity, however, these models have not proved invertible to allow estimation of surface and canopy characteristics needed to study specific ecological features or processes. The value of these models lies in their utility in understanding the dependence of microwave backscatter on system and imaging parameters (frequency, polarization, and viewing geometry of the transmitted microwave radiation) and the basic geometric characteristics of the vegetated surface being studied. In addition, these models have also been useful in developing an understanding of the effects of temporally varying factors which influence microwave backscatter, including soil moisture (Wang *et al.*, 1994b), air temperature and flooding. This understanding has proven critical in developing approaches to use SAR data in algorithms to estimate specific surface characteristics (Dobson *et al.*, 1995c; Rignot and Way, 1994).

1.5 Geographic Information System

Geographical Information System (GIS) is a system of hardware, software and procedures designed to support the capture, management manipulation; analysis modeling display of spatially referenced data for solving complex planning and management problems (Burroghs, 1986). GIS provides ample opportunity to integrate, analyze and generate scenarios based on human knowledge and geospatial parameters. Combination of remote sensing and GIS is making tasks of planning and decision-making much easier (Lillesand and Kiefer, 1999).

1.6 Problem Identification

Tropical realms of the world are a unique place where the world's biological diversity is concentrated. Conservation of this complex biologically diverse region needs to be taken up on priority basis. Therefore, nature reserves are created mainly to preserve and protect species of plants and animals. The aim of conservation has important aspect: to plan resource management on the basis of accurate inventory and to take protective measures ensuring untimely extinction. Reserves, which are usually large enough to protect whole sets of ecosystems may be unique in itself, rare or typical of the region are often designated as national park, sanctuary or biosphere reserve. These protected areas, when managed in scientific and construction way provide major sustainable benefits to society.

The terai with its characteristics complex of Sal forests, tall grasslands and swamps maintained by periodic flooding, is one of the most threatened ecosystems in India. Most of the terai has succumbed to anthropogenic pressures with agriculture and homesteads replacing the rich natural vegetation of the past. In this scenario the Dudwa Tiger Reserve stands out as the primary Protected Area Complex of the terai with one of its components having the status of a National Park. It is the only National Park and Tiger Reserve representative of Tarai-bhabar Biogeographic subdivision of the Upper Gangetic Plains (7a) Biogeographic province (Rodgers and Panwar, 1988). The vegetation of the area is of North Indian Moist Deciduous type.

Protected areas in the lowland Terai of Indo- Nepal contain some of the last remaining examples of sub-tropical tall grasslands in the Indian sub-continent (Bell and Oliver, 1992). These grasslands are key sites for biodiversity conservation, not only as a restricted area habitat, but also for the range of endangered faunal species which they support (IUCN, 1993). Fire, cutting and grazing of grassland retard succession from early successional grasslands dominated by *Saccharam spontaneum* to forest, allowing other grassland assemblages to become established (Lehmkuhl, 1994).

Optical remote sensing data has been used in the past extensively to derive biophysical parameters related to forest structure and composition. However, the stand volume could not be estimated directly from optical data owing to poor correlation

between tree height, girth and reflectance. In India only recently large scale (1:50,000) forest mapping has gained momentum. This kind of study can form a basis for working plan studies and stock mapping by Forest Department as the Forest Department also undertakes such studies on the same scale (Kacchwaha, 1990). Singh, 1985 provided area statistics under different vegetation types based on Landsat- 3 satellite data of November, 1981.

Research Objectives

There are two scientific objectives of the present study:

1. To map forest types and canopy density using optical ETM and microwave ASAR data.
2. To study and compare the forest stand volume and dry biomass with optical and microwave ASAR backscattering response.

Research Questions

1. Is it possible to map the forest type/ cover using ASAR data?
2. Is optical and/ or microwave ASAR C- Band could be used for forest stand volume and woody biomass estimation and which is better in terms of backscatter response/ behavior?

CHAPTER- 2

REVIEW OF LITERATURE

Numerous studies have demonstrated that approaches using optical remotely sensed data do not work for most terrestrial biomass densities, because there is a saturation effect at very low levels of biomass. The cloud penetration and sensitivity to vegetation capability of the Synthetic Aperture Radar (SAR) systems with their longer wavelengths from the microwave region of the electromagnetic spectrum approximately of 1 mm. to 1m has merits in assessment and management of natural resources in most of the region with persistent clouds. Currently, radar remote sensing appears to offer the greatest promise for obtaining estimates of biomass using remote sensing techniques. The dependence of microwave backscatter on total above-ground biomass has been documented in monospecific pine forest (Kasischke *et al.*, 1994a; LeToan *et al.*, 1992), mixed deciduous and coniferous forests (Ranson *et al.*, 1994; Rignot *et al.*, 1994; Moghaddam *et al.*, 1994). These studies all show the same results: (1) the sensitivity of microwave backscatter to biomass variations saturates after a certain level is reached; and (2) the biomass dependence of microwave backscatter varies as a function of radar wavelength and polarization. In summary, the saturation point is higher for longer wavelengths, and the HV polarization is most sensitive and VV the least (Waring *et al.*, 1994).

However, Microwave backscatter is correlated with total biomass and various components of biomass (e.g., branch biomass, needle biomass, bole biomass) or other physical characteristics (e.g., tree height, basal area) (Dobson *et al.*, 1995c; Hussin *et al.*, 1991). Since different radar frequencies and polarization combinations are sensitive to different layers of a forest canopy, it should be possible to use multiple channels of microwave data to estimate total aboveground biomass. Ranson *et al.*, 1994; Ranson and

Sun, 1995b, used a ratio of P-band HV (PHV) and C-band HV (CHV) to estimate total biomass in mixed coniferous/deciduous forests. Dobson *et al.*, 1995b, estimated aboveground biomass over a mixed coniferous/deciduous forest using the different combinations of the SAR data sets and found it useful. The study of the synergism between optical and radar Remote Sensing also became more feasible using ERS-1 SAR and Landsat TM (Kuplich *et al.*, 2000a).

Mapping of forest biomass using radar has been studied by various workers (eg. Sader *et al*., 1989; Hussain *et al*., 1991; Le Toan *et al*., 1992). So the relationship between microwave Remote Sensing and forest total above ground biomass have been studied extensively since early 1990's at different forest sites (Le Toan *et al*., 1992; Dobson *et al*, 1992a). Furthermore, the nature of microwave interaction with forest is sensitive to its forest biomass as a result of its geometry etc., (Baker *et al*., 1994; Beaudoin *et al*., 1994; Imhoff, 1995a; Kasischke *et al.*, 1995). According to Le Toan *et al.,* 1992, as most of the backscatter energy originates from the upper crown layer, in C-band, it is of practically not much useful for biomass estimation due to shorter wavelength (e.g., Radarsat, SIR- C, ERS-1), Israelsson, 1994.

There is a strong relationship between SAR backscatter L- band around 40-60 t/ha. (Imhoff, 1995; Luckman *et al*., 1997) in 4-10 years old tropical regenerating forests (Uhl *et al.*, 1988; Freanside and Guimaraes, 1996). In brief, C- band (50 t/ha), L-band (100 t/ha) and P- band (200 t/ha) according to (Sader, 1989; 1992; Le Toan *et al*., 1992) and a volume of approximately 200m^3 /ha at P- band for poplar stands in MAESTRO 1 Campaign , Israelsson, 1994.

RADARSAT provides data at different incidence angles. ENVISAT ASAR will have in addition the polarization diversity. For different incidence angles, the bare soil, when the surface is smooth in terms of the wavelength, will have a large angular variation of its backscatter compared to the canopy. In general, this will result in a reduced sensitivity of the signal with biomass for increasing incidence. The sensitivity to biomass is then higher at low incidence angles for RADARSAT and ENVISAT.

The two like polarizations of ENVISAT are not expected to bring additional information. It is not the case of the cross- polarizations, where the backscatter results

only from the canopy volume scattering, the ground surface contribution being negligible. The relationships with biomass can be expected by the increase of the canopy backscatter with the increasing biomass. Thus, cross polarizations is expected to provide more generalized direct- then inverse- relationships with biomass compared to like polarizations.

For higher values of biomass, the signal saturates. To explain the signal saturation the canopy may be assumed to be a homogenous medium with a single category of scatters (here, needles). In the high biomass case, the attenuation of the incoming wave is important enough to cause the soil contribution to be negligible. In this case, the backscattering co- efficient is found independent of the number of scatters. The saturation level depends only on the distribution in size, orientation, and dielectric constant of the scatters. As an example, the saturation observed observed with SIR- C at C- band, 54º, (HH) is – 11.5 dB for respectively *Pinus pinaster* (Maritime pine), and *Pinus nigra* (Corsican pine) for the Landes and the Loze're forest. The observations could be interpreted using the theoretical curve of backscattering co- efficient at C (HH) – 55º versus the cylindrical radius of the main scatter, of a homogenous medium formed by cylindrical needles with a uniform orientation distribution between 0 and 2 p. The effective cylindrical radius of the needles of *Pinus pinaster* is actually larger than the needle radius of *Pinus nigra*.

CHAPTER- 3

SAR IMAGING PRINCIPLES

3.1. Radar Imaging

Radar is a commonly used acronym for Radio Detection and Ranging. Radio waves are that part of the electromagnetic spectrum that have wavelengths considerably longer than visible light, as shown in table below.

Table 3.1. The radar wavebands

Band Name	Wavelength (cm)	Frequency (GHz)
Ka	0.75 -1.13	26.5 -40
Ku	1.67- 2.40	12.5 -18
K	0.75 - 1.67	18 -26.5
X	2.40 - 3.75	8 -12.5
C	3.75- 7.5	4 -8
S	7.5 -15	2 -4
L	15 -30	1 -2
P	30 -130	0.230-1

Imaging radar is an active illumination system, in contrast to passive optical imaging systems that require the Sun's illumination. An antenna, mounted on an aircraft or spacecraft, transmits a radar signal in a ***side-looking direction*** towards the earth's surface. The reflected signal, known as the echo, is ***backscattered*** from the surface and received a fraction of a second later at the same antenna, as shown in below. The brightness, or amplitude (A), of this received echo is measured and recorded and the data are then used to construct an image. For coherent Radar systems such as Synthetic Aperture Radar (SAR), the phase of the received echo is also measured and used to construct the image.

Radar uses a single frequency for illumination; therefore there is no color associated with raw Radar imagery (unlike optical imagery which is illuminated by all the various colours from the ambient visible light.) However, Radar provides at least two

significant benefits from its not being dependent on natural light: the ability to image through clouds, and the ability to image at night. The wavelength of the microwaves used in Radar are longer than those of visible light, and are less responsive to the boundaries between air and the water droplets within the clouds. The result is that, for Radar, the clouds appear homogeneous with only slight distortions occurring when the waves enter and leave the clouds.

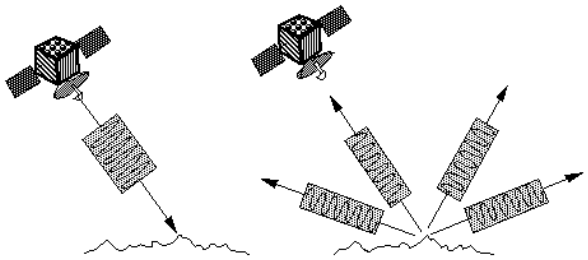

Fig. 3.1. Echoes received back by ASAR antenna

3.2. Radar Principles

Radar sensors are usually divided into two groups according to their modes of operation. Active sensors are those that provide their own illumination and therefore contain a transmitter and a receiver, while passive sensors are simply receivers that measure the radiation emanating from the scene under observation.

1.	Active systems	- radar imaging systems (Radar = Radio Detection and Ranging)
2.	Scatterometers	- altimeters
3.	Passive systems	- microwave radiometers

The basic principle of radar is transmission and reception of pulses. Short microsecond) high energy pulses are emitted and the returning echoes recorded,

providing information on:

- magnitude

- phase
- time interval between pulse emission and return from the object
- polarization
- Doppler frequency

The two types of imaging radars most commonly used are:

- RAR (Real Aperture Radar)

- SAR (Synthetic Aperture Radar)

Real Aperture radars are often called SLAR (Side Looking Airborne Radar). Both Real Aperture and Synthetic Aperture Radar are side-looking systems with an illumination direction usually perpendicular to the flight line. The difference lies in the resolution of the along-track, or azimuth direction. Real Aperture Radars have azimuth resolution determined by the antenna beamwidth, so that it is proportional to the distance between the radar and the target (slant-range). Synthetic Aperture Radar uses signal processing to synthesise an aperture that is hundreds of times longer than the actual antenna by operating on a sequence of signals recorded in the system memory.

These systems have azimuth resolution (along-track resolution) that is independent of the distance between the antenna and the target. The nominal azimuth resolution for a SAR is half of the real antenna size, although larger resolution may be selected so that other aspects of image quality may be improved. Generally, depending on the processing, resolutions achieved are of the order of 1-2 metres for airborne radars and 5-50 metres for spaceborne radars.

Fig. 3.2. Side-looking radars

3.2.1. Real Aperture Radar (RAR)

A narrow beam of energy is directed perpendicularly to the flight path of the carrier platform (aircraft or spacecraft). A pulse of energy is transmitted from the radar antenna, and the relative intensity of the reflections is used to produce an image of a narrow strip of terrain. Reflections from larger ranges arrive back at the radar after proportionately larger time, which becomes the range direction in the image. When the next pulse is transmitted, the radar will have moved forward a small distance and a slightly different strip of terrain will be imaged.

These sequential strips of terrain will then be recorded side by side to build up the azimuth direction. The image consists of the two dimensional data array. In this figure, the strip of terrain to be imaged is from point A to point B. Point A being nearest to the nadir point is said to lie at near range and point B, being furthest, is said to lie at far range. The distance between A and B defines the swath width. The distance between any point within the swath and the radar is called its slant range. Ground range for any point within the swath is its distance from the nadir point (point on the ground directly underneath the radar).

Range resolution

For a Radar system to image separately two ground features that are close together in the range direction, it is necessary for all parts of the two objects' reflected signals to be received separately by the antenna. Any time overlap between the signals from two objects will cause their images to be blurred together.

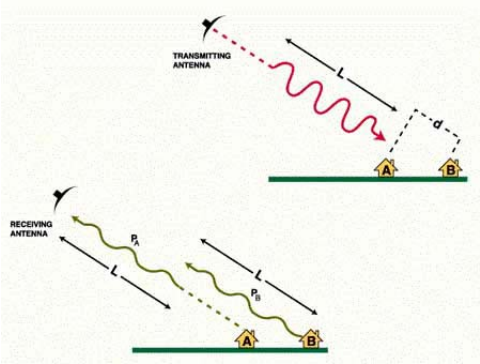

Fig. 3.3. Range resolution

For the radar to be able to distinguish two closely spaced elements, their echoes must necessarily be received at different times. In the upper part of the figure, the pulse of length L is approaching buildings A and B. The slant range distance between the two buildings is d. Since the radar pulse must travel two ways, the two buildings lead to two distinguished echoes if: $d > L/2$.

The part of the pulse backscattered by building A is PA, and the part of the pulse backscattered by building B is PB. It appears in the lower part of the figure that to reach the target and come back, PB has covered an extra distance 2d, and thus is at a slightly shorter distance than L behind PA. Because of this, the end of PA and the beginning of PB overlap when they reach the antenna. As a consequence, they are imaged as one single large target which extends from A to B. If the slant range distance between A and B were slightly higher than L/2, the two pulses would not overlap and the two signals

would be recorded separately. Range resolution (across track resolution) is approximately equal to L/2, i.e. half the pulse length. Ground range resolution is:

Where c: speed of light, t: pulse duration and q: incidence angle.

Azimuth resolution

As mentioned above, the azimuth resolution is affected by the beamwidth. As the antenna beam fans out with increasing distance from the earth to the platform carrying the pulse transmitting source and receiver, the azimuth resolution deteriorates. The beamwidth of the antenna is directly proportional to the wavelength of the transmitted pulses and inversely proportional to the length of the antenna.

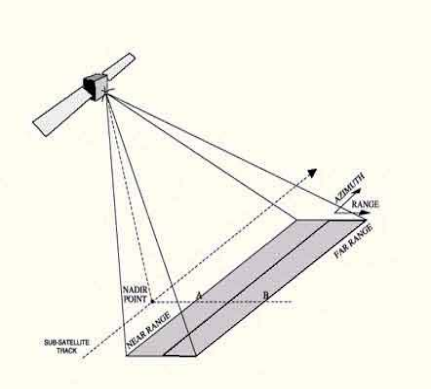

Fig. 3.4. Azimuth Resolution

So, for any given wavelength, antenna beamwidth can be best controlled by one of two different means:

- by controlling the physical length of the antenna, or
- by synthesizing an effective length of the antenna

Those systems where beamwidth is controlled by the physical antenna length are referred to as Real Aperture, or Noncoherent Radars and the natural resolution of such an orbiting radar instrument, observing from 1000 km, is typically 10 km on the ground.

While these systems enjoy relative simplicity of design and data processing, the resolution difficulties restrict them to short-range, low altitude operation and the use of relatively short wavelengths. These restrictions limit the area of coverage obtainable and the short wavelengths experience more atmospheric dispersion.

The term azimuth is used to indicate linear distance or image scale in the direction parallel to the ***radar*** flight path. In an ***image***, azimuth is also known as ***along-track*** direction, since it is the relative along-track position of an object within the ***antenna***'"s field of view following the radar's line of flight. Azimuth is predominately used in radar terminology. The azimuth direction is perpendicular to the ***range*** direction. The resolution of an image in the azimuth directions for a ***SAR*** image is constant and is independent of the range. For two objects to be resolved, they must be separated in the azimuth direction by a distance greater than the ***beamwidth*** on the ground.

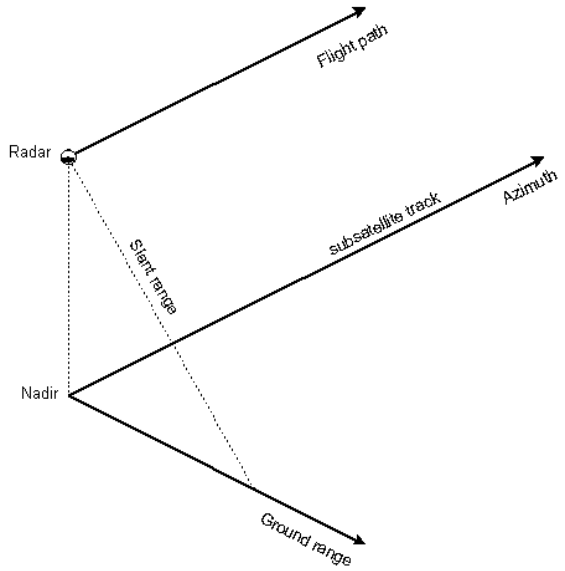

Fig. 3.5. Azimuth line

Spatial Resolution

The spatial resolution of a Real Aperture Radar system is determined by, among

other things, the size of the antenna used. For any given wavelength, the larger the antenna the better the spatial resolution. Other determining factors include the pulse length and the antenna ***beamwidth***. The pulse length of the radar signal is determined by the length of time that the antenna emits its burst of energy.

Consider an image to be a set of values A(x,y), where the x coordinate is in the direction of platform motion and the y coordinate is in the direction of illumination. Then the value of y, or ***range direction*** , and its resolution (range resolution) is based on the pulse length, the arrival time of the echo, and the timing precision of the radar. The value of x, which is ***azimuth*** direction (also referred to as the along-track direction) , and its resolution (azimuth resolution) depends on the position of the platform that carries the transmitting antenna and the beamwidth of the radar.

Beamwidth

Beamwidth is a measure of the width of the radiation pattern of an ***antenna***. For ***SAR*** applications, both the vertical beamwidth, affecting the width of the illuminated ***swath***, and the horizontal or ***azimuth*** pattern, which determines, indirectly, the azimuth resolution, are frequently used. Beamwidth may be measured in the one-way or two-way form, and in either voltage or power.

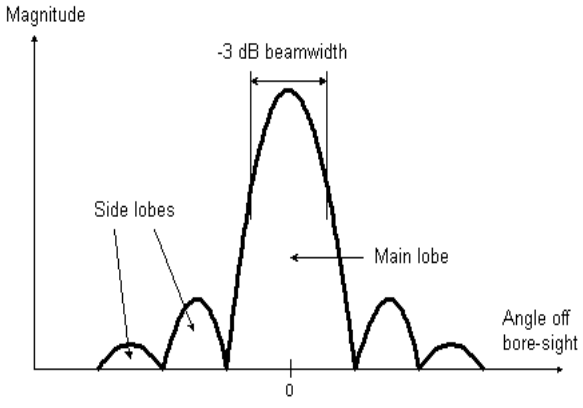

Fig. 3.6. Beam width

Look angle/ Depression angle

Depression angle usually refers to the line of sight from the radar to an illuminated object as measured from the horizontal plane at the *radar*. For image interpretation, use of the term is not recommended because it does not account for the effects of Earth curvature, and it does not conveniently include effects of local slope in the scene. It is more appropriate for an engineering description of the vertical *antenna* pattern at the radar itself.

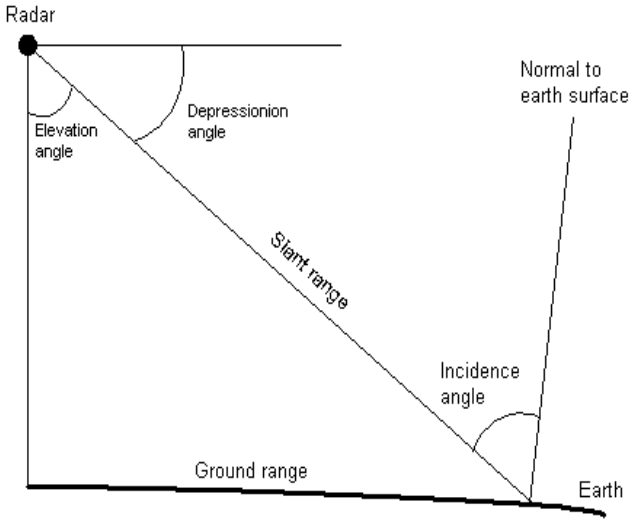

Fig. 3.7. Depression angle

Elevation Displacement

Elevation displacement, also referred to as geometric distortion, is the image displacement in a **remote sensing** image toward the **nadir** point in **radar** imagery due to sensor/target imaging geometries. In a **radar image** the displacement is toward the sensor and can become quite large when the sensor is nearly overhead. The displacement increases with decreasing **incidence angle**. The four characteristics resulting from the geometric relationship between the sensor and the terrain that are unique to radar imagery are **foreshortening**, pseudo-shadowing, **layover**, and **shadowing**. **Topographic** features

like mountains, as well as artificial targets like tall buildings, will be displaced from their desired orthographic position in an image. The effect may be used to create **stereo images**. It may be removed from an image through independent knowledge of the terrain profile. In many applications, an approximate correction may be derived through shape-from-shading techniques. Elevation displacement will be greater in **slant range** than **ground range** due to the fact that the image is more compressed in a slant range presentation. Elevation displacement is also most pronounced at **near range**.

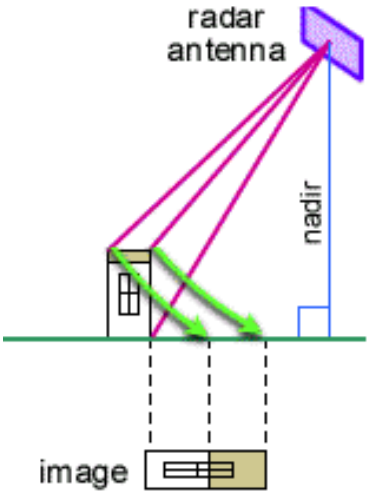

Fig. 3.8. Elevation displacement

Foreshortening

Foreshortening is the spatial distortion whereby terrain slopes facing a ***side-looking radar's (SLAR)*** illumination are mapped as having a compressed scale relative to its appearance, as if the same terrain were level. Foreshortening is a special case of ***elevation displacement***. The effect is more pronounced for steeper slopes and for radars that use steeper ***incidence*** angles.

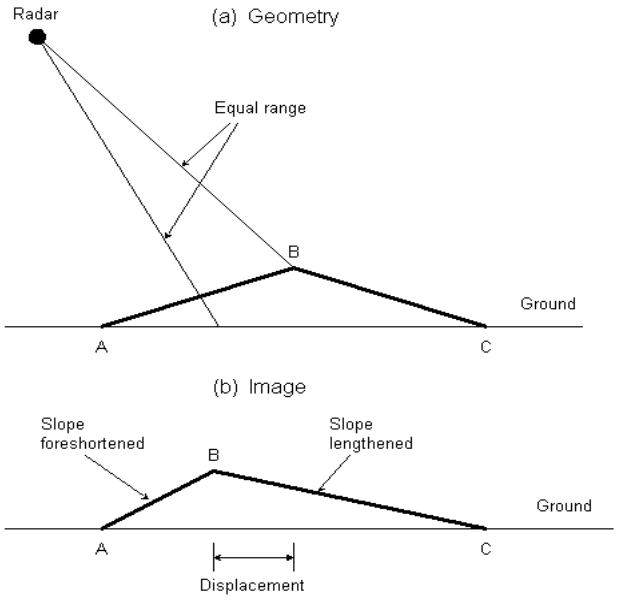

Fig. 3.9. Foreshortening

Ground Range

Ground Range is the perpendicular distance from the ground track to a given object on the Earth's surface. Also defined as the range direction of a side-looking radar image as projected onto the nominally horizontal reference plane, similar to the spatial display of conventional maps. Ground range projection requires a geometric transformation from slant range to ground range; for spacecraft data, a geoid model of the Earth is used, whereas for airborne radar data, a planar approximation is sufficient. This can lead to relief or elevation displacement, foreshortening, and layover on radar images. However, if terrain elevation information is used, the effect on viewing geometry can be minimised.

Imaging Geometry

The imaging geometry of a ***radar*** system is different from the framing and scanning systems commonly employed for optical remote sensing. Similar to optical

systems, the platform travels forward in the flight direction (A) with the ***nadir*** (B) directly beneath the platform. The ***microwave*** beam is transmitted obliquely at right angles to the direction of flight illuminating a ***swath*** (C) which is offset from nadir. ***Range*** (D) refers to the ***across-track*** dimension perpendicular to the flight direction, while ***azimuth*** (E) refers to the ***along-track*** dimension parallel to the flight direction. This ***side-looking*** viewing geometry is typical of imaging radar systems (airborne or spaceborne).

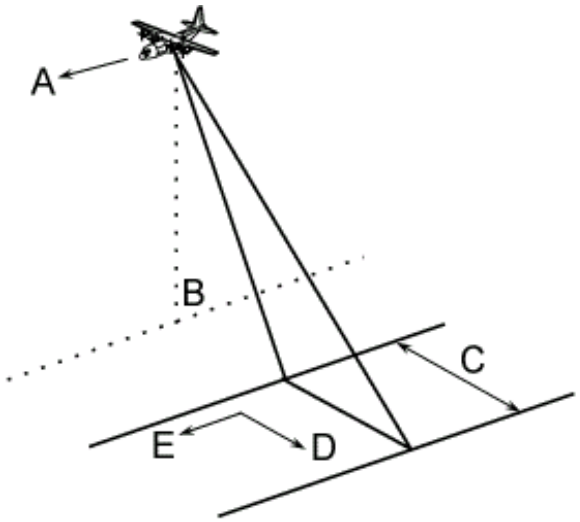

Fig. 3.10. Imaging geometry

The portion of the image swath closest to the nadir track of the radar platform is called the ***near range*** (A) while the portion of the swath farthest from the nadir is called the ***far range*** (B). The ***incidence angle*** is the angle between the ***radar beam*** and ground surface (A) which increases, moving across the swath from near to far range. The look angle (B) is the angle at which the radar ***looks*** at the surface. In the near range, the viewing geometry may be referred to as being steep, relative to the far range, where the viewing geometry is shallow. At all ranges the radar ***antenna*** measures the radial line of sight distance between the radar and each target on the surface. This is the ***slant range*** distance (C). The ***ground range*** distance (D) is the true horizontal distance along the ground corresponding to each point measured in slant range.

Incidence Angle

The incidence angle is the angle defined by the incident ***radar beam*** and the vertical (normal) to the intercepting surface. In general, reflectivity from distributed scatterers decreases with increasing incidence angle. The incidence angle is commonly used to describe the angular relationship between the radar beam and the ground, surface layer or a target. A change of the radar illumination angle often affects the radar ***backscattering*** behaviour of a surface or target. The incidence angle changes across the radar image ***swath***; it increases from ***near range*** to ***far range***. In the case of satellite ***radar imagery***, the change of incidence angle for flat terrain across the imaging ***swath*** tends to be rather small, usually on the order of several degrees. In the case of an inclined surface (slope), the local incidence angle (L) is defined as the angle between the incident radar beam and a line that is normal to that surface. The local incidence angle determining, in part, the ***brightness***, or image ***tone***, for each picture element (pixel) and slope facet, is a key element in the prominent rendition of terrain features in radar imagery.

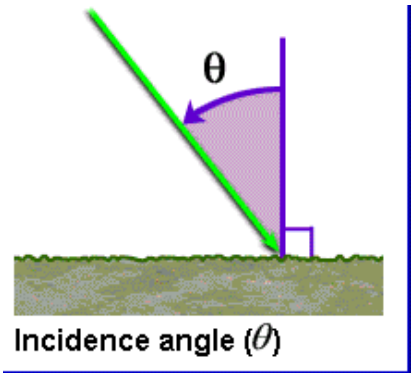

Fig. 3.11. Incidence Angle

Microwave interactions with the surface are complex and different scattering mechanisms may occur in different angular regions. Returns due to surface scattering are normally strong at low incidence angles and decrease with increasing incidence angle, with a

slower rate of decrease for ***rougher*** surfaces. Returns due to volume scattering from an heterogeneous medium with low dielectric constant tend to be more uniform for all incidence angles. Thus, radar backscatter has an angular dependence, and there is potential for choosing optimum configurations for different applications.

Layover

Layover is an extreme form of ***elevation displacement*** or ***foreshortening*** in which the top of a reflecting object, such as mountain, is closer to the ***radar*** (in ***slant range***) than are the lower parts of the object. The image of such a feature appears to have fallen over towards the radar. Also defined as the displacement of the top of an elevated feature with respect to its base on the radar image. The peaks look like dip-slopes. The effect is more pronounced for radars having smaller incidence angle.

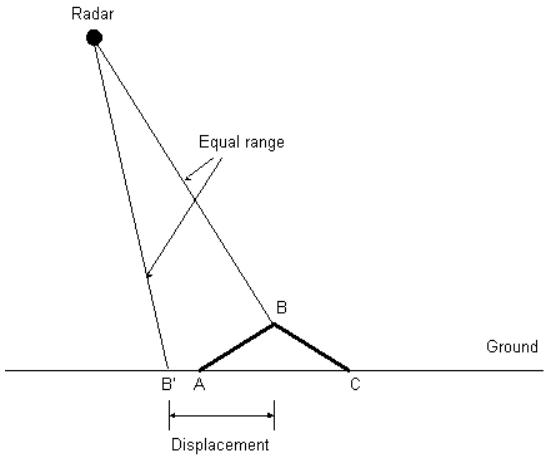

Fig. 3.12. Layover

Optical vs. microwave image geometry

The figure below presents a comparison between respective geometries of radar image and oblique aerial photos. The reason for the major differences between the two image's geometry is that an optical sensor measures viewing angles, while microwave imagers determine distances.

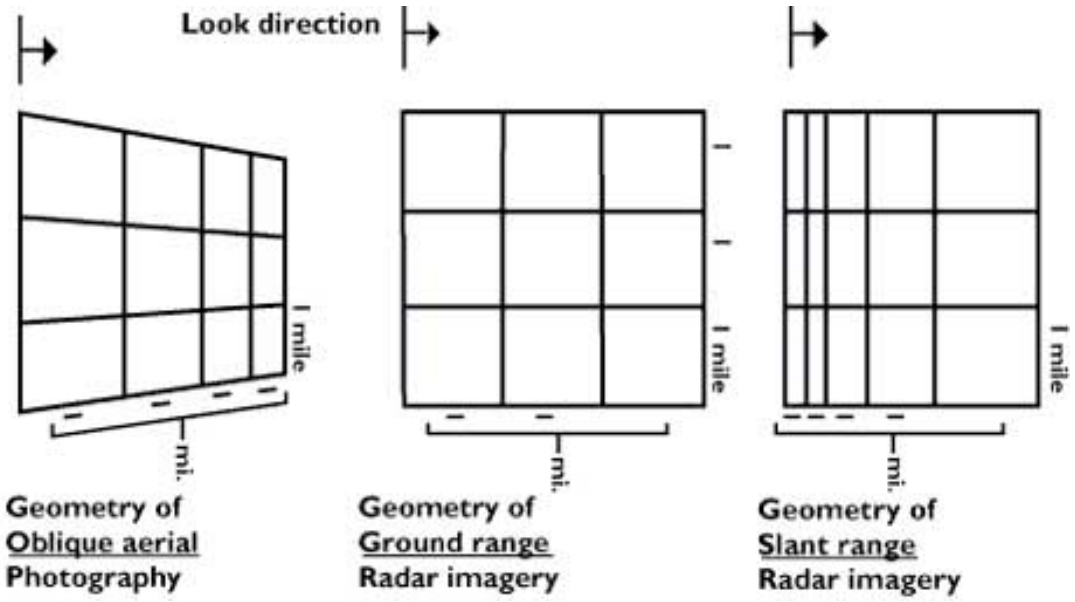

ig. 3.13. Optical Vs microwave image geometry

Radar Polarisation

Radar polarisation is the orientation of the electric (E) vector in an electromagnetic wave, frequently horizontal or vertical, in conventional imaging radar systems. Polarisation refers to the orientation of the plane of the electric field (E), as opposed to the magnetic field (M).

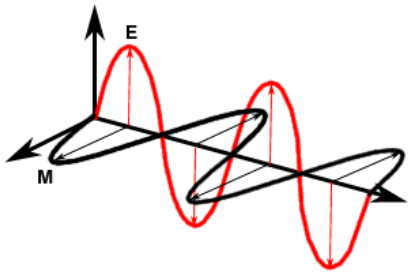

Fig. 3.14. Radar polarisation

Remote sensing radars are usually designed to transmit either vertically polarised or horizontally polarised radiation. This means that the electric field of the wave is in a vertical plane or a horizontal plane. Likewise, the radar can receive either vertically or horizontally polarised radiation, and sometimes both. The planes of transmitted and received polarisation are designated by the letters H for Horizontal and V for Vertical. Thus the polarisation of a radar image can be ***HH***, for horizontal transmit, horizontal receive, ***VV*** for vertical transmit, vertical receive, ***HV*** for horizontal transmit vertical receive, and vice versa (***VH***).

When the polarisation of received radiation is the same as the transmitted radiation, the image is said to be like-polarised When the polarisation of received radiation is the opposite of the transmitted radiation, the image is said to be cross-polarised cross polarisation requires multiple-scattering by the target and therefore results in weaker ***backscatter*** than like-polarisation Satellite radars generally use like-polarisation because the cross-polarised signals are too weak to produce a good ***image***.

Polarisation is established by the ***antenna***, which may be adjusted to be different on transmit and on receive. Reflectivity of ***microwaves*** from an object depends on the relationship between the polarisation state and the geometric structure of the object. Possible states of polarisation, in addition to vertical and horizontal, include all angular orientations of the E vector, and time varying orientations leading to elliptical and circular polarisations.

Backscatter

Radar images are composed of many picture elements referred to as pixels. Each pixel in the radar image represents an estimate of the radar ***backscatter*** for that area on the ground. Darker areas in the image represent low backscatter, while brighter areas represent high backscatter. Bright features mean that a large fraction of the radar energy was reflected back to the radar, while dark features imply that very little energy was

reflected. Backscatter for a target area at a particular wavelength will vary for a variety of conditions, such as the physical size of the scatterers in the target area, the target's electrical properties and the moisture content, with wetter objects appearing bright, and drier targets appearing dark. (The exception to this is a smooth body of water, which will act as a flat surface and reflect incoming pulses away from a target. These bodies will appear dark). The wavelength and polarisation of the Radar pulses, and the observation angles will also affect backscatter.

A useful rule-of-thumb in analysing radar images is that the higher or brighter the backscatter on the image, the rougher the surface being imaged. Flat surfaces that reflect little or no radio or microwave energy back towards the radar will always appear dark in radar images. Vegetation is usually moderately rough on the scale of most radar wavelengths and appears as grey or light grey in a radar image. Surfaces inclined towards the radar will have a stronger backscatter than surfaces which slope away from the radar and will tend to appear brighter in a radar image. Some areas not illuminated by the radar, like the back slope of mountains, are in shadow, and will appear dark. When city streets or buildings are lined up in such a way that the incoming radar pulses are able to bounce off the streets and then bounce again off the buildings (called a double-bounce) and directly back towards the radar they appear very bright (white) in radar images. Roads and freeways are flat surfaces and so appear dark. Buildings which do not line up so that the radar pulses are reflected straight back will appear light grey, like very rough surfaces.

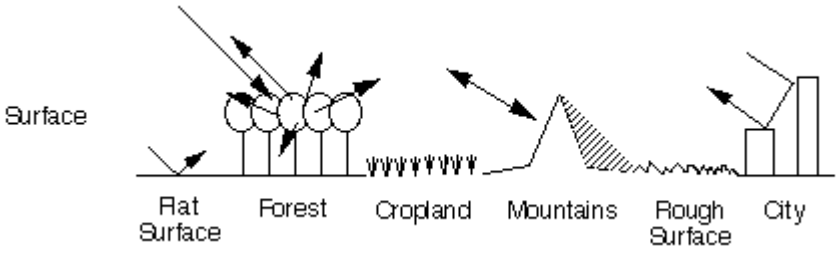

Fig. 3.15. Backscatter from various surfaces types

3.2.2. Synthetic Aperture Radar

Synthetic Aperture Radars were developed as a means of overcoming the limitations of real aperture radars. These systems achieve good azimuth resolution that is independent of the slant range to the target, yet use small antennae and relatively long wavelengths to do it.

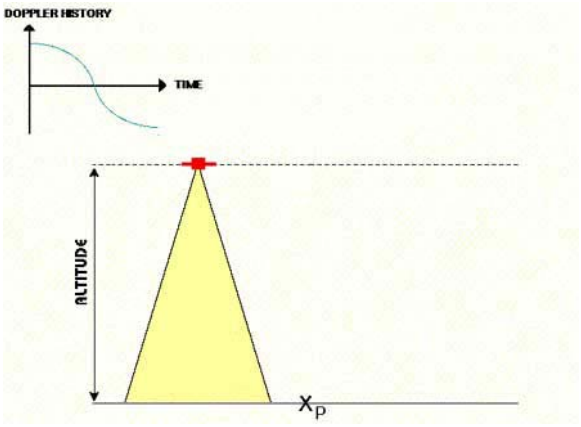

Fig. 3.16. Synthetic aperture radar

SAR Principle

A synthetic aperture is produced by using the forward motion of the radar. As it passes a given scatterer, many pulses are reflected in sequence. By recording and then combining these individual signals, a "synthetic aperture" is created in the computer providing a much improved azimuth resolution. It is important to note that some details of the structure of the echoes produced by a given target change during the time the radar passes by. This change is explained also by the Doppler effect which among others is used to focus the signals in the azimuth processor.

Synthetic Aperture Radar takes advantage of the ***Doppler*** history of the radar echoes generated by the forward motion of the spacecraft to synthesis a large antenna,

enabling high azimuthal resolution in the resulting image despite a physically small antenna. As the radar moves, a pulse is transmitted at each position. The return echoes pass through the receiver and are recorded in an echo store.

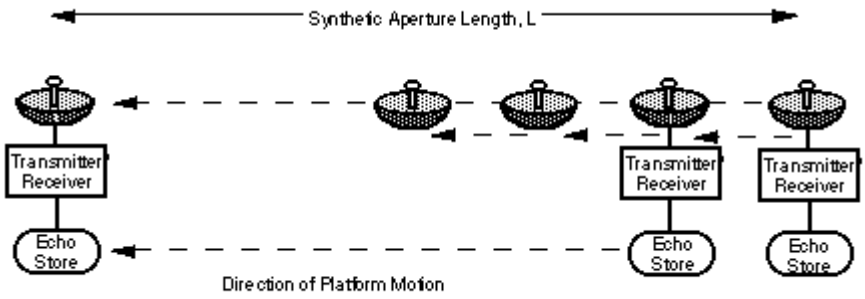

Fig. 3.17. Constructing a synthetic antenna

SAR is a ***coherent***, active, microwave imaging method that improves natural radar resolution by focusing the image through a process known as synthetic aperture processing. This typically requires a complex integrated array of onboard navigational and control systems, with location accuracy provided by both Doppler and inertial navigation equipment. For a C band instrument, (such as ERS-1, ERS-2 or ASAR) 1000 km from its target, the area on the ground covered by a single transmitted EM pulse, known as the radar footprint, is on the order of 5 km long in the along-track (azimuth) direction. In SAR, the satellite must not cover more than half of the azimuth antenna length between the emission of successive pulses, so as not to degrade the **range resolution**. For example, a 10 m antenna should advance only 5 m between pulses, to produce a 5 m long final elementary resolution cell, or ***pixel***. Therefore, each 5 km long footprint is a collection of signals, each one of which is a mixture of a thousand 5 m samples, each of which contributes to a thousand signals. Focusing is the reconstruction of the contribution of each 5 m cell, which results in an improvement of resolution of approximately a thousand times of a Real Aperture Radar. This effectively provides a synthetic aperture of a 20 km antenna.

Because the signals received by a SAR system are recorded over a long time period, the system translates the real antenna over a correspondingly long distance, which becomes the effective length of the antenna. The **azimuth resolution** with this synthetic antenna length is greatly improved, due to the effective narrowing of the beamwidth. The azimuth resolution is also essentially independent of range, because at long range an object is in the beam longer, meaning that returns from it are recorded over a longer distance.

3.5. Parameters affecting radar backscatter (Geometric characteristics)

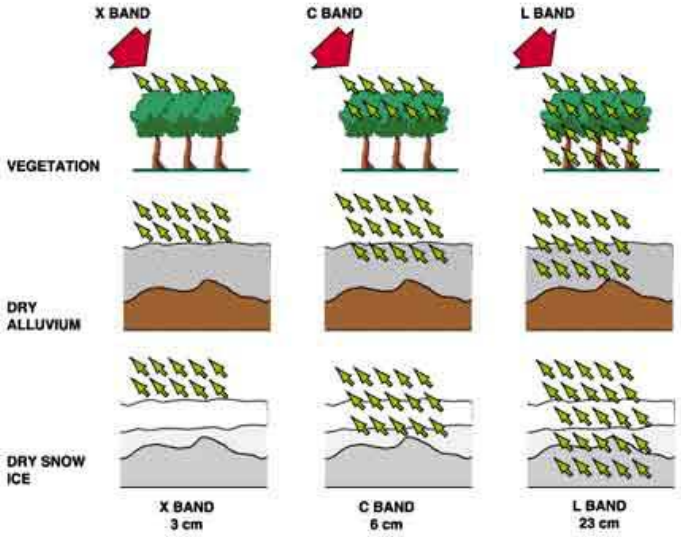

Fig. 3.18. Different terrain and their impact on various wavelength bands

Different surface features exhibit different scattering characteristics:

1. urban areas : very strong backscatter
2. forest : intermediate backscatter
3. calm water : smooth surface, low backscatter
4. rough sea : increased backscatter due to wind and current effects

The radar backscattering coefficient σ^0 provides information about the imaged surface. It is a function of:

1. radar observation parameters: (frequency **f**, polarisation **p** and incidence angle of the electromagnetic waves emitted)
2. surface parameters: (roughness, geometric shape and dielectric properties of the target).

Influence of frequency

The frequency of the incident radiation determines:

- the penetration depth of the waves for the target imaged;
- the relative roughness of the surface considered.

Penetration depth tends to be longer with longer wavelengths. If we consider the example of a forest, the radiation will only penetrate the first leaves on top of the trees if using the X-band (λ = 3 cm). The information content of the image is related to the top layer and the crown of the trees. On the other hand, in the case of L-band (λ = 23 cm), the radiation penetrates leaves and small branches; the information content of the image is then related to branches and eventually tree trunks.

But it should be noted that:

- penetration depth is also related to the moisture of the target;
- microwaves do not penetrate water more than a few millimeters.

Influence of polarization

Polarization describes the orientation of the electric field component of an electromagnetic wave. Imaging radars can have different polarization configurations. However, linear polarization configurations HH, VV, HV, VH are more commonly used. The first term corresponds to the polarization of the emitted radiation, the second term to the received radiation, so that X_{HV} refers to X band, H transmit, and V receive for example. In certain specific cases, polarization can provide information on different layers of the target, for example flooded vegetation. The penetration depth of the radar wave varies with the polarization chosen. Polarization may provide information on the form and the orientation of small scattering elements that compose the surface or target. More than one bounce of backscattering tends to depolarize the pulse, so that the cross polarized return in this case would be larger than with single bounce reflection.

Influence of roughness

Roughness is a relative concept depending upon wavelength and incidence angle. A surface is considered "rough" if its surface structure has dimensions that are comparable to the incident wavelength.

An example of the effect of surface roughness can be observed in the zones of contact between land and water.

Inland water bodies tend to be relatively smooth, with most of the energy being reflected away from the radar and only a slight backscatter towards the radar. On the contrary, land surfaces tend to have a higher roughness.

Water bodies generally have a dark tonality on radar images, except in the case of wind-stress or current that increases the water surface roughness, which provokes a high backscatter.

In the microwave region, this difference between respective properties of land and water can be extremely useful for such applications as flood extent measurement or coastal zones erosion. This animation illustrates the range of backscatter from water surfaces.

Influence of incidence angle

The incidence angle is defined by the angle between the perpendicular to the imaged surface and the direction of the incident radiation. For most natural targets, backscatter coefficient σ^0 varies with the incidence angle.

Experimental work was conducted by Ulaby et al. (1978) using five soils with different surface roughness conditions but with similar moisture content. It appeared that, when using the L band (1.1 GHz), the backscatter of smooth fields was very sensitive to near nadir incidence angles; on the other hand, in the case of rough fields, the backscatter was almost independent of the incidence angle chosen.

Influence of moisture

The complex dielectric constant is a measure of the electric properties of surface materials. It consists of two parts (permittivity and conductivity) that are both highly dependent on the moisture content of the material considered.

In the microwave region, most natural materials have a dielectric constant between 3 and 8, in dry conditions. Water has a high dielectric constant (80), at least 10 times higher than for dry soil.

As a result, a change in moisture content generally provokes a significant change in the dielectric properties of natural materials; increasing moisture is associated with an increased radar reflectivity.

In the specific case of vegetation, penetration depth depends on moisture, density and geometric structure of the plants (leaves, branches).

For flat terrain, the local reflection angle is the same as the incidence angle; most of the incident energy is reflected away from the sensor, resulting in a very low return signal. Rough surfaces, on the other hand, will scatter incidence energy in all directions and return a significant portion of the incident energy back to the antenna.

The shape and orientation of objects must be considered, as well as their surface roughness, when evaluating radar returns. For instance a particularly bright response will come from a corner reflector, which will produce a double bounce, as shown above. It is also worth noting that some features, such as corn fields, might appear rough when seen in both the visible and microwave portion of the spectrum, whereas other surfaces, such as roads, may appear rough in the visible range but look smooth in the microwave spectrum. In general, SAR images will manifest many more smooth, or specular, surfaces than those produced with optical sensors.

Since one factor affecting backscatter is the ***polarisation*** used, those SAR systems that can transmit pulses in either horizontal (H) or vertical (V) polarisation and receive in either H or V, such as the ASAR sensor, can better utilise this property for image interpretation.

In addition, SAR measures the phase of the incoming pulse and can therefore measure the phase difference in the return of the HH and VV signals. This difference can be thought of as a difference in the round-trip times of HH and VV signals and is frequently the result of the structural characteristics of the scatterers, or targets. The phase information in the products from these SAR can used to derive an estimate of the correlation coefficient for the HH and VV returns, which can be considered as a measure of how alike the HH and VV scatterers are.

Electrical Characteristics

The electrical characteristics of terrain features interact with their geometric characteristics to determine the intensity of radar returns. One measure of an object's electrical character is the 'complex dielectric constant', which is a parameter that indicates the reflectivity and conductivity of various materials. As reflectivity and conductivity increases, so does the value of this constant.

In the microwave region of the spectrum, most natural materials have a dielectric constant in the range of 3 to 8 when dry, whereas water has a dielectric constant of approximately 80. This means that the presence of moisture in either soil or vegetation will result in significantly greater reflectivity. Other examples of sources of high reflectivity are metal bridges, silos, and railroad tracks.

3.4. ASAR Design

The orbit selected for ENVISAT will provide a 35-day repeat cycle, the same as the ERS-2 mission. Since the ***orbit*** track spacing varies with latitude (the orbit track spacing at 60° latitude is half that at the equator), the density of observations and/or revisit rate is significantly greater at higher latitudes than at the equator. The flexible ***swath*** positioning in Image Mode greatly increases the potential temporal coverage ***frequency*** compared to ERS. Coverage is also affected by the different swath widths of IS1 to IS7. ASAR operates simultaneously with the other ENVISAT instruments.

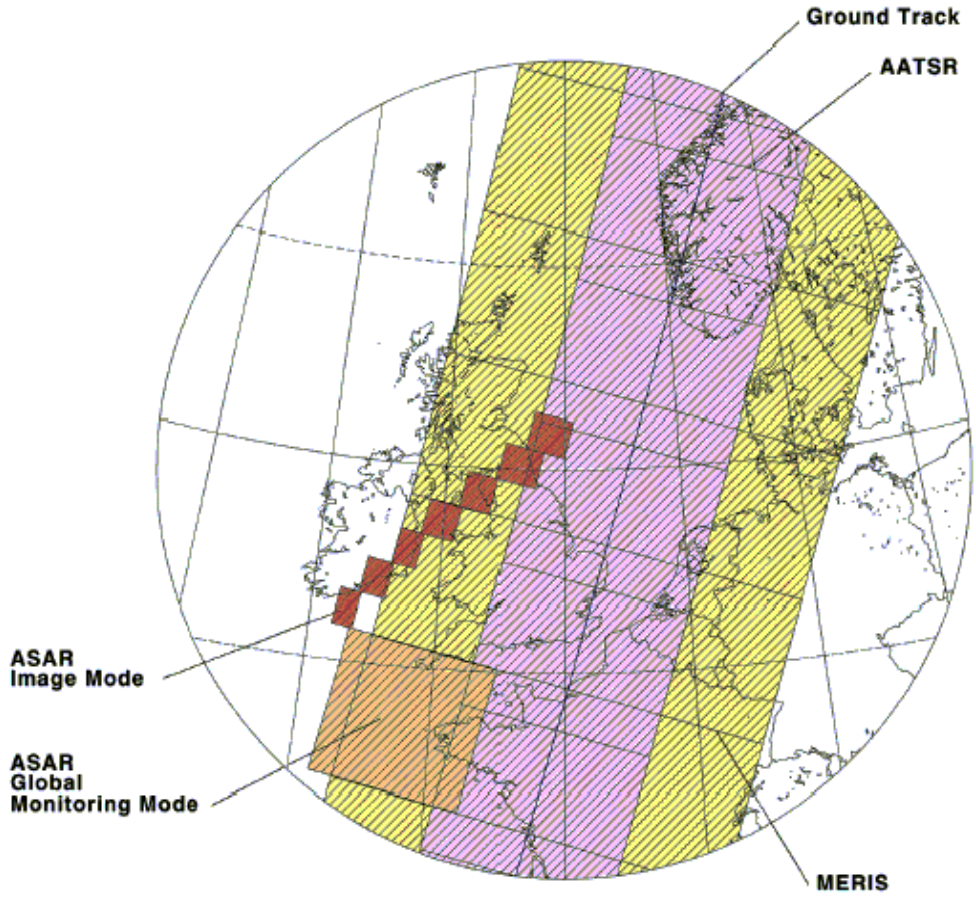

Fig. 3.19. Comparative simultaneous coverage of ASAR Image (red), Wide Swath - Global (orange), AATSR (violet) and MERIS (yellow).

The ENVISAT Swath and Orbit Visualisation (ESOV) software provides visualisation of the ENVISAT orbits, instrument swaths and ground station visibility. It is a free tool available to any user involved in ENVISAT data acquisition planning.

Dual Polarisation

ASAR provides dual-channel data. In Alternating ***Polarisation*** Mode (AP Mode), it provides one of three different channel combinations as VV and HH; HH and HV; VV and VH respectively.

For many vegetation studies, the use of different polarisations, in particular cross polarisation, will improve the discrimination between vegetation (volume scattering) and soil (surface scattering). In the case of forestry, the use of cross polarisation will improve the forest/non-forest discrimination and the retrieval of low biomass values (forest regeneration, regrowth, and plantation).

SAR Signal

The sequence of received pulses are arranged in a two-dimensional format, with dimensions of range and ***azimuth***, to form the SAR signal. The signal is typically described by the considering the signal received from a single scatterer on the ground, or point target. In this case, at each azimuth position, a single pulse echo from the point target is received. The delay of the received pulse depends on the distance from the radar to the target, and this distance varies as the spacecraft travels along the flight path. Also, pulses are received for as long as the target is illuminated by the antenna beam. This illumination time determines the azimuth extent of the raw SAR signal from a point target, or ***synthetic aperture***. The changing range, synthetic aperture, and resulting SAR signal are illustrated in the following figure.

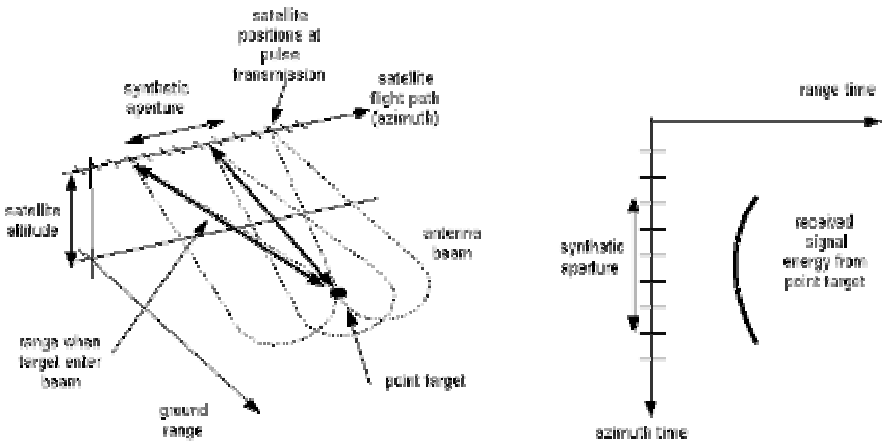

Fig. 3.20. ASAR signal

ASAR consists of a coherent, active phased array SAR (i.e., distributed transmitter and receiver elements) which is mounted with the long axis of the antenna aligned with the satellite's flight direction (i.e., Y-axis). The SAR antenna with its two-dimensional beam pattern images a strip of ground to the right side of the flight path which has potentially unlimited content in the direction of motion (i.e., the azimuth direction) but is bounded in the orthogonal direction (i.e., the range direction) by the antenna elevation beamwidth. The objective of the SAR system is to produce a two-dimensional representation of the scene reflectivity at high resolution, with axes defined in the range and azimuth direction.

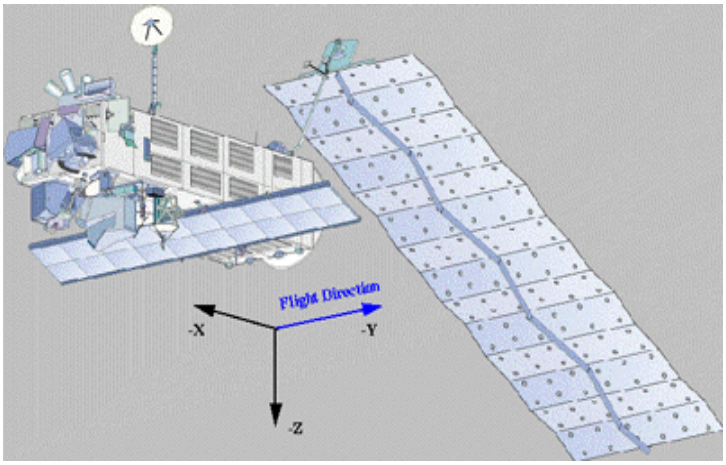

Fig. 3.21. SAR flight direction (i.e. Y-axis)

Instrument

The ASAR, operated at C-band (5.331 GHz), can be regarded as an advanced version of the SAR flying on ERS-1/2. It can be operated continuously for 30 minutes in a high-resolution mode for each orbit. Its application covers observations of land and sea characteristics under all weather conditions.

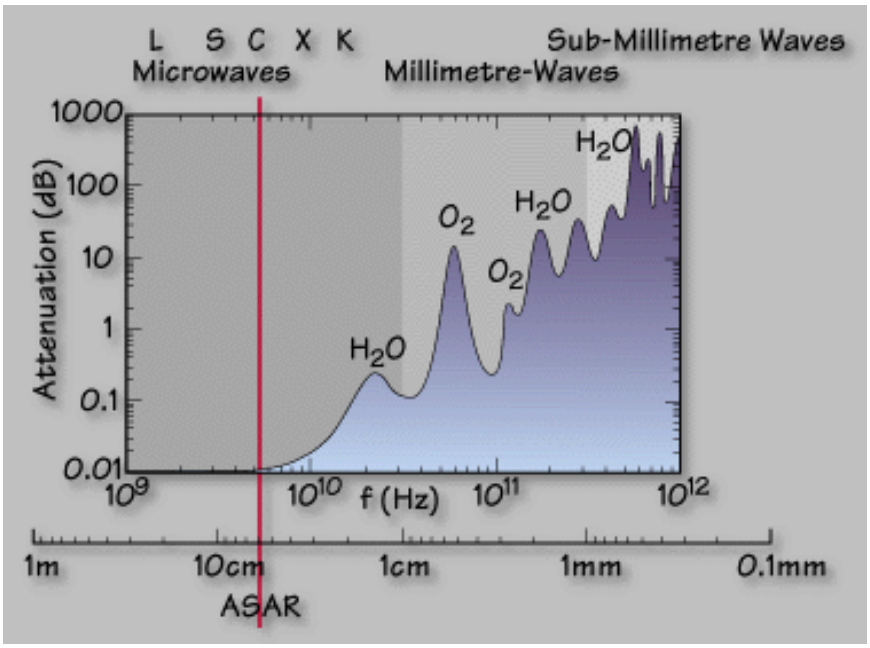

Fig. 3.22. The ASAR operation

The ASAR, operated at C-band (5.331 GHz)

In order to provide the possibility to adapt to various observing requirements, ASAR incorporates the capabilities to steer the beam to image different swath positions. Additionally, imaging can be performed in horizontal and vertical polarization. These features provided by the active array antenna requires a dedicated calibration scheme. The table summarizes the ASAR capabilities.

Table. 3.2. ASAR capabilities

Instrument Parameters	Image Mode	Alternating Polarisation	Wide Swath	Global Monitoring	Wave Mode
Swath width	up to 100 km	up to 100 km	> 400 km	> 400 km	5 km vignette
Operation time	up to 30 min per orbit			rest of orbit	
Data Rate	up to 100 Mbit/s			0.9 Mbit/s	
Power	1365 W	1395 W	1200 W	713 W	647 W

The use of the ASAR generic processor for near real time and off-line processing in the processing and archiving centres (PACs) and national stations offering ESA services is a simplification for processing and product validation. This allows full product compatibility between the different processing centres.

Operations

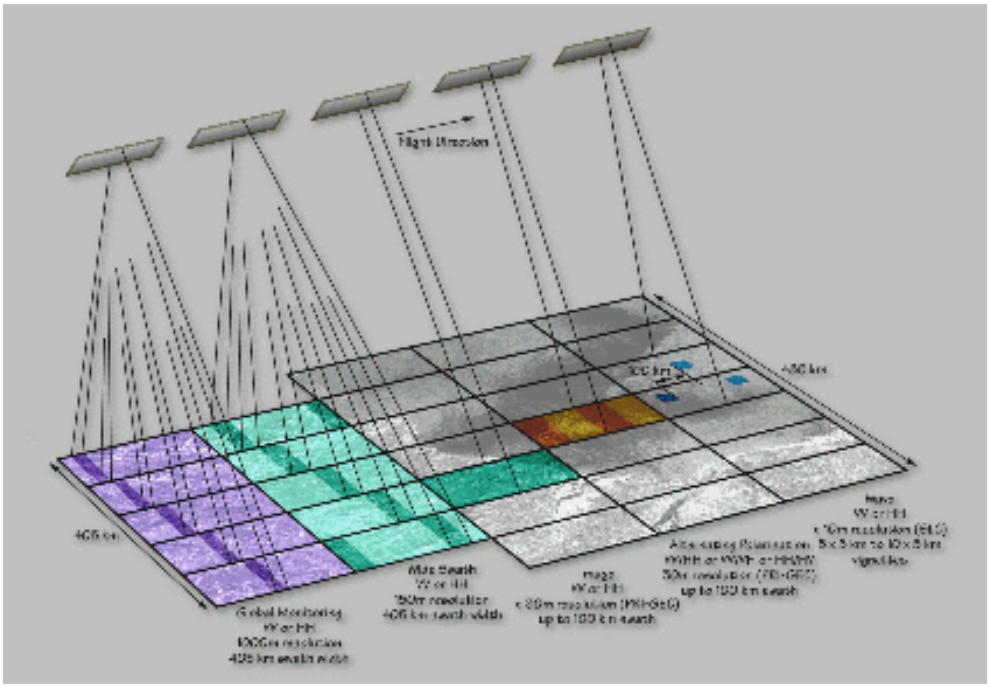

Fig. 3.23. Modes of ASAR operation

Global Monitoring Mode (GM)

The Global Monitoring Mode provides low resolution images (1 km) using ScanSAR technique over a 405 km swath at HH or VV polarisation. The mode has a low data data rate due to a slightly reduced along-track duty ratio and the use of digital filtering for reduction in the across-track direction. The same subswaths as defined for the Wide Swath Mode are used.

Wave Mode (WM)

In Wave Mode, the ASAR instrument, measures changes in backscatter from the sea surface due to ocean wave action. Therefore it generates vignettes, minimum size of 5 km x 5 km, similar to ERS AMI wave mode, spaced 100 km along-track in HH or VV polarization. The position of the wave vignette across track being selected as either

constant or alternating between two across-track positions over the full swath range.

Examples of simulated ASAR wave mode spectra:

- Simulated ASAR cross-spectra versus buoy measurements
- Comparison of real part of ERS and ASAR - Respective spectra
- Comparison of complete ERS and ASAR - Cross spectra
- Comparison of complete ERS and ASAR - Wave mode spectra

Image Mode (IM)

In Image Mode the ASAR generates high spatial resolution products (30 m) similar to the ERS SAR. It images one of the seven swaths located over a range of incidence angles spanning from 15 to 45 degrees in HH or VV polarisation.
In the table below the range of the values is due to the different orbit positions. The values are given for Level 1b products.

Table. 3.3. ASAR image swath geometry

ASAR swath	Swath width [km]	Near- range incidence angle	Far- range incidence angle
IS1	108.4 - 109.0	14.1 - 14.4	22.2 - 22.3
IS2	107.1 - 107.7	18.4 - 18.7	26.1 - 26.2
IS3	83.9 - 84.3	25.6 - 25.9	31.1 - 31.3
IS4	90.1 - 90.6	30.6 - 30.9	36.1 - 36.2
IS5	65.7 - 66.0	35.5 - 35.8	39.2 - 39.4
IS6	72.3 - 72.7	38.8 - 39.1	42.6 - 42.8
IS7	57.8 - 58.0	42.2 - 42.6	45.1 - 45.3

Alternating Polarization Mode (AP)

Alternating Polarization Mode provides high resolution products in any swath as

in Image Mode but with polarisation changing from subaperture to subaperture within the synthetic aperture. Effectively a ScanSAR technique is used but without varying the subswath. The results are in two images of the same scene in different polarisations combination (HH/VV or HH/HV or VV/VH) with appoximately 30 m resolution (except IS1). Radiometric resolution is reduced compared to Image Mode.

Wide Swath Mode (WS)

In the Wide Swath Mode the ScanSAR technique is used providing images of a wider strip (405 km) with medium resolution (150 m) in HH or VV polarization. The total swath consists of five subswaths and the ASAR transmits bursts of pulses to each of the subswaths in turn in such a way that a continuous along-track image is build up for each subswath.

Space Segment

The major driver for the Polar Platform/Envisat satellite configuration has been the need to maximise the payload instrument mounting area and to meet the viewing requirements within the constraints of the Ariane 5 fairing and interfaces. Additionally, the configuration also has been driven by the reuse of the SPOT Mk II service module concept and the ERS payload accommodation experience (concept of instrument electronics in an internal enclosure with externally mounted antennas).

In flight, the major spacecraft longitudinal axis (the Xs-axis) is normal to the orbit plane, the Ys-axis is closely aligned to the velocity vector and the Zs-axis is Earth pointing. This configuration concept provides a large, modular, Earth-facing mounting surface for payload instruments and an anti-sun face for radiative coolers, free of occultation by satellite subsystem equipment.

Fig. 3.24. The EnviSat satellite

Ground Segment

The Envisat ground segment provides the means and resources to manage and control the mission, to receive and process the data produced by the instruments, and to disseminate and archive the generated products. Furthermore, it provides a single interface to the users to allow optimum utilization of the system resources in line with the user needs. The ground segment can be split into two major elements:

- which is responsible for the command and control of the satellite;
- the payload data segment (PDS), which is responsible for the exploitation of the instrument data.

CHAPTER- 4

STUDY AREA

4.1. General

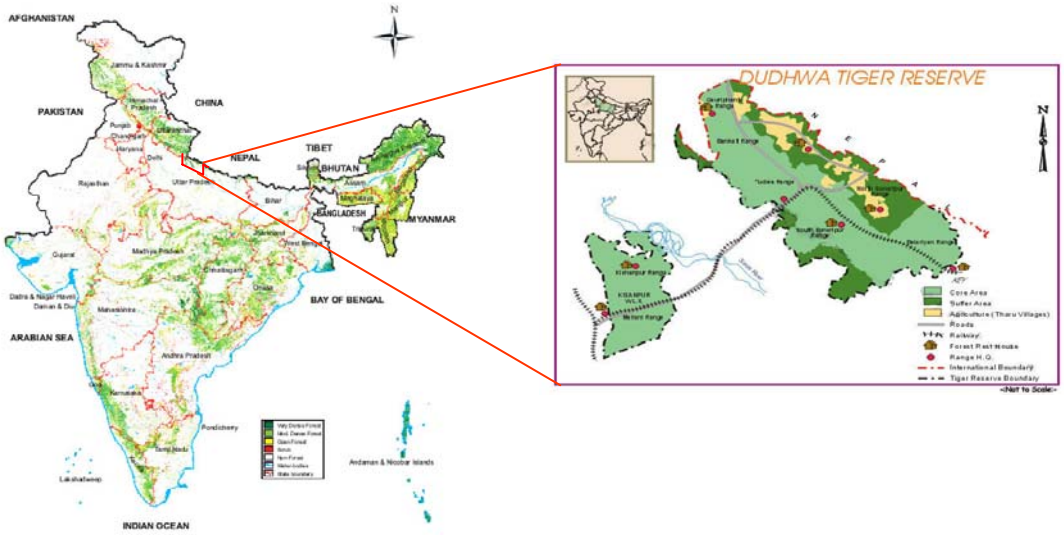

Fig. 4.1. The study area (Source: FSI)

The Dudwa Tiger Reserve comprises of the Dudwa National Park and the Kishanpur Wild life Sanctuary. The Park is located on the Indo-Nepal border in the Nighasen Tehsil of district Lakhimpur-Kheri and lies between 28º18'- 28º42' N and 80º 28'- 80º57' E. The total area of the Park is 68110.58 ha. Reserved forest area of 6974.06 ha serves as its northern and southern buffer inhabited by the Tharu tribal. The areas, which constitute the Dudwa National Park and its buffer, were once part of North Kheri Forest Division. The State Government declared its intent to create a National Park by a notification in the official gazette in October 1975 and established on February 1, 1977.

The two protected Areas constituting the Tiger Reserve, though separated physically, are by themselves compact and consist of continuous forest tracts. These represents one of the few remaining examples of a highly diverse and productive terai ecosystem, supporting a large number of endangered species, obligate species of tall wet

grasslands and species of restricted distribution.

The Reserve is presently accessible by rail and road. The Dudwa branch-line of the North-east Railways links Dudwa/Palia with Lucknow, Barielly and Gonda. The Dudwa Railway Station is in the heart of the Park about 4km from the tourist complex at Dudwa. By road Dudwa can be accessed from Lucknow via Sitapur-Lakhimpur-Gola-Khutar-Mailani-Bhira-Palia-Dudwa. There are regular bus services, both private and Government owned, from Palia and Lakhimpur to various parts of the State.

4.2. Terrain

In general the area of the Park is a vast alluvial plain scoured with the channels of numerous water courses large and small. There are no prominent eminences, the only irregularities on the surface being formed by the river bed and their high banks. This has resulted in the formation of a series of fairly elevated plateaus separated by steams flowing from northwest to south-east and each border by low alluvial belts of varying width. The general slope of the area is from northwest to southeast. The altitude above m.s.l. ranges from 182 m. in the extreme north to 150 m. in the farthest southeast.

4.3. Geology and Soil

The area of the Park is a vast alluvial plain, the daob of the Mohana and Suheli rivers. The under-lying soil consists of the alluvial formation the Gangetic Plains, showing a succession of beds of sand and loam. These vary in thickness and depth according to the configuration of the ground. The subsoil at depths of 12m to 21m, a layer of hard clay with narrow single beds.

The surface soil is sandy in the more elevated portions and along the high banks of the rivers, loamy in the level uplands and clayey in the depressions.

1. Low Alluvium-
   i. Pure Sand- This is infact the bed of the Sarda and the Ull rivers and is generally under water during the rains.
   ii. Recent loamy sand- The sand is much coarse and shallower than that found in the

high alluvium. The subsoil is micaceous. At times small boulders of quartzite, gneiss and other Himalayan rocks are found embedded in the sand of 3-4.5m. This type of soil is found in portions of Sarda block.

2. High and Middle Alluvium-

i. A rich loamy sand with a variable proportion of clay. This supports the best forests and is found in the Sal areas. The soil has a fair amount of humus.

ii. A moist sandy loam mixed with a fair amount of decaying vegetable matter is met with in depressions and watercourses covered with grasses. The depth of this soil varies from 0.6 to 0.9m.It is usually quite stiff when dry. Due to prolonged submergence it usually does not support tree growth but in areas where its thickness has increased due to deposition of silt from adjoining high grounds, it supports a good crop of Sal and Terminalia spp.

iii. A micaceous sand with little or no clay and marked by an almost complete absence of humus is the typical soil of the Sal chanders. It is exceedingly poor, containing particles of manganese dioxide, which bind it and render it stiff and hard during the greater part of the year.

iv. A stiff clay with a large amount of decayed and partly decayed vegetative matter is the soil type found in the lower parts of the Ull river. This type of soil is characterized by extremely poor aeration of the surface soil and water logging conditions. The depth of the soil varies from a few cm. in the chandars to about 2.4 m elsewhere. In most of the areas the soil varies from 1.2 to 2.4m in depth. The portion rich in humus never exceed 0.9 m. and are usually limited 0.3 to 0.6m under trees and only a few cm under grassy patches.

4.4. Climate

There are three distinct seasons approximately as cold weather which commences from mid- October to mid- March (days are bright, cool and the nights are cold and foggy). January is the coldest with mean maximum temperature of 22.2ºC (72ºF) and mean daily minimum temperature of 9.1ºC (48.4ºF). Hot weather commences from mid-

March to mid- June where May and June are the hottest with the maximum temperature ranging between 40º- 45ºC (104ºF to 113ºF). Rainy season starts from mid- June to mid-October (the total annual rainfall being 150 cm.) and the prevalent winds are westerly, gatherings in strength with the onset of summer. Hot winds (loo) blow very strongly from the middle of the April up to the end of May. These are then replaced by easterly winds, which are prevalent during the rainy season. Northern winds also occur during the month of June. Storms are rare. The temperature ranges between a minimum of 9.1ºC (average) in winter to maximum of up to 40-45º C in the peak summer. Temperatures as low as 2.8ºC and as high as 45ºC have been recorded. Records of temperature have not been maintained in the Reserve.

4.5. Water Resources

The Reserve is bestowed with a number of perennial water sources. The Suheli and Mohana rivers, Johara, Nakua, and Newra nalas (streams), are the major rivers and streams of the Park. In all twenty rivers and streams are associated with the Reserve. The Suheli and Mohana river flow roughly along the southern northern boundaries of the Park. There are also a large number of large of perennial *taals* or lakes such as the bankeys, Kakraha, Chedia, Puraina, Bhandara, Chapra, Amaha, Bhadi, Mutna, Churaila, Ludaria, Khajua, Chaitua, Dhanghari, Bhadraula, Teria etc. located variously in the Park. These contribute significantly in making the habitat of the Park unique. Many areas have depressions that rainwater for some time after monsoon and provide drinking water to wild animals.

4.6. Forest/ Vegetation

The rich fertile Indo- Gangetic plains support a luxuriant growth of forest which offers a combination of gldes and natural perennial lakes and provides a unique habitat for animals. According to Champion and Seth's (1968), following forest types exist in the area:

1. Northern Tropical Semi- Evergreen Forest (Sub- Group 2B)

This forest Sub- Group comes under Group 2 which includes forest tree species like *Mallotus phillipensis*, *Syzygium cumini*, *Ficus racemosa*, *Ehtretia laevis, Trewia nudiflora, Schleichera oleosa*.

2. North Indian Moist Deciduous Forest (Sub- Group 3C)

This forest Sub- Group comes under Group 3 which includes five types of forest as- Sal forests which includes tree species like *Shorea robusta*, *Mallotus phillipensis*, *Syzygium cumini*, *Terminalia alata*, *Ehtretia laevis*. The same composition is again characterized by another forest type as Sal Mixed Forests. The third type is called as Moist Mixed Deciduous Forest comprising of tree species like *Mallotus phillipensis*, *Syzygium cumini*, *Ficus racemosa*, *Ehtretia laevis, Trewia nudiflora, Schleichera oleosa, Dalbergia sissoo*. The fourth forest type is Upland Grassland comprising of *Imperate cylindrica*, *Saccharum spontaneum*, *Sancharum munja*, *Desmostachya bipinnata* and Lowland Grassland which comprises tree species like *Phraginites karka, Saccharum narenga*, *Sclerostachya fusca* , *Desmostachya bipinnata*.

3. Tropical Seasonal Swamp forests (Sub- Group 4D)

There are two types of forests which comes under this Sub- Group 4D as *Barringtonia* Swamp Forest which includes tree species like *Mallotus phillipensis*, *Barringtonia acutangula,, Ficus racemosa*. The other forest type is *Syzygium* Swamp Low Forests which includes tree species like *Mallotus phillipensis*, *Syzygium cumini*, *Trewia nudiflora* etc.

4. North Indian Dry Deciduous Forest (Sub- Group 5B)

This forest Sub- Group 5B comes under Group 5 consisting of Khair- Sissoo Forest which includes tree species like *Acacia catechu*, *Dalbergia sissoo*, *Bombax ceiba, Adina cordifolia*.

4.7. Fauna

The Reserve has a vast and varied heritage of fauna having a unique in diversity. The Dudwa Tiger Reserve is the only place in the country to hold a potentially viable population of the nominate sub-species of the swamp deer –*Cervus duvauceli duvauceli.* Of the seven species of deer found in the country, five occur in the Reserve. It is also home to a sizable tiger population. Some critically endangered species such as the Bengal florican (*Hubaropsis bengalensis)* and hispid hare (*Caprolagus hispidus)* find a home here. Dudwa is also the place where the Great Indian One-Horned Rhinoceros has been successfully reintroduced. Thirteen species of mammals, nine species of birds, and eleven species of reptiles and amphibians found here are considered to be endangered and are listed in Schedule-1 of the Wild life (Protection) Act.

It was only during 1980s that the Terai Conservation Area (TCA) attracted attention to many researchers with special reference to selected featured faunal species. Prominent among them are- the ecology of swamp deer (Singh, 1984; Qureshi *et al.*, 1991); rhino habitat and monitoring of reintroduced rhinos (Sale and Singh, 1987; Sinha and Sawarkar, 1991); ecology of Bengal florican (Rahmani *et al.*, 1990; Sankaran and Rahmani, 1991); study on bird diversity (Javed, 1996) and ecology of Black necked stork (Maheshwaran, 1998).

4.8. Block

The Dudwa National Park consists of 27 Blocks (Anonymous, 2001) viz., Tribal habitations, Kiratpur Block, Sumerpur Block, Belghat Block, Laudaria Block, Nagrah Block, Mohrania Block, Gulra Block, Chandpara Block, Sarota Block, Lauki Block, Maholi Block, Kakraha Block, Barbatta Block, Sohna Block, Rehta Block, Sathiana Block, Badruala Block, Phersia Block, Dignia Block, Mahadeva Block, Chotta Palia Block, Amargarh Block, Masankhamb Block, Pachperi Block, Badhi Block and Tehri Block respectively.

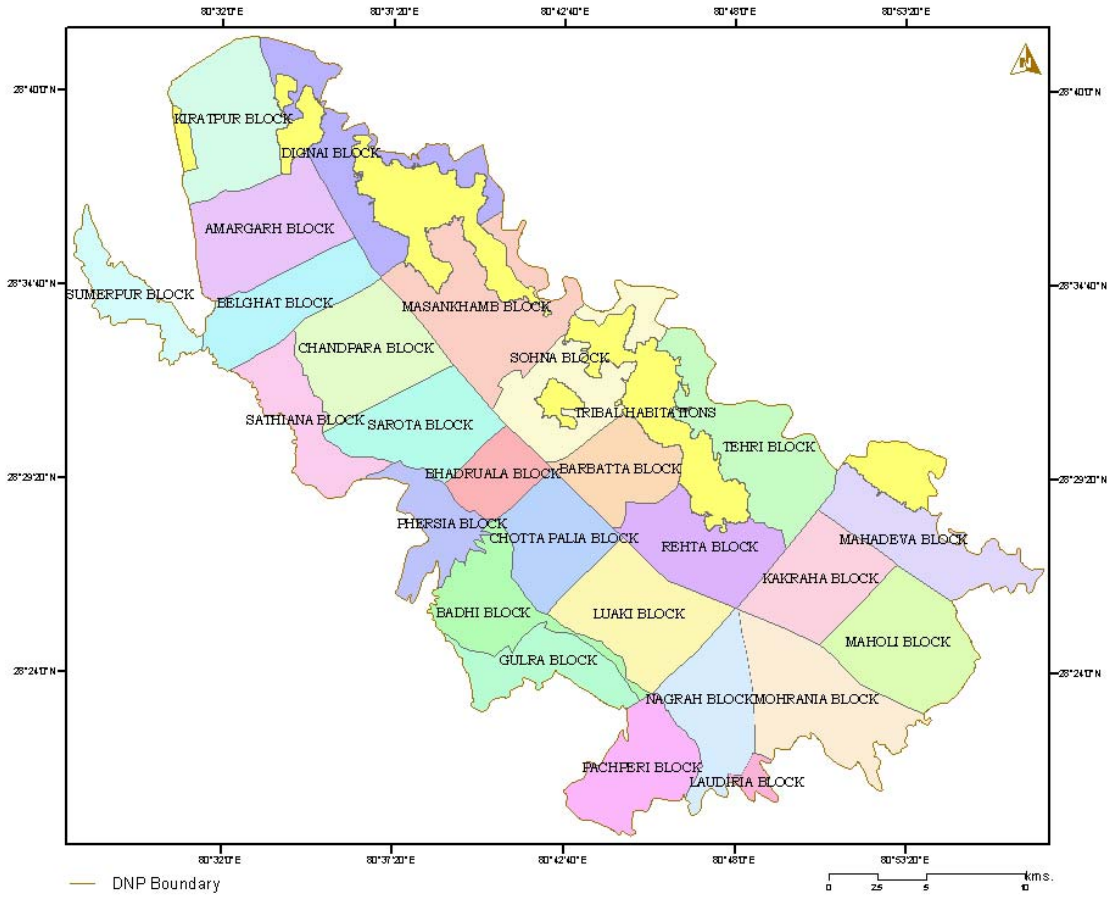

Fig. 4.2. Block map of DNP

Table. 4.1. Block level distribution of DNP

Block	Area in ha	Area (km^2)	%
Tribal Habitations	6974.06	69.74	10.24
Kiratpur Block	2913.29	29.13	4.28
Sumerpur Block	1332.05	13.32	1.96
Belghat Block	2244.45	22.44	3.30
Laudiria Block	260.27	2.60	0.38
Nagrah Block	2373.43	23.73	3.48
Mohrania Block	3442.75	34.43	5.05
Gulra Block	1754.79	17.55	2.58
Chandpara Block	2997.22	29.97	4.40
Sarota Block	2462.44	24.62	3.62
Luaki Block	3051.51	30.52	4.48
Maholi Block	3047.35	30.47	4.47
Kakraha Block	2392.91	23.93	3.51
Barbatta Block	1821.94	18.22	2.67
Sohna Block	2587.65	25.88	3.80
Rehta Block	2432.18	24.32	3.57
Sathiana Block	1806.92	18.07	2.65
Bhadruala Block	1215.24	12.15	1.78
Phersia Block	1481.44	14.81	2.18
Dignai Block	2608.28	26.08	3.83
Mahadeva Block	2466.29	24.66	3.62
Chotta Palia Block	2125.17	21.25	3.12
Amargarh Block	3075.76	30.76	4.52
Masankhamb Block	3664.67	36.65	5.38
Pachperi Block	2253.77	22.54	3.31
Badhi Block	2117.32	21.17	3.11
Tehri Block	3207.43	32.07	4.71
Total	68110.58	681.11	100.00

4.9. Problems of the study area

The rich fertile Indo- Gangetic plain, once rich in flora and fauna in the past has suffered a lot in the recent times due to human interference. Realising the importance of protection of wildlife, Dudwa National Park was notified and established on February 1, 1977.

a) Biotic Pressure

The park is completely surrounded by habitation. The northern and north- western boundary of the park is along the Indo- Nepal international border. The forest on the Nepal side has been cleared for the settlement of people. This has not only resulted in the elimination of buffer along the entire 70 kms. Length of the international borders but has

also increased pressure of the Nepalese citizen entering the park for timber, fuelwood and fodder.

There are three major road and rail networks passing through the park in the core zone. The Dudwa- Gauriphanta, Dudwa- Chandan Chowki road passes through the core zone. The road network disturbed 16% of the park. Thus, serving as a network for indulge in illegal activities such as smuggling across the international border and illegal removal fuelwood, fodder and thatch grasses from within the park boundaries.

b) Forest fire

The rail and road traffic several forests fire each year mostly due to the negligence of travelers. The extend of loss with respect to flora and fauna due to forests fire is high. Detection, extend and intensity of damage due to forest fire in almost real- time using satellite data is possible (especially MODIS and microwave data).

c) Human settlements within park

There are 37 Tharu villages occupying the buffer of the park. These are revenue villages. The 3747 family households adding upto approximately 23,000 individuals having about 18,000 cattle herds depend to a large extend on the park and its buffer for their requirement of fuel, fodder, food, small timber and thatch grass. The increasing human and cattle population has increased the biotic pressure not only on the buffer zone but only core zone as well.

d) Seasonal Flood

On the Suheli river, 2.5 km down stream from the park boundary, a barrage has been built by the State Irrigation Department ostensibly to provide irrigation facilities to 17,000 ha (approx.) of agricultural land. However, since its inception it has been irrigated only 345 ha per annum. The barrage has resulted in siltation of the river which in turn, has adverse effect on the plant community, especially on grassland and Khair- Shisham forest. In some areas, ecological profile has changed from grassland to marsh land and vice- versa. While, in others several species of trees including Sal and Shisham have started drying up due to long water- logging.

CHAPTER- 5

MATERIALS AND METHODS

Materials

The methodology consists of geo-spatial analysis of database generated from the satellite images, ancillary database and information collected from the field.

The study was completed using data from various sources as under:

A) Remote Sensing data

Table. 5.1. Remote sensing data

Data used	Path/ Row	Spatial Resolution (m)	Spectral Resolution (µm)	Band	Swath (Km)	Date of Acquisition
Landsat ETM	144/ 40	30	Band 1: 0.450- 0.515	Blue	185	09 Nov 1999
			Band 2: 0.525- 0.605	Green		
			Band 3: 0.360- 0.690	Red		
			Band 4: 0.760- 0.900	Near IR		
			Band 5: 1.550- 1.750	Mid IR		
			Band 6: 10.40- 12.5	Thermal IR		
			Band 7: 2.080- 2.35	Mid IR		
EnviSat ASAR	144/ 40	25	Horizontal/ Horizontal	C-Band (5.3 GHz)	82	24 March 2005
			Horizontal/ Vertical	C-Band (5.3 GHz)		
ETM NDVI	144/ 40	30	Band 3: 0.360- 0.690	Red	185	09 Nov 1999
			Band 4: 0.760- 0.900	Near IR		

1. Landsat Satellite

The first Landsat satellite launched in July 1972. Of the sensors carried, the Multispectral Scanner (MSS) with 80 m pixels and four spectral bands was found to provide information of unforeseen value. In July 1982, the launch of Landsat 4 witnessed the inclusion of Thematic Mapper (TM) with 30 m resolution and 7 spectral bands.

The newest in this series is Landsat 7, launched on 15th April 1999, with new Enhanced Thematic Mapper (ETM+) sensor. This sensor has 7 spectral bands as TM but has an added Panchromatic band (15 m) and a higher resolution Thermal band of 60 m.

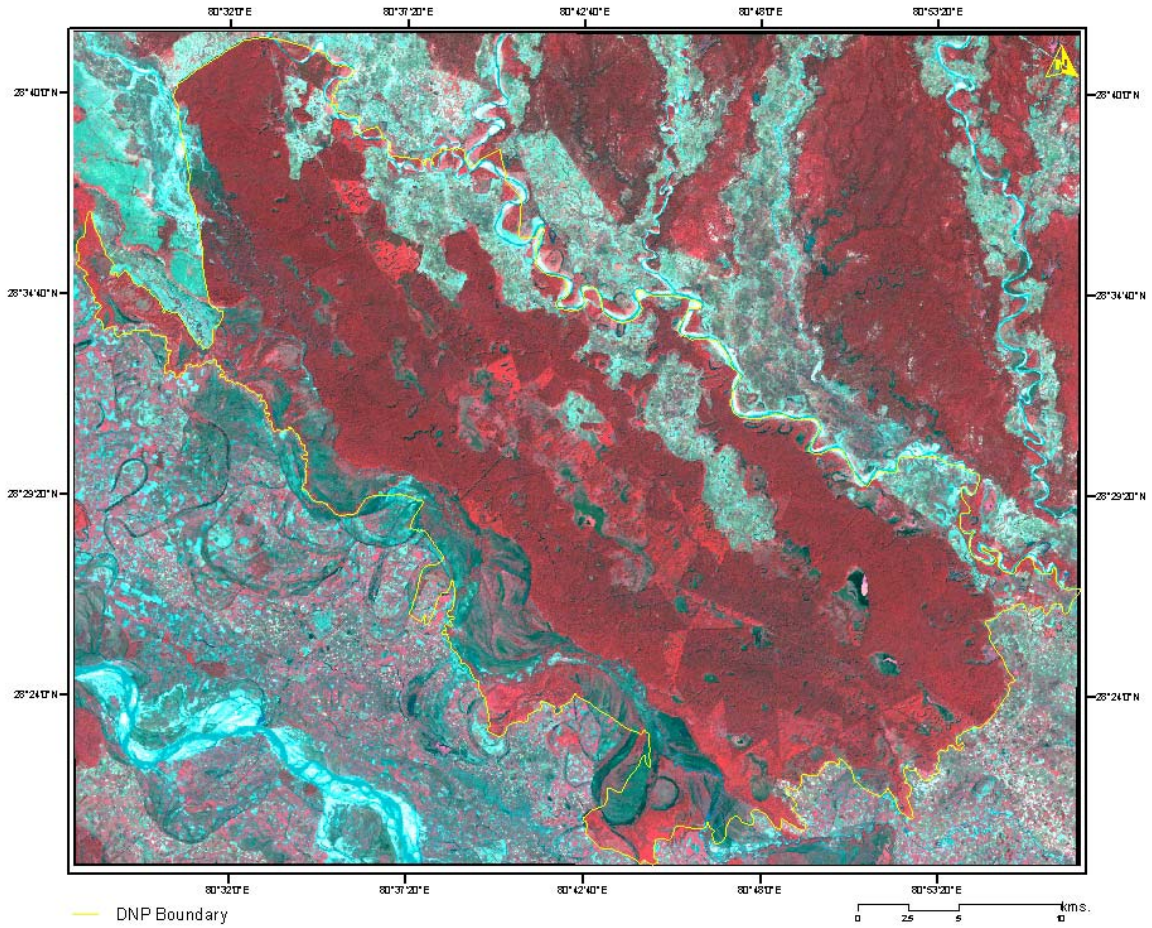

Fig: 5.1: Landsat ETM FCC (4R, 3G, 2B) of DNP

2. Environmental Satellite (EnviSat)

On February 28th, 2002 the European Space Agency (ESA) launched its European Environmental Satellite (EnviSat), which carries an Advanced Synthetic Aperture Radar System/ Sensor (ASAR) operated in C- band (5.3 GHz) wavelength. The ASAR on EnviSat features enhanced capability in terms of coverage, range of incidence angles, polarization and modes of operations. (Table. 5.2).

In this study, ASAR, C- band data acquired on 24th of March, 2005 in AP Mode (HH and HV polarizations) having a beam swath of IS - 3 i.e., an incidence angle of 25.8º to 31.2º is being used. It has the ground range of 82 Km. with ≈ 25m spatial resolution.

Table. 5.2. Characteristics of EnviSat-1 satellite and its ASAR sensor

System	EnviSat 1
Orbit Altitude	800 Kms., sun-synchronous, 10:00 a.m. crossing, 35 days repeat cycle
Orbit Inclination Angle	98.6 º
Sensor	ASAR (Advanced Synthetic Aperture Radar)
Ground Range Swath width [x]	56- 405 Kms.
Off- nadir viewing	Track 17º to 45º
Revisit time	35 days
Frequency	C- band, 5.331 GHz.
Polarization	HH/ HV/ VH/VV
Spatial Resolution	30 m
Calibration Accuracy	± 0.5 dB
Range Sampling rate [MHz]	19.21
Pulse repetition frequency [Hz] [x]	1709- 2067

[x] Dependent on the selected configuration

(Source: http://envisat.esa.int/handbooks/asar/toc.htm)

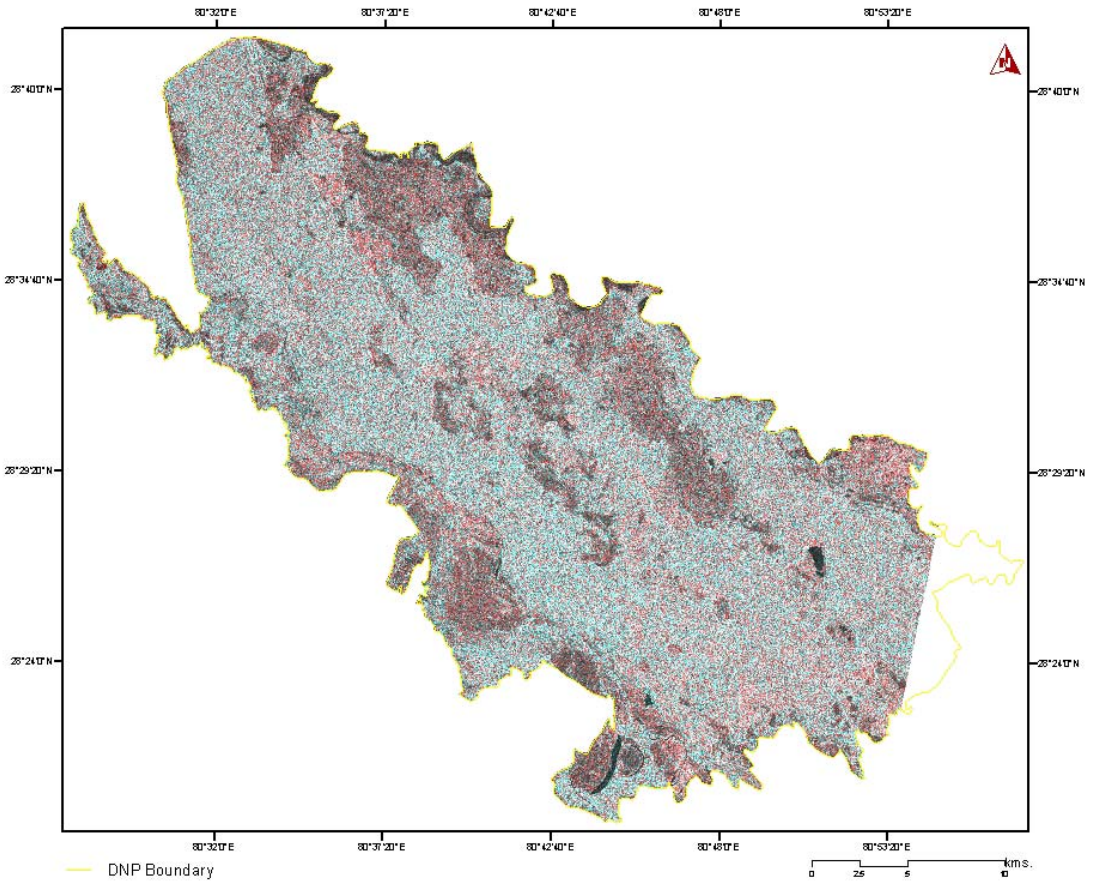

Fig: 5.2: ASAR FCC (HV R, HH G, HH B) of DNP

3. NDVI Image

NDVI is a band ratio calculated using (Infrared - Red) / Infrared + Red) (Rouse *et al*., 1973). It is highly correlated with vegetation parameters such as green leaf biomass and green leaf area and hence is of considerable value for vegetation segmentation (Curran and Franquin, 1980; Hatfield, 1983; Holben and Frasher, 1984; Jackson *et al*., 1983; Justice *et al*., 1985; Roy, 1993; Tucker *et al*., 1981). Moreover, it reduces variation due to surface topography (Holben and Frasher, 1984) and compensates for variation in radiance as a function of Sun elevation for different parts of the scene, which is highly valuable in continental studies.

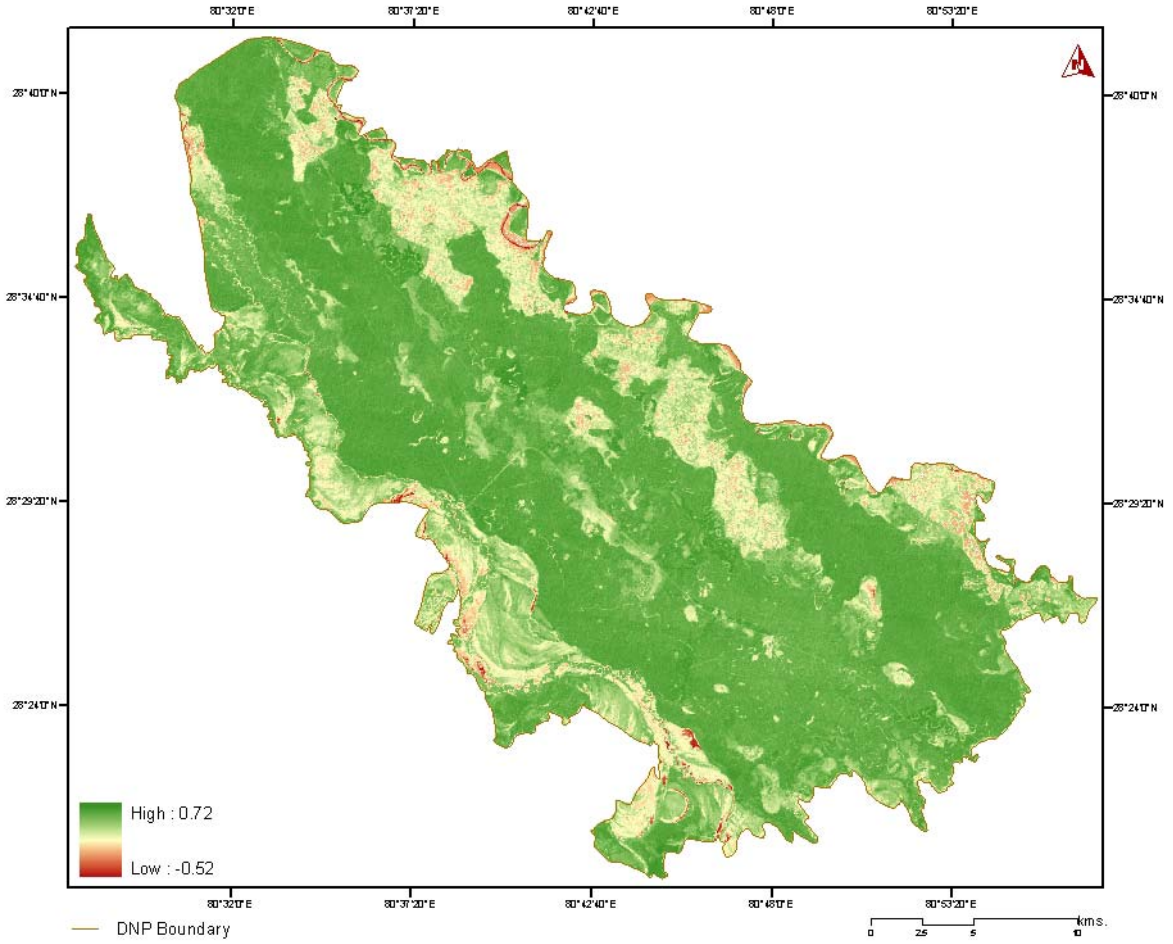

Fig: 5.3: NDVI image of DNP

B) Ancillary data

1. Topographic Sheet 62D (1: 50,000).
2. Dudwa National Park Management Plan.

C) Instruments used

1. Global Positioning System (GPS)
2. Rangers Compass
3. Camera
4. Relascop

5.2. Methods

It includes three main stages as under:

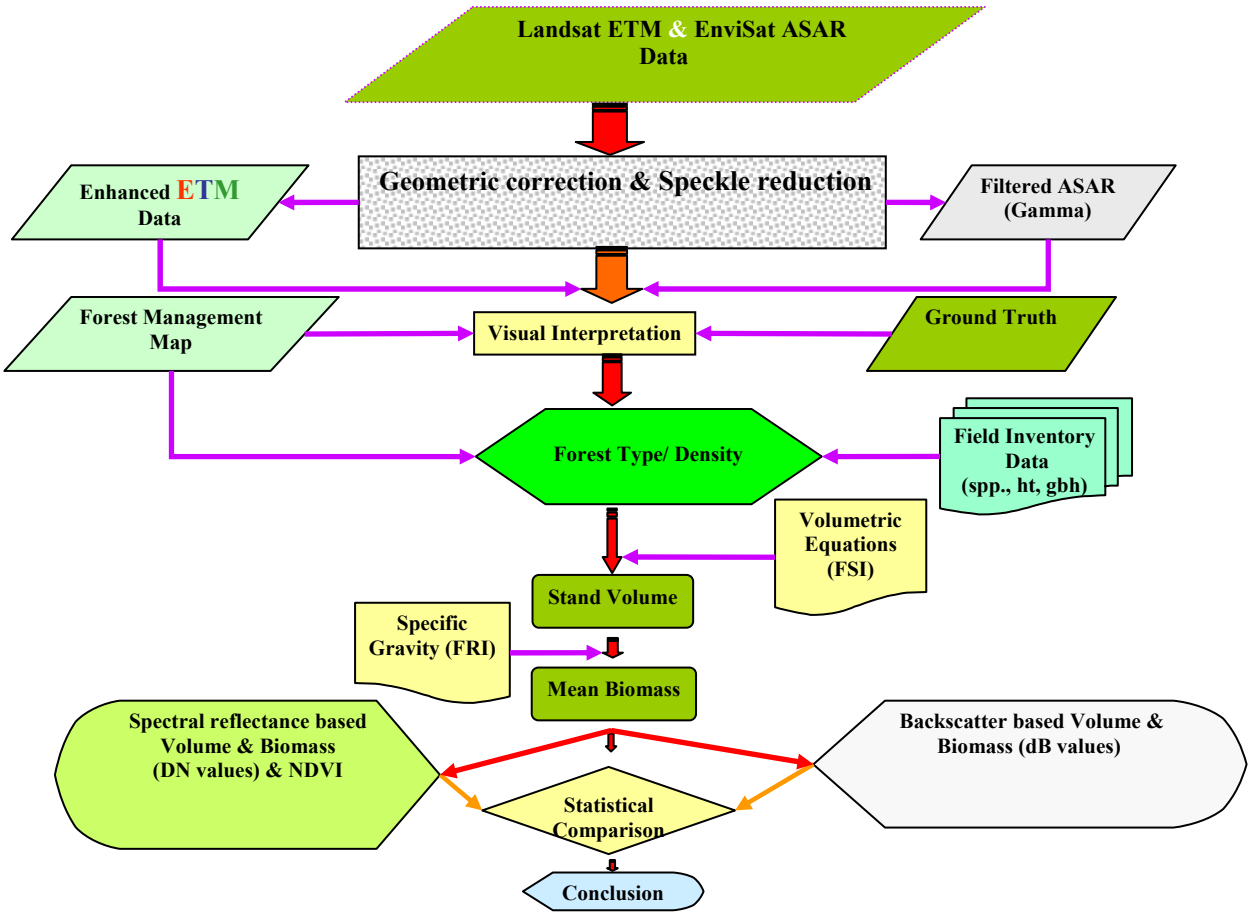

Fig. 5.4. Flowchart of Methodology

5.2.3. Image processing, speckle removal and preliminary interpretation

It is the foremost initiation part of the research comprising of the satellite data order, data pre- processing and creation of the base map for the reconnaissance survey of the study area.

The research/ study was felt the need of the hour for the protection/ conservation of the protected area in terms of the wildlife and its natural environments in support of the terai conservation area. The technology of remote sensing combined with Geographical Information System has led to the exploration of the natural forest of this belt in terms of the forest volume and dry aboveground biomass. This includes reviewing of literature related to the research theme and procurement of satellite data.

Pre- Processing of Image Data:

It involves processing of the image data for rectification, visualization and for interpretation of the satellite data. Different geo- processing softwares were employed for these purposes. There are two corrections:

Radiometric correction

It is the processing of satellite data to remove the undesirable influence of atmospheric interference and system noise. It addresses variations in the pixel intensities (Digital Numbers) that are not caused by the object or scene being scanned. This includes differing sensitivities or malfunctioning of the detectors, topographic effects and atmospheric effects.

Geometric correction

It addresses errors in the relative position of pixels. These errors are induced by sensor viewing geometry or terrain variations (Gautam, 2005). For this, Geo-referencing of the satellite data both ETM and ASAR were executed on the basis of the topographical map with uniformly distributed Ground Control Points (GCP s) in a sub- pixel accuracy followed by re-sampling in cubic- convolution domain. The datasets were then co-registered for further analysis.

Digital Processing of Radar ASAR Data

All radar images contain some degree of speckle, a grainy or salt-and-pepper pattern. Speckle arises from the coherent nature of radar waves, causing random constructive and destructive interferences and hence, random bright and dark areas in radar imagery. Speckle reduces the image quality and contrast. It can be reduced through image processing techniques but cannot be completely eliminated. The various filtering techniques includes as -

Speckle Filtering

Proposed first by Kuan, the Gamma MAP Filtering is used to remove the speckles from radar data. It smoothes the image data, without removing edges or sharp features in the image. To apply it, the *a priori* knowledge of the probability density function of the scene is required. The scene reflectivity is assumed to be Gaussian (normal) distributed. However, this is not quite realistic since it implicitly assumes a negative reflectivity. Lopes modified the Kuan MAP filter by assuming a gamma distributed scene and setting up two thresholds. Also First Order Statistics Filters (Standard deviation, Mean, Median and Variance filters) can also be employed. Median filter is especially recommended as it retains the original image feature boundaries in output image. (Figure. 5.5).

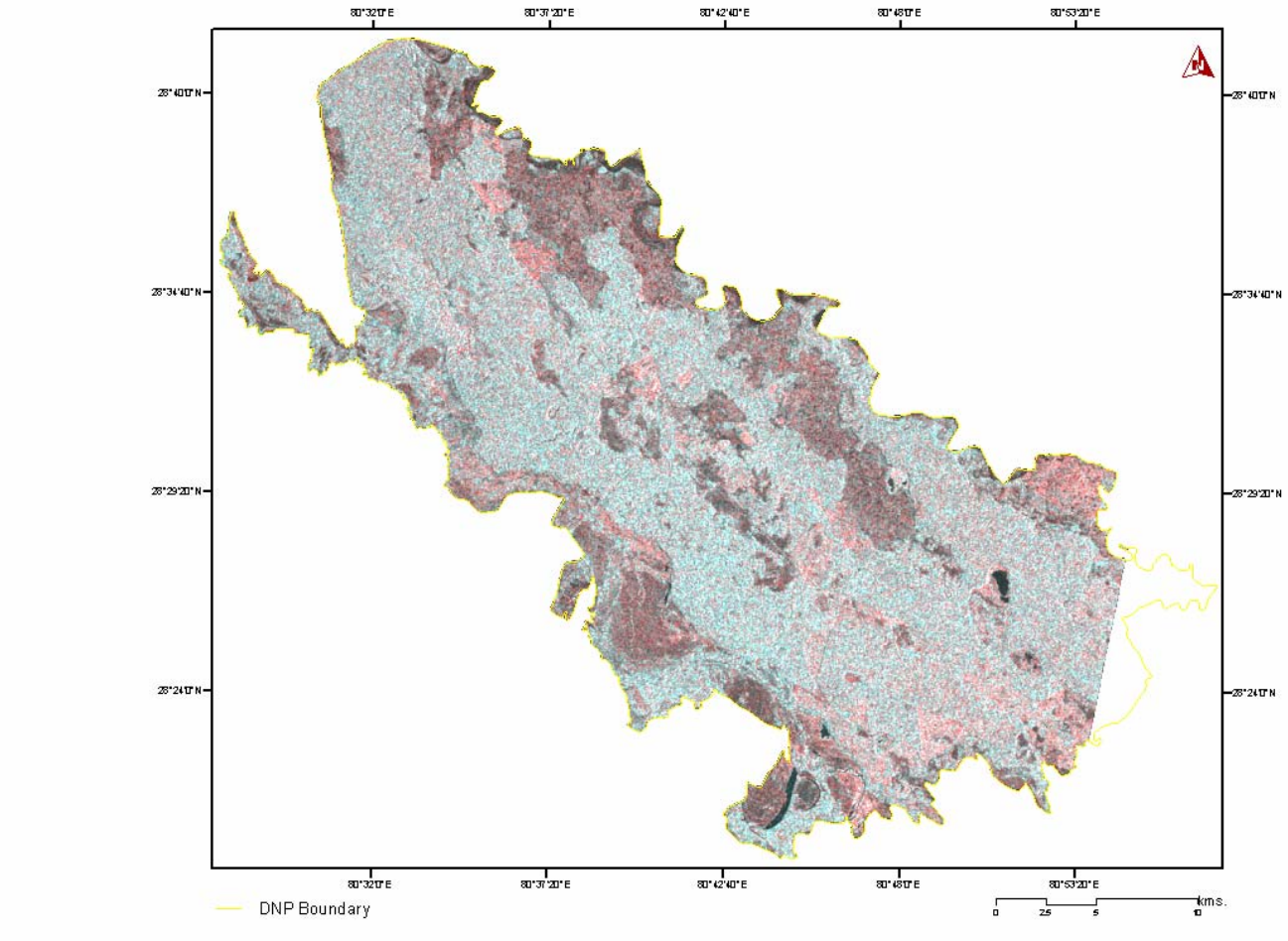

Fig: 5.5: Gamma Filtered ASAR FCC (HV R, HH G, HH B) of DNP

Estimation and retrieval of the Backscattering Coefficient

Using the filtered ASAR data, the backscattering co- efficient of the different classes/ forest were retrieved using the standard Radar Equations in a model. Thus, capturing of all the backscattered co-efficient of all the sample plot for each forest type classes.

To perform a precise absolute image calibration and derive the radar backscatter coefficient for objects a detailed knowledge of the local slope (i.e., local incident angle) in required. Since this information is usually not possible "flat terrain" is assumed during processing (based on the ellipsoid WGS84) and the final intensity image is therefore proportional to the radar brightness of the illuminated scene. The relationship between the value of the image pixels (DN) the radar brightness (***β °***) and the radar backscattering co-efficient (**σ °**) can be written as-

$$DN^2 = \text{constant}.\ \beta^{o} = \text{constant}.\ \sigma^{\circ} / \sin(\alpha) = \text{constant}(\alpha).\ \sigma^{\circ} \ldots\ldots\ldots\ldots\ldots 1$$

The constant factor is hereafter referred as "absolute calibration constant" (*K*) which is derived in the ASAR case from measurements over precision transponders. This factor is processor and product type dependent and might between different between different beams for same product type. The constant **(α)** term is equal to the absolute calibration constant divided by the sine of the local incidence angle **α**.

Finally the pixel Digital Numbers (DN) were converted to backscatter coefficient σ^{o} (herein called backscatter) via equation (2):

$$\sigma^{\circ} = 10 \log_{10} \frac{[\sum (DN)^2]}{n} + K \ldots\ldots\ldots\ldots\ldots\ldots 2$$

where DN^{2} = Pixel intensity value at image line and column " *i,j*", *n* is the number of pixels extracted from the images and *K* is the absolute calibration constant (Kuplich, 2000).

Raw data of the ENVISAT, ASAR precision image was imported by the ENVI image processing software. This raw image is basically the intensity image. From the intensity image the following quantities were calculated for C (3.8 – 7.5 cm.) frequency: the backscatter co- efficient – σ^{o}_{HH}, σ^{o}_{HV} (for HH, and HV polarization respectively.

iii) **GIS Environment**

Database creation is the operation of encoding the data and writing them into the database. Different geo- spatial software was used for the preparation of the entire database. This involves the following steps as:

In the vector data model, the world is represented as a mosaic of interconnecting **lines**, **points** and **arc** representing the locations and boundaries of geographical entities (Aronoff, 1989). **Lines** and **arcs** are a series of ordered points. The simple points, lines and polygons entities are essentially static representative of phenomena in terms of *X,Y* Co- ordinates and supposed to be unchanging and do not contain information about temporal and spatial variability (Burrough and McDonnell, 1998). In the present study, linear features such as forest block/ compartments were considered as a line feature whereas landuse/ cover map and boundary were considered as a polygon. The vector model is very useful for describing discrete features (Davis, 2001).

Topology is one of the most useful relationships maintained in many spatial databases. It is defined as the mathematics of connectivity or adjacency of points or lines that determines spatial relationships in GIS. It logically determines exactly how and where points and lines connect on a map. So, in order to remove the data redundancy and to maintain its spatial relationships, the steps of ***Clean*** and ***Built*** is very important.

***Sampling Intensity*:**

On the basis of the total area and the nature of the species composition in each forest type, it was feasible to perform the sampling intensity at 0.01 %.

Table. 5.3. Sampling intensity

Percent sampling	**0.10%**	**0.01%**
Area to be sampled (km.^{2})	0.6811	0.06811
Area to be sampled (m.^{2})	681100	68110
Size of Plot (m.^{2})	400	400
No of Plots	1702	170

Table. 5.4. Total number of plots at 0.01% intensity.

Class/ Density	**km.^{2}**	**No. of Plots**
Sal Forest (>60%)	83.59	20
Sal Forest (40-60%)	113.16	28
Sal Forest (<40%)	166.95	41
Sal Mixed Forest (>60%)	10.45	2
Sal Mixed Forest (40-60%)	22.80	5
Sal Mixed Forest (<40%)	2.93	1
Moist Mixed Deciduous Forest	24.04	6
Barringtonia Swamp Forest	11.27	3
Syzygium Swamp Low Forest	21.10	5
Khair-Sissoo Forest	7.19	2
Teak Plantation	1.85	1
Eucalyptus Plantation	6.14	1
Sissoo Plantation	4.98	1
Teak-Eucalyptus Plantation	5.95	1
Teak- Sissoo Plantation	0.29	1
Gulchaman Plantation	1.47	1
Tropical Semi- Evergreen Forest	7.13	2
Lowland Grassland	69.23	17
Upland Grassland	43.41	11
River	6.31	-
Waterbody	4.36	-
Openland	15.54	-
Agriculture	50.97	-
Total	**681.10**	-

Total No. of Plots to be measured = 150 at 0.01% Sampling intensity.

According to the vegetation type/ density classes so collected from the ground truth, the following number of sampling plots was enumerated.

Table. 5.5. Vegetation type/ density wise distribution of sample plots

S. No.	Vegetation Type/ Density	No. of Sample Plots	Size (m^2)
1	Dense Sal Forest (>60%)	66	400
2	Moderately Sal Forest (40-60%)	31	400
3	Open Sal Forest (<40%)	39	400
4	Dense Sal Mixed Forest (>60%)	20	400
5	Moderately Sal Mixed Forest (40-60%)	18	400
6	Open Sal Mixed Forest (<40%)	3	400
7	*Syzygium* Swamp Low Forest	18	400
8	*Eucalyptus* Plantation	12	400
9	Sissoo Plantation	9	400
10	Teak Plantation	22	400
11	Teak- Eucalyptus Plantation	8	400
12	Gulchaman Plantation	3	400
13	Khair- Sissoo Forest	3	400
14	Tropical Semi- Evergreen Forest	4	400
15	Mixed Moist Deciduous Forest	5	400
16	Lowland Grassland	11	1
17	Upland Grassland	11	1
	Total	283	

5.2.4. Reconnaissance survey and field inventory

Field work activities were carried out in the month of October 2005 and March 2006 to get the insight of the study area and obtain necessary information {(20×20 m^2) sample plots laid for species, height and girth at breast height (gbh)}.

i) ***Reconnaissance survey***

The reconnaissance survey was carried out in order to be familiar with the study area. The False Color Composite images of both ETM and ASAR hardcopies along with the GPS Receiver, Topographical and Park Management Maps were utilized for this purpose. The tonal and textural variations in both ETM and ASAR images were recorded with corresponding GPS reading in Geographic Spheroid and WGS- 84 Datum for classification purpose in the final preparation of the forest Type/ Density Maps.

The ground truth information was collected using the above mentioned equipments (viz., satellite images, topographical map, GPS receiver, Ranger Compass, Camera, Releiscope and Field Performa designed exclusively for this purpose. The image

elements were correlated with the ground realities that formed the basis for the development of image interpretation keys. Thus, based on the preliminary reconnaissance survey and visual interpretation of the satellite data, forest type and cover/ density were classified as under: (Table 5.6 and 5.7).

Table.5.6. Interpretation key for forest/ vegetation cover mapping using optical data

S. No.	Tone	Texture	Pattern	Physiography/ Location	Vegetation/ Land use Type	Prominent Species
A	Forest					
1	Light pink to green	Smooth	Regular	Along river, streams and wet depressions	Tropical Semi-Evergreen Forest	*Mallotus phillipensis*, *Syzygium cumini*, *Ficus racemosa*, *Ehtretia laevis, Trewia nudiflora, Schleichera oleosa*
2	Bright red to medium red	Smooth to medium	Irregular	Mostly on uplands and peripheral areas	Moist Mixed Deciduous Forest	*Mallotus phillipensis*, *Syzygium cumini*, *Ficus racemosa*, *Ehtretia laevis, Trewia nudiflora, Schleichera oleosa, Dalbergia sissoo*
3	Dark red	Smooth	Regular	Mainly on old alluvial plain and 'damar' (upland) areas	Dense Sal Forest (> 60%)	*Shorea robusta*, *Mallotus phillipensis*, *Syzygium cumini*, *Terminalia alata*, *Ehtretia laevis*
4	Dark to medium red	Smooth	Regular	Occurs on high/ low alluvial areas	Moderately Closed Sal Forest (40-60%)	*Shorea robusta*, *Mallotus phillipensis*, *Syzygium cumini*, *Terminalia alata*, *Miliusa velutina*
5	Medium to light red	Coarse	Regular	On alluvial areas	Open Sal Forest (< 40%)	*Shorea robusta*, *Mallotus phillipensis*, *Syzygium cumini*, *Miliusa velutina* with occasional gap plantations of *Tectona grandis*
6	Red to brown	Coarse	Irregular	On gentle slopes around grasslands	Dense Sal Mixed Forest (> 60%)	*Shorea robusta*, *Mallotus phillipensis*, *Syzygium cumini, Lagerstromia parviflora* with plantations of *Tectona grandis*
7	Light red with brownish tinge	Medium to coarse	Irregular	Along gentle slopes, rivers and grasslands	Moderately Closed Sal Mixed Forest (40- 60%)	*Shorea robusta*, *Mallotus phillipensis*, *Syzygium cumini, Lagerstromia parviflora* with plantations of *Tectona grandis*
8	Red with dark red tinge	Medium	Irregular	Along rivers and grasslands	Open Sal Mixed Forest (< 40%)	*Shorea robusta*, *Mallotus phillipensis*, *Syzygium cumini, Lagerstromia parviflora* with plantations of *Tectona grandis*
9	Dark green to bright red	Coarse to medium	Regular	Along perennial rivers on degraded areas	Tropical Seasonal Swamp forest 1.*Barringtonia* Swamp Forest	*Mallotus phillipensis*, *Barringtonia acutangula,, Ficus racemosa*
10	Bright red	Medium	Regular	Along perennial areas	Tropical Seasonal Swamp forest 2. *Syzygium cuminii* Swamp Low Forest	*Mallotus phillipensis*, *Syzygium cumini*, *Trewia nudiflora*
11	Dirty red	Coarse	Irregular	In lowland along	Khair- Sissoo	*Acacia catechu*, *Dalbergia sissoo*,

	to green			rivers and near habitations	(*Acacia catechu* and *Dalbergia sissoo*) Forest	*Bombax ceiba, Haldina cordifolia*
12	Pink to bright red	Smooth	Regular	Along roads	Plantation	*Tectona grandis*
13	Dark green to black	Smooth to Coarse	Regular	Along railway tracts	Plantation	*Eucalyptus hybrida*
14	Magenta to dark red	Smooth	Irregular	Along roads and tracts	Plantation	*Dalbergia sissoo*
15	Dirty pink	Coarse	Irregular	Along tracts, roads	Plantation	Gulchaman
16	Pink to medium red	Coarse	Irregular	Near the grassland	Plantation	*Tectona grandis- Eucalyptus hybrida*
17	Dirty pink to light green	Smooth	Regular	Near the lowland and roads	Plantation	*Tectona grandis- Dalbergia sissoo*
B	Moist Sal Savannah					
18	Dark green to dirty red	Medium	Irregular	Upland areas	Upland Grassland	*Imperate cylindrica*, *Saccharum spontaneum*, *Sancharum munja*, *Desmostachya bipinnata*
19	Bright green	Smooth	Regular	Lowland areas and along fresh alluvial of rivers	Low land Grassland	*Phraginites karka, Saccharum narenga*, *Sclerostachya fusca* , *Desmostachya bipinnata*
C	Wetlands					
20	Black	Smooth	Regular	Inside forest and roads	Waterbody	
21	Bright blue to black	Smooth	Regular	Natural course	River	
D	Non- Forest					
22	Cyan	Coarse	Irregular	Open areas	Openland	
23	Cyan to green	Coarse	Regular	Alluvial plains, croplands	Agriculture/ Tribal habitation	Sugarcane, Rabi crops (Wheat, Mustard)

Table. 5.7. Interpretation key for forest/ vegetation cover mapping using ASAR data

S. No.	Tone	Texture	Pattern	Physiography/ Location	Vegetation/ Land use Type	Prominent Species
A	Forest					
1	Dark tan	Coarse	Irregular	Along river, streams and wet depressions	Tropical Semi-Evergreen Forest	*Mallotus phillipensis*, *Syzygium cumini*, *Ficus racemosa*, *Ehtretia laevis, Trewia nudiflora, Schleichera oleosa*
2	Cyan with red and white tinge	Smooth to medium	Regular	Mainly on old alluvial plain and 'damar' (upland) areas	Dense Sal Forest (> 60%)	*Shorea robusta*, *Mallotus phillipensis*, *Syzygium cumini*, *Terminalia alata*, *Ehtretia laevis*
3	Red and white with cyan tinge	Medium	Irregular	Occurs on high/ low alluvial areas	Moderately Closed Sal Forest (40-	*Shorea robusta*, *Mallotus phillipensis*, *Syzygium cumini*, *Terminalia alata*, *Miliusa velutina*

					60%)	
4	Cyan with white tinge	Coarse	Irregular	On alluvial areas	Open Sal Forest (< 40%)	*Shorea robusta*, *Mallotus phillipensis*, *Syzygium cumini*, *Miliusa velutina* with occasional gap plantations of *Tectona grandis*
5	Cyan with white tinge	Smooth	Irregular	Along perennial areas	Tropical Seasonal Swamp forest *1. Syzygium cuminii* Swamp Low Forest	*Mallotus phillipensis*, *Syzygium cumini*, *Trewia nudiflora*
6	Bright red	Smooth	Regular	Along roads	Plantation	*Tectona grandis*
7	Brown with blue tinge	Smooth	Regular	Near Grassland	Plantation	*Eucalyptus hybrida*
8	Red with blue and white tinge	Smooth	Regular	Along roads and tracts	Plantation	*Dalbergia sissoo*
9	Dark brown	Coarse	Irregular	Roads	Plantation	Gulchaman
10	Red with white tinge	Coarse	Irregular	Near the grassland	Plantation	*Tectona grandis- Eucalyptus hybrida*
B	Moist Sal Savannah					
11	Brown to red	Smooth	Regular	Upland and lowland areas along fresh alluvial of rivers	Grassland	*Imperate cylindrica*, *Saccharum spontaneum*, *Sancharum munja*, *Desmostachya bipinnata, Phraginites karka, Saccharum narenga*, *Sclerostachya fusca*
C	Wetlands					
12	Blackish blue	Coarse	Irregular	Inside forest and roads	Waterbody	
13	Black	Smooth	Regular	Natural course	River	
D	Non- Forest					
14	Brown to red	Coarse	Irregular	Open areas	Openland	
15	Brown to dark	Coarse	Regular	Alluvial plains, croplands	Agriculture/ Tribal habitation	Sugarcane, Rabi crops (Wheat, Mustard)

*iii) **Ancillary Data Collection***

Based on the forest type as described by Champion and Seth (1968) for the terai region (Dudwa National Park), a specially designed sample plot size of 20 x 20 m^2 were intensively laid as per the 0.01 sampling intensity. The field data were recorded in terms of forest type, canopy density, tree species- wise, height and girth at breast height enumeration. The total of 252 plots with Eucalyptus Plantation (12), Teak- Eucalyptus Plantation (8), Gulchaman Plantation (1), Khair- Sissoo Forest (1), Moist Mixed Deciduous Forest (2), Sal Forest (136), Sissoo Plantation (9), Sal Mixed Forest (41), *Syzygium* Swamp Low Forest (18), Teak Plantation (22) and Tropical Semi- Evergreen Forest (2) were collected.

iv) ***Secondary Data Collection***

Review of literature related to the present study area, plans and other documents were part of the field research. It includes procurement of Management Plan, Park Boundary Map and corresponding Block Maps.

5.2.3. Final image interpretation, stand volume and biomass estimation

i) Selection of mapping scale (Mapping Unit)

The scale for mapping the forest type / cover maps of the satellite data has been fixed in 1: 40,000 as the representative fraction unit.

ii) Forest Type mapping using optical data

On screen visual interpretation of optical data (4R, 3G, 2B bands combination) was carried out to map the different forest types/ classes in conjunction with information from topographical maps, management plan and ground truth following the standard visual interpretation technique (Browden and Pruitt, 1983). A total of 15 classes have been identified (forest type) using on- screen visual interpretation technique. These classes are Sal Forest, Eucalyptus Plantation, Teak - Eucalyptus Plantation, Teak- Sissoo Plantation, Gulchaman Plantation, Khair- Sissoo Forest, Moist Mixed Deciduous Forest, Sissoo Plantation, Sal Mixed Forest, *Barringtonia* Swamp Forest, *Syzygium* Swamp Low Forest, Teak Plantation, Tropical Semi-Evergreen Forest, Upland Grassland, Lowland Grassland. The land cover includes agriculture/ tribal habitations, openland, river and waterbody.

iii) Forest Density mapping using optical data

The same on- screen visual interpretation cum classification was carried out using optical data (4 R, 3G, 2B bands combination) following the standard one for mapping the different forest canopy cover. Using optical data, a total of 19 classes (forest canopy density) has been identified using on- screen visual interpretation technique. These classes are Dense Sal Forest (>60%), Moderately Closed Sal Forest (40-60%), Open Sal Forest (<40%), Eucalyptus Plantation, Teak- Eucalyptus Plantation, Teak- Sissoo Plantation, Gulchaman Plantation, Khair- Sissoo Forest, Moist Mixed Deciduous Forest,

Sissoo Plantation, Dense Sal Mixed Forest (>60%), Moderately Closed Sal Mixed Forest (40-60%), Open Sal Mixed Forest (<40%), *Barringtonia* Swamp Forest, *Syzygium* Swamp Low Forest, Teak Plantation, Tropical Semi- Evergreen Forest, Upland Grassland, Lowland Grassland including other land cover classes as agriculture/ tribal habitations, openland, river and waterbody.

iv) Forest Type mapping using ASAR data

Using Gamma filtered ASAR (HV R, HH G, HH B combinations), the on- screen visual interpretation was similarly conducted using the standard interpretation keys in mapping the forest type. A total of 9 forest type classes can be classified using this dataset. These classes are Sal Forest, Eucalyptus Plantation, Teak - Eucalyptus Plantation, Gulchaman Plantation, Sissoo Plantation, *Syzygium* Swamp Low Forest, Teak Plantation, Tropical Semi- Evergreen Forest, Grassland and other land cover classes as agriculture/ tribal habitations, openland, river and waterbody.

v) Forest Density mapping using ASAR data

Following the same procedure, a total of 11 forest density classes can be distinctively classified in terms of forest canopy cover/ density using the same dataset (HV R, HH G, HH B). These classes are Dense Sal Forest (>60%), Moderately Closed Sal Forest (40-60%), Open Sal Forest (<40%), Eucalyptus Plantation, Teak- Eucalyptus Plantation, Gulchaman Plantation, Sissoo Plantation, *Syzygium* Swamp Low Forest, Teak Plantation, Tropical Semi- Evergreen Forest, Grassland followed by other lancover classes as agriculture/ tribal habitations, openland, river and waterbody.

vi) Stand volume, Growing stock and Biomass Estimation.

Using the measured field data (dbh, Ht.) of trees with 252 plots, the calculated aboveground volume (m^3) using Volumetric Equations are utilized for the generation of aboveground volume map (m^3/ha) with std. deviation for all the 15 forest type classes (prepared from optical data). Again, using these volume information with specific gravity of trees, the generation of aboveground biomass map in (t / ha) with std. deviation for all the 15 forest type classes is prepared.

vii) Classification Assessment

Accuracy assessment of coarse resolution land cover maps poses a great challenge to the remote sensing community. Statistically valid sampling strategy was adopted to assess commission, omission and overall accuracy (Rosenfield & Fitzpatrick-Lins, 1986; Stehman, 1996). Finally, the contingency table was tested using Kappa Statistics (Khat coefficient) (Lillesand & Kiefer, 1999).

Database creation

i) Creation of volume database using Volumetric Equations

Identification of tree species and timber volume estimation using local, general and standard volume equation developed by Forest Survey of India (1996) in m^3 for the existing tree species were developed in a database. And if the species is not encountered in the literature, then the common equation for U.P. (Terai region) is being used.

Table. 5.8. Equations used in developing the tree species volume.

Species	Volume Equations (m^3)
Shorea robusta Gaertn. f.	$\sqrt{V} = 0.16306 + 4.8991D - 1.57402 \sqrt{D}$
Mallotus philippensis Mull.-Arg	$V = 0.14749-2.87503 D+19.61977 D^2-19.11630 D^3$
Acacia catechu Willd.	$V/D^2 = 0.16609/ D^2-2.78851/ D+ 17.22127-11.60248 D$
Dalbergia sissoo Roxb.	$\sqrt{V} = 0.3165 + 4.54751D - 1.46921 \sqrt{D}$
Tectona grandis Linn. f.	$V = 0.08847-1.4693 D+11.98979 D^2 +1.970560 D^3$
Terminalia tomentosa Wight & Arn.	$V/ D^2 = 0.18149/ D^2 - 2.85865/ D + 18.60799$
Cassia fistula, Linn.	$V = 0.066 + 0.287D^2H$
Eucalyptus hybrida,	$V = -0.0015 + 0.2401D^2H$
Adina cordifolia, Hook.j.	$V = 0.0043H + 0.278D^2H$
Gmelina arborea, Linn.	$V = 0.25058 – 3.55124 + 16.41720D^2 - 8.32129 D^3$
Grewia tileafolia, Rottl.	$V = - 0.035+ 0.307 D^2 H$
Lannea coromandelica, Houtt.	$V/D^2 = 0.14004/ D^2 – 2.35990/ D + 11.90726$
Madhuca latifolia, Gmel.	$V = - 0.002557 + 0.260114 D^2 H$
Syzygium cumini, Linn.	$V = 0.08481 – 1.81774D +12.63047D^2 – 6.33263 D$
Albizzia procera, Benth.	$V = 0.009134 + 0.17315D^2 H$
Pterocarpus marsupium, Roxb.	$V = 0.013437 + 0.217379 D^2 H$
Michelia champaca, Linn.	$V = - 2.1537 + 0.0745 D$
Bauhinia variegate, Linn.	$V = - 0.04262 + 6.09491 D^2$
Bombax malabaricum, D.C. Schlott & Endl.	$V = - 0.032 - 0.61 D + 7.208 D^2$
Ficus spp., Linn.	$\sqrt{V} = 0.3629 + 3.95389 D – 0.84421\sqrt{D}$
U.P. (Terai region)	$V/D^2 = - 0.00342/ D^2 – 0.0922/D + 2.28178 + 9.46641 D$

(Source: FSI, 1996)

ii) Biomass Estimation from Growing Stock database

A sufficient number of field measurements is a prerequisite for developing aboveground biomass estimation models and for evaluating biomass estimation results. For estimating total biomass, the natural ecosystem was divided into trees and grasses. The estimated volume or growing stock using the derived volumetric equations was converted into dry biomass by using specific gravity or wood density as the product of specific gravity and volume (Rajput *et al.,* 1996; Limaye and Sen, 1956):

Biomass (tonnes) = Volume (m^3) x Specific Gravity

Wood specific gravity is an important factor in converting forest volume data to biomass and may also strongly depend on location, climate, and possibly management. However, it is a convenient indicator for life history strategy in trees and one with direct importance for ecosystem studies, and highly correlated with the density of carbon per unit volume and is thus of direct applied importance for estimating ecosystem carbon storage and fluxes.

Table: 5.9. Specific gravity of different tree species

Species	Specific gravity
Shorea robusta Gaertn. f.	0.726
Mallotus philippensis Mull.-Arg	0.571
Acacia catechu Willd.	0.875
Dalbergia sissoo Roxb.	0.669
Tectona grandis Linn. f.	0.578
Terminalia tomentosa Wight & Arn.	0.696
Cassia fistula, Linn.	0.746
Eucalyptus hybrida,	0.697
Adina cordifolia, Hook.j.	0.583
Gmelina arborea, Linn.	0.445
Grewia tileafolia, Rottl.	0.829
Lannea coromandelica, Houtt.	0.497
Madhuca latifolia, Gmel.	0.737
Syzygium cumini, Linn.	0.647
Albizzia procera, Benth.	0.579
Pterocarpus marsupium, Roxb.	0.587
Michelia champaca, Linn.	0.426
Bauhinia variegate, Linn.	0.629
Bombax malabaricum, D.C. Schlott & Endl.	0.329
Ficus spp., Linn.	0.523

Grasslands of the study area were divided into two categories based on topography and the duration of the water availability in the area viz., grassland in the lowland and upland etc. (Appendix 2).

CHAPTER- 6

RESULTS

6.6. Forest/ Vegetation strata

The vegetation classification scheme attempted in this study is based on broad phenological physiognomic vegetation cover types. The study has identified 23 cover classes with a description of 19 vegetation cover including 4 non- forest cover types (agriculture, openland, waterbody and river) from the optical data (Fig. 6.1 and 6.2) whereas 9 type against 11 density classes using ASAR data (Fig. 6.3 and 6.4). The vegetation cover types depict physiognomic community characteristics and geographical distribution pattern (thermal and local specific parameters). These are close to the forest type description given by Champion and Seth, 1968.

While explaining the heterogeneous vegetation of this large area, any fine lines of compositional or physiognomic distinctions between its division and sub-divisions are not attempted. The cover classes have been organized to give an overall picture of the vegetation and land cover of the National Park area fully realizing that there are all kinds of variations and overlaps existing in its composition. A brief description of vegetation cover type is given in the following text. The area statistics of different vegetation cover types is given in Table. 6.1. and Table. 6.2 compares the Champion and Seth, 1968, forest type classification with the one used in this study.

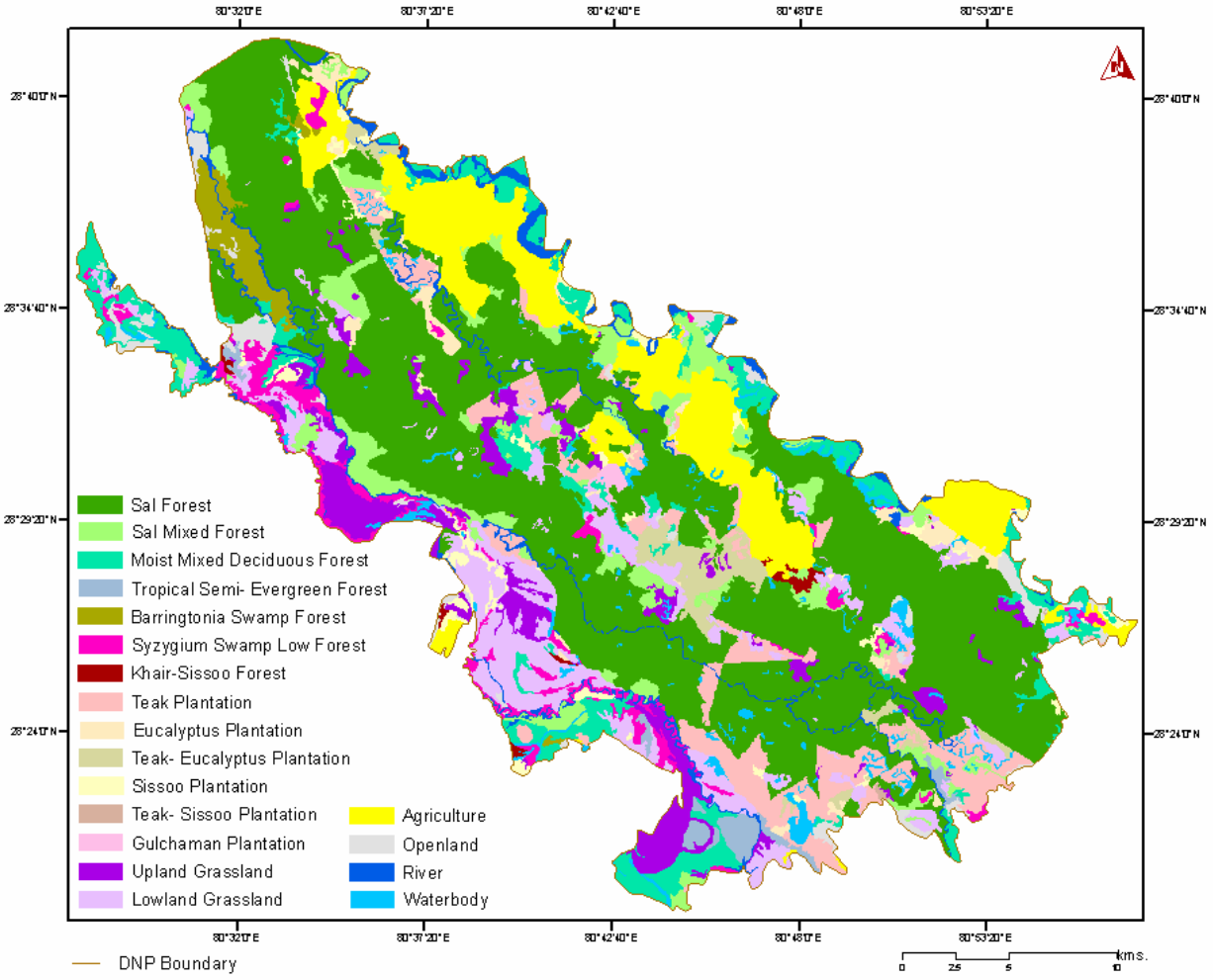

Fig. 6.1: Forest type map preparation using optical data

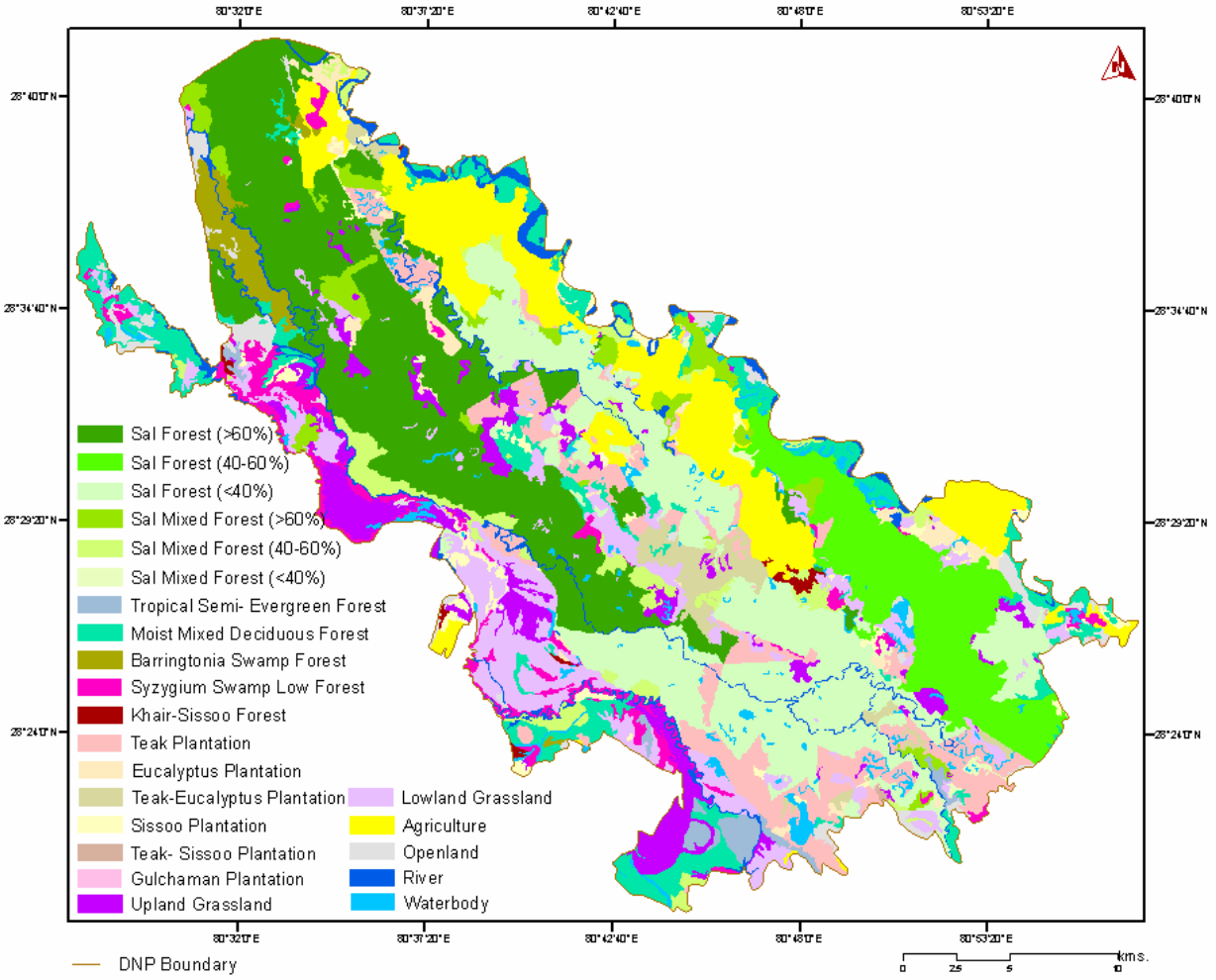

Fig. 6.2: Forest density map preparation using optical data

Sal Forests with Sal (*Shorea robusta*) as the key species occurring on higher alluvial terraces (damars) with loamy soils (majority). Other important associated species found were *Terminalia alata* and *Lagerstromia parviflora*. The middle storey comprised of *Mallotus phillipensis* and *Millusa velutina*. Profuse growth of *Syzygium cumini* and *Scheleichera oleosa* along streams also occurred. Using optical satellite data, sal forests occupies a total area of about 281.89 km^2 (41.38 %) against 370.82 km^2 (54.45%) using ASAR satellite data. On the basis of the canopy density, this forest is sub- divided into 3 classes as-*Dense Sal Forest* (> 60%) occupying an area of 18.47 % (optical) against 23.5 3% (ASAR), *Moderately Closed Sal Forest* (40-60%) occupying an area of 7.78 % (optical) against 11.15 % (ASAR) and *Open Sal Forest* (< 40%) occupying an area of about 15.13 % against 19.77 % (ASAR) respectively.

Sal Mixed Forests are confined on the gentle slopes, old river terraces around grasslands in the Park area. The over- wood being scattered old Sal and *Terminalia alata* with majority middle aged trees. *Mallotus phillipensis*, *Syzygium cumini, Lagerstromia parviflora with* plantations of *Tectona grandis* were also associated. It occupies about 39.52 km^2 with 5.8 % (optical satellite data) only. On the basis of the canopy density, this forest is sub- divided into 3 classes as- *Dense Sal Mixed Forest* (> 60%) occupying an area of 17.50 km^2 with 2.57%, *Moderately Closed Sal Mixed Forest* (40-60%) occupying an area of 19.51 km^2 with 2.86 % against *Open Sal Mixed Forest* (< 40%) occupying an area of 2.51 km^2 with 0.37 % respectively. ***Tropical Semi- Evergreen Forest*** occurs in more or less permanently wet/ moist soils of fine clay and rich in humus. It occupies about 6.96 km^2 with 1.02 % (optical satellite data) against 2.29 km^2 (0.34%) using ASAR data. It prominently occurred along the perennial streams (nalahs) and also near swamps (taals). Prominent tree species viz., *Mallotus phillipensis*, *Syzygium cumini*, *Ficus racemosa*, *Ehtretia laevis, Trewia nudiflora, Schleichera oleosa.* Climbers like *Tiliacora acuminate* and cane (*calamus tenuis*) commonly occurred. Fern (*Lygodium fleuosum*) was conspicuous. ***Moist Mixed Deciduous Forest*** is conspiciuos with the absence of sal trees in these forests occupying about 46.01 km^2 with 6.76 % (optical data) only. The presence of miscellanoeuous species viz., *Mallotus phillipensis*, *Syzygium cumini*, *Ficus racemosa*, *Ehtretia laevis, Trewia nudiflora, Schleichera oleosa, Dalbergia sissoo* has made these forests highly diversed occurred on sandy alluvium.

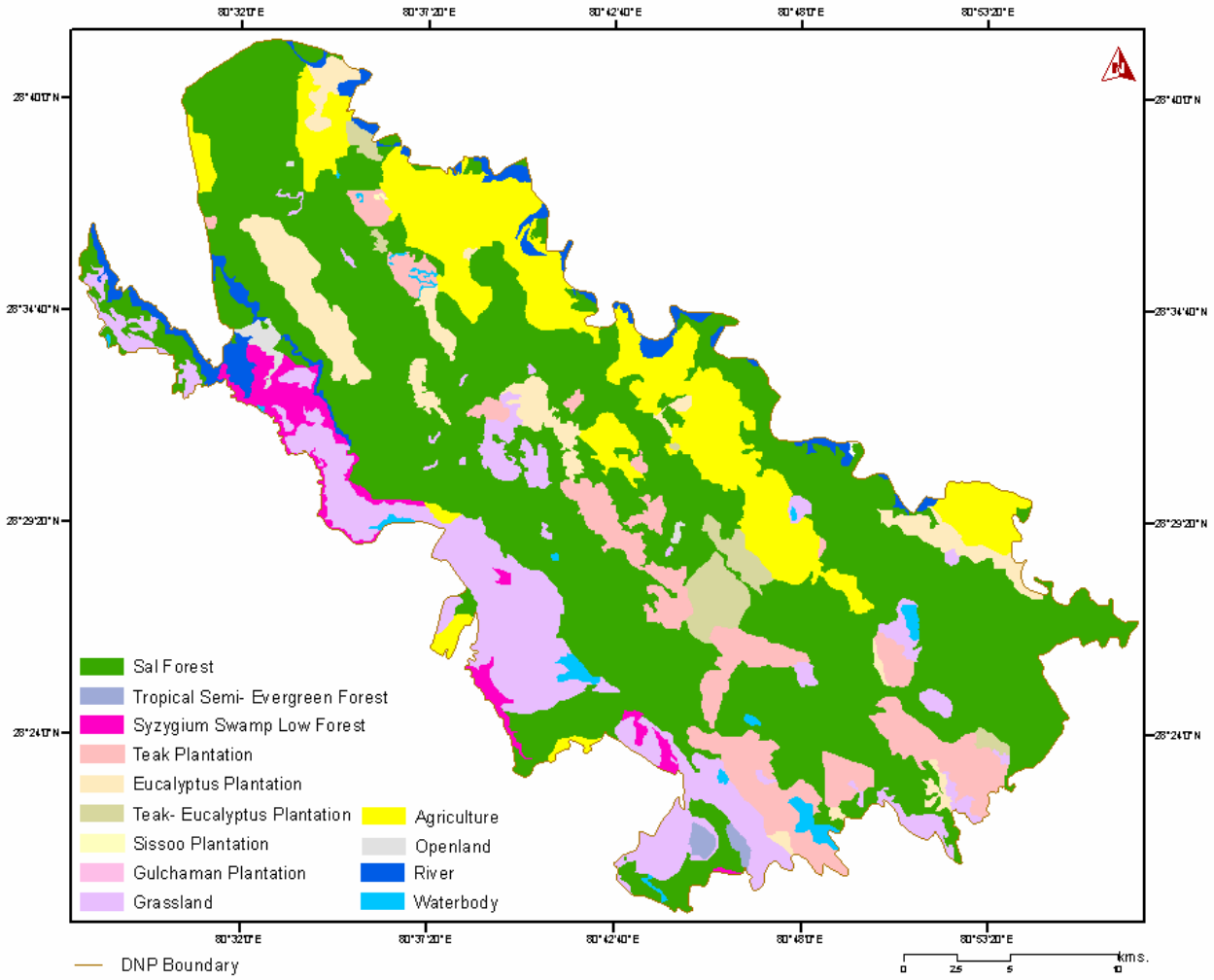

Fig. 6.3: Forest type map preparation using ASAR data

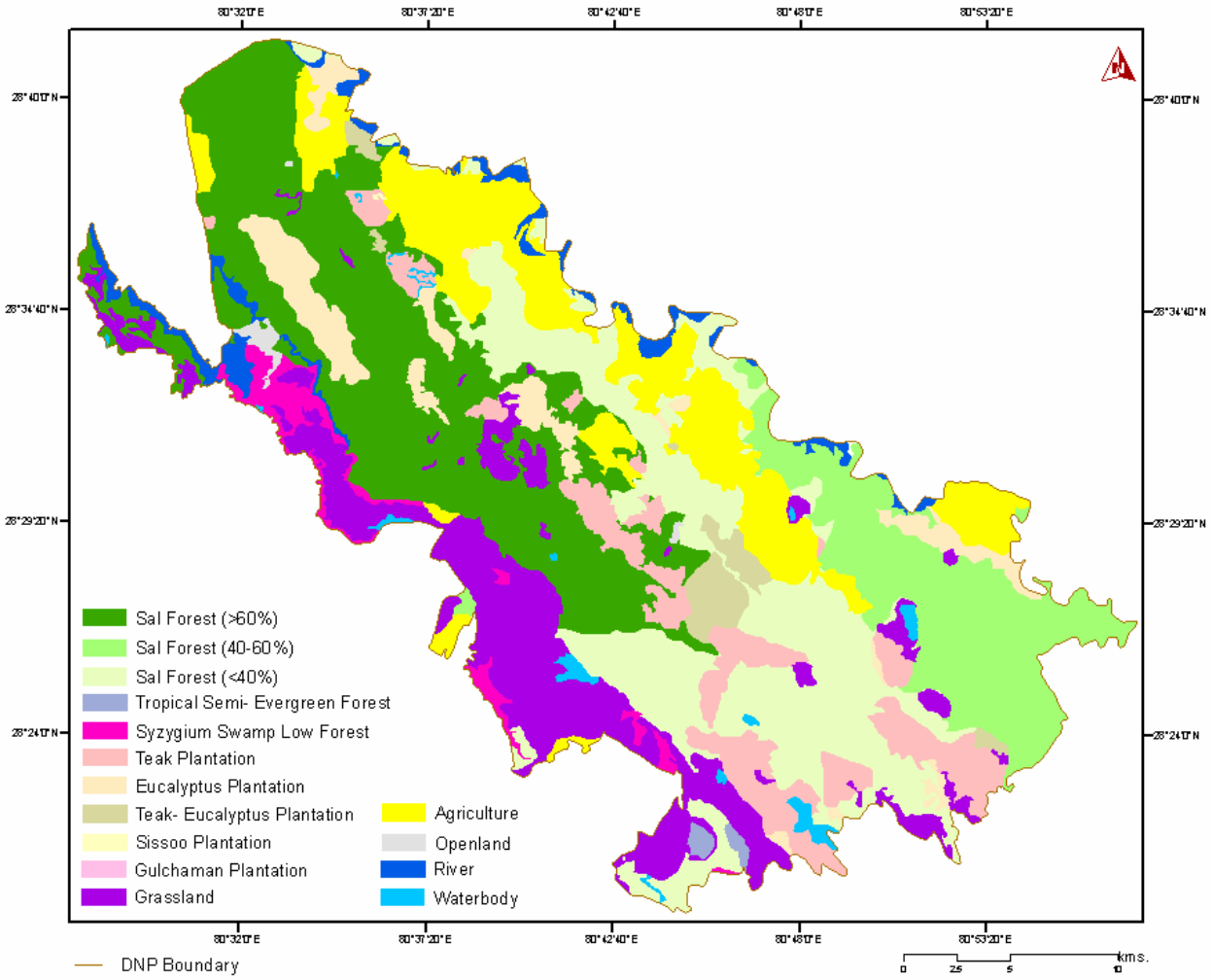

Fig. 6.4: Forest density map preparation using ASAR data

Table. 6.1. Area under different forest/ vegetation categories

S. No.	Class	Optical		ASAR	
	Forest Type/ Density	Area (km.^{2})	Area (%)	Area (km.^{2})	Area (%)
1	Sal Forest (>60%) (DSF)	125.83	18.47	160.26	23.53
2	Sal Forest (40-60%) (MSF)	53.00	7.78	75.94	11.15
3	Sal Forest (<40%) (OSF)	103.06	15.13	134.62	19.77
4	Sal Mixed Forest (>60%) (DSMF)	17.50	2.57	-	-
5	Sal Mixed Forest (40-60%) (MSMF)	19.51	2.86	-	-
6	Sal Mixed Forest (<40%) (OSMF)	2.51	0.37	-	-
7	Tropical Semi- Evergreen Forest (TSEF)	6.96	1.02	2.29	0.34
8	Moist Mixed Deciduous Forest (MMDF)	46.01	6.76	-	-
9	*Barringtonia* Swamp Forest (BSF)	9.64	1.42	-	-
10	*Syzygium* Swamp Low Forest (SSLF)	19.13	2.81	14.07	2.07
11	Khair-Sissoo Forest (KSF)	2.05	0.30	-	-
12	Teak Plantation (TP)	37.85	5.55	39.58	5.81
13	Eucalyptus Plantation (EP)	9.15	1.34	33.10	4.86
14	Teak-Eucalyptus Plantation (TEP)	18.64	2.73	18.21	2.67
15	Sissoo Plantation (SP)	9.29	1.36	0.10	0.01
16	Teak- Sissoo Plantation (TSP)	0.24	0.04	-	-
17	Gulchaman Plantation (GP)	1.26	0.19	9.33	1.37
18	Upland Grassland (UG)	34.27	5.03	77.30	11.35
19	Lowland Grassland (LG)	48.77	7.16	-	-
	Landuse/ Cover				
20	Agriculture (Ag)	68.78	10.10	91.09	13.37
21	Openland (Op)	13.30	1.95	2.36	0.35
22	River (R)	20.50	3.01	16.93	2.49
23	Waterbody (Wb)	13.88	2.04	5.93	0.87

Table. 6.2. Forest type/ crown density using satellite data.

Sl. No.	Vegetation Types (Mapped) using satellite data	Champion and Seth (1968) Forest Equivalents	Forest Groups/ Sub-Group
1	Tropical Semi- Evergreen Forest	Tropical Semi- Evergreen Forest Northern Tropical Semi- Evergreen Forest	Group 2 Sub- Group 2B
2	Moist Mixed Deciduous Forest	Tropical Moist Mixed Deciduous Forest North Indian Moist Deciduous Forest	Group 3 Sub- Group 3C
3	Dense Sal Forest Moderately Closed Sal Forest Open Sal Forest	Tropical Moist Deciduous Forest North Indian Moist Deciduous Forest	Group 3 Sub- Group 3C
4	Sal Mixed Forest	Tropical Moist Deciduous Forest North Indian Moist Deciduous Forest	Group 3 Sub- Group 3C
5	Tropical seasonal Swamp forests 1.*Barringtonia* Swamp Forest 2.*Syzygium cuminii* Swamp Low Forest	Littoral and Swamp Forest Tropical Seasonal Swamp forest 4D/ SS2 *Barringtonia* Swamp Forest 4D/ SS3 *Syzygium cuminii* Swamp Low Forest	Group 4 Sub- Group 4D
6	Khair- Sissoo (*Acacia catechu* and *Dalbergia sissoo*) Forest	Tropical Dry Deciduous Forest North Indian Dry Deciduous Forest 5B/ IS2 Khair- Sissoo Forest	Group 5 Sub- Group 5B

7	Plantations (Teak, Sissoo, Eucalyptus, Gulchaman)	Mainly Teak (*Tectona grandis*) and Safeda (*Eucalyptus spp*.)	
8	Upland Grassland	Tropical Moist Deciduous Forest North Indian Moist Deciduous Forest 3 C/C2/DSI- Moist Sal Savannah	Group 3 Sub- Group 3C
9	Lowland Grassland	Tropical Moist Deciduous Forest North Indian Moist Deciduous Forest 3 C/ISI- Low Alluvial Savannah Woodland	Group 3 Sub- Group 3C

Teak (*Tectona grandis*) and *Eucalyptus hybrida* have been successfully introduced. ***Tropical Seasonal Swamp forest (Barringtonia Swamp Forest)*** was found in swamp depressions along streams which remain under water continuously for a long period during the rains or where deep black heavy waterlogged soils occurred. *Barringtonia acutangula* dominated as tree specis along with *Mallotus phillipensis*, *Ficus racemosa* were the prominent co- associates. It occupies about 9.64 km^2 with 1.42 % using optical data only. ***Tropical Seasonal Swamp forest (Syzygium cumini Swamp Low Forest)*** occurred in swamp depressions along streams with *Syzygium cumini* (Jamun) with long clean boles as the main constituent tree species along with *Mallotus phillipensis* and *Trewia nudiflora*. *Corchorus austuans, Dioscorea belophylla* and *Ageratum conyzoides* were the main important herbs in this type of forest. This forest occupies about 19.13 km^2 with 2.81 % (optical satellite data) as compare to 14.07 km^2 (2.07 %) using ASAR data. ***Khair- Sissoo Forest*** occurred on new sandy alluvium along streams and rivers (Suheli, Mohana, Ghagra and Sharda) with Khair (*Acacia catechu*) and Sissoo (*Dalbergia sissoo*) tree species. These forests were mixed with heavy growth of grasses. Regeneration of both species was scarce, as these forests are prone to fire. Flooding and prolonged water logging of these forests result into poor and stunted growth of Khair and sissoo. *Bombax ceiba, Haldina cordifolia* and *Catununaregam spinosa* were co- associates. It occupies about 2.05 km^2 with 0.30 % with optical satellite data only.

Teak Plantations (*Tectona grandis*) are found extensively have been raised as gap planting as well after clear felling silvicultural system, occupying about 37.85 km^2 with 5.55 % with optical satellite data as compare to 39.58 km^2 (5.81 %) using ASAR data. ***Eucalyptus Plantation*** had taken up extensive mass scale plantations (*Eucalyptus hybrida*) recently a decade and shows successful in grasslands or 'grassy blanks'. It occupies about 9.15 km^2 with 1.34 % using optical satellite data against 33.10 km^2 (4.86%) using ASAR satellite data. ***Teak- Eucalyptus Plantation*** an admixture of teak (*Tectona grandis*) and Safeda (*Eucalyptus hybrida*) occupies about 18.64 km^2 with 2.73 % suing optical satellite data as compare to 18.21 km^2 (2.67 %) using ASAR satellite data. ***Sissoo Plantation*** was taken up with Sissoo (*Dalbergia sissoo*) along the streams occupying about 9.29 km^2 with 1.36 % using optical satellite data against 0.10 km^2 (0.01%) using ASAR satellite data. ***Gulchaman Plantation*** was executed in a small portion of the park with Gulchaman tree occupying about 1.26 km^2 with 0.19 % using optical satellite data against 9.33 km^2 (1.37%) using ASAR satellite data. ***Teak- Sissoo Plantation*** comprising both teak (*Tectona grandis)* and shisham (*Dalbergia sissoo*) occupying about 0.24 km^2 with 0.04 % using optical satellite data only.

Upland Grassland characterized by the occurrence of 'grassy blanks' or 'phantas' inside the moist Sal forests. These grasslands occurred on well- drained soils occupying large areas and scattered. Some of them have scattered tree growth species such as *Bombax ceiba*, *Syzygium cerasoides, Dalbergia sissoo, Haldina cordifolia* and *Acacia catechu.* The dominant grasses vary from place to place depending upon the soil type, drainage and management conditions. *Arundo donax, Phragmites karka* and *Sclerostachya fusca* were thus found in swampy locations while *Themeda arundinaceae*

occurred in fairly well drained soils and *Imperata cylindrical*, *Desmostachya bipinnata, Cymbopogan jwarancusa, Saccharum spontanum* and *S. bengalense* were found over clayey soil. It occupies about 34.27 km^2 with 5.03 % using optical satellite data. ***Lowland Grassland*** occurred in low lying areas/ depressions which were water logged or marshy in nature having areas with alluvial soils, mostly sandy with clayey patches. The prominent species were *Bombax ceiba, Haldina cordifolia, Butea monosperma, Dalbergia sissoo, Albizzia lebbeck, Scheleichera oleosa* and *Syzygium cumini.* Prominent grasses were *Saccharum spontenum, Arundo donax, Phragmites karka, Themeda arundinacea, Sclerostachya fusca* and *Saccarum narenga*. These grasslands have interspersed swamps. It occupies about 48.77 km^2 with 7.16 % using optical data only. ***Grassland*** *class* is the combination of Upland and lowland Grassland that are included in the ASAR mapping due to the difficulty in the separation of these different types occupying an area of 77.31 km^2 (11.35 %).

Agriculture/ Tribal habitation occupy around 68.78 km^2 with 10.10 % (optical data) while 91.09 km^2 (13.37 %) using ASAR data are the cultivated land in the buffer zone of the park. The main crops sown were rice, maize, wheat, barley, gram, lentil, pea, potato and mustard. Jute, sunhemp and kenaf are also cultivated for the extraction of fibres. **Openland** class signifies the area comprising of the Lantana camera and barren land adjacent to buffer and forested areas next to agricultural lands. The trees are very few with palatable grasses grown for cattle are the characteristics of openland. It occupies about 13.30 km^2 with 1.95 % using optical satellite data as compare to 2.36 km^2 (0.35%) using ASAR data.

River occupy along the buffer in the Indo- Nepal border in the north (river Mohana) and River Suheli in the south covering a total area about 20.50 km^2 with 3.01 % using optical data as compare to 16.93 km^2 (2.49 %) with ASAR data. **Waterbody** are found scattered in the whole park. Most of the taals and ponds remain seasonally dry during lean season. It also finds its way deep inside the teak plantation and mixed forest. It occupies about 13.88 km^2 with 2.04 % using optical data as compare to 5.93 km^2 (0.87 %) using ASAR data.

6.7. Stand volume and growing stock

Sal Forest includes sal contributing a mean volume of 0.47 m^3 (± 1.17 S.D.) followed by rohini of 0.49 m^3 (± 1.16 S.D.) with other associates like amaltas contributing 0.49 m^3 (± 1.22 S.D.), asna of 0.50 m^3 (± 1.17 S.D.), chilla of 0.48 m^3 (± 1.19 S.D.) respectively with a mean volme of 631.86 m^3/ha (± 352.42 S.D.) leading to the total volume of sal forest as 17.81 Mm^3. ***Sal Mixed Forest*** contributes around 563.16 m^3/ha (± 350.84 S.D.) leading to mean volume of this forest as 2.22 Mm^3. ***Eucalyptus Plantation*** comprising of 0.495 m^3 mean volume (± 1.160 S.D.) eucalyptus species leading to 312.54 m^3/ha (± 144.08 S.D.) as mean volume per ha and a total volume of 0.28 Mm^3. ***Barringtonia Swamp Forest*** consisting of rohini contributes a mean volume of 0.49 m^3 (± 1.16 S.D.) followed by gular (*Ficus racemosa*) of 0.53 m^3 (± 1.18 S.D.), gutel of 0.51 m^3 (± 1.13 S.D.), and kari (*Miluisa spp.*) of 0.49 m^3 (± 1.15 S.D.) along with ***Gulchaman Plantation*** consisiting of gulchaman alone contributes around 0.16 m^3 (± 0.15 S.D.) with rohini contribute around 0.12 m^3 (± 1.34 S.D.) and jamun of 0.14 m^3 (± 1.49 S.D.). So the mean volume of 212.47 m^3/ha (± 24.12 S.D.) leading to 0.23 Mm^3 as total volume of these two forests.

Syzygium Swamp Low Forest consists of jamun alone contributing around a mean volume of 0.49 m^3 (± 1.16 S.D.) followed by gutel of 0.51 m^3 (± 1.13 S.D.), haldu of 0.06 m^3 (± 0.06 S.D.), kachnar of 0.35 m^3 (± 0.86 S.D.), semal of 0.73 m^3 (± 0.75 S.D.) leading to a mean volume of 288.40 m^3/ha (± 165.96 S.D.) with a total volume of this forest 0.55 m^3. ***Sissoo Plantation*** consists of sisham alone contributing around a mean volume of 0.49 m^3 (± 1.18 S.D.) followed by jamun of 0.48 m^3 (± 1.21 S.D.), khair of 0.48 m^3 (± 1.21 S.D.) with a mean volume of 390.53 m^3/ha (± 286.54 S.D.) leading to the total volume of sissoo plantation 0.36 Mm^3. ***Moist Mixed Deciduous Forest*** consisting of rohini contributing around 0.45 m^3 mean volume (± 0.9 S.D.) followed by sisham of 0.41 m^3 (± 0.53 S.D.), kari of 0.39 m^3 (± 0.94 S.D.), jamun of 0.45 m^3 (± 0.99 S.D.) and *Putranjeva roxburghii* of 0.56 m^3 (± 0.68 S.D.) with 248.36 m^3/ha (± 60.15 S.D.) as the mean volume per ha leading to 1.14 Mm^3 as the total volume of this type of forest.

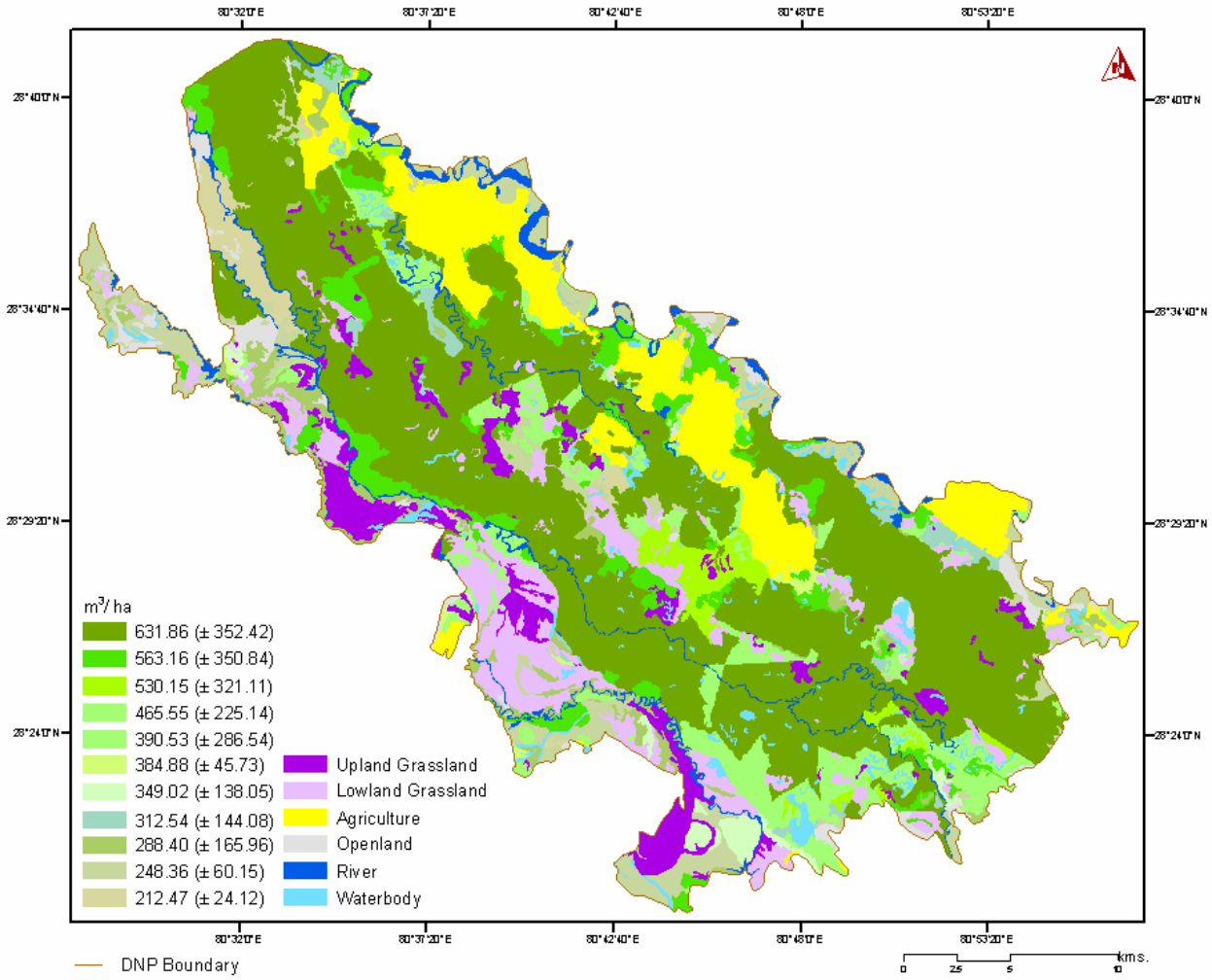

Fig. 6.5: Mean Volume map of DNP

Khair- Sissoo Forest consisting of sisham contributing 0.66 m^3 mean volume (± 0.32 S.D.) followed by rohini of 0.47 m^3 (± 1.06 S.D.), jamun of 0.47 m^3 (± 1.05 S.D.) and kari of 0.03 m^3 (± 0.01 S.D.) with khair of 0.31 m^3 (± 0.14 S.D.) with 384.88 m^3/ha (± 45.73 S.D.) as the mean volume per ha leading to 0.08 Mm^3 as the total volume of this type of forest. ***Teak- Sissoo*** and ***Teak- Eucalyptus Plantation*** consisting of teak contributing around 0.51 m^3 mean volume (± 1.18 S.D.), sisham of 0.50 m^3 (± 1.16 S.D.) and eucalyptus of 0.50 m^3 (± 1.16 S.D.) leading to 530.15 m^3/ha (± 321.11 S.D.) as the mean volume per ha of both these plantations leading to 0.74 Mm^3 as the total volume. ***Tropical Semi- Evergreen Forest*** consisting of arjun contributing around 1.66 m^3 mean volume (± 1.27 S.D.) , followed by gutel of 0.54 m^3 (± 0.40 S.D.) and *Morus indica* (mulberry) of 1.35 m^3 mean volume (± 1.35 S.D.) with a mean volume of 349.02 m^3/ha (± 138.05 S.D.) per ha which leads to 0.24 Mm^3 as the total volume of this type of forest. ***Teak Plantation*** consisting teak alone contributes around 0.49 m^3 mean volume (± 1.16 S.D.) with a mean volume of 465.55 m^3/ ha (± 225.14 S.D.) leading to total volume of teak plantation as 1.99 Mm^3.

Table. 6.3. Stand Volume and growing stock in DNP

Sl. No.	Forest / Land Cover Type	Mean Volume (m^3/ha)	Area (ha)	Total Volume/ Growing Stock (Mm^3)
1	Sal Forest	631.86 (± 352.42)	28187.34	17.81
2	River	River	2052.22	-
3	Eucalyptus Plantation	312.54 (± 144.08)	918.20	0.285
4	*Syzygium* Swamp Low Forest	288.40 (± 165.96)	1910.16	0.55
5	Openland	Openland	1328.13	-
6	Waterbody	Waterbody	1386.34	-
7	Lowland Grassland	Lowland Grassland	4877.26	-
8	Sissoo Plantation	390.53 (± 286.54)	928.90	0.36
9	Moist Mixed Deciduous Forest	248.36 (± 60.15)	4597.37	1.14
10	Upland Grassland	Upland Grassland	3426.01	-
11	Khair- Sissoo Forest	384.88 (± 45.73)	204.20	0.07
12	Agriculture	Agriculture	6878.50	-
13	Teak- Sissoo and Teak- Eucalyptus Plantation	530.15 (± 321.11)	1390.50	0.73
14	*Barringtonia* Swamp Forest and Gulchaman Plantation	212.47 (± 24.12)	1089.98	0.23
15	Sal Mixed Forest	563.16 (± 350.84)	3953.67	2.22
16	Tropical Semi- Evergreen Forest	349.02 (± 138.05)	695.83	0.24
17	Teak Plantation	465.55 (± 225.14)	4285.99	1.99
		Total	**68110.58**	**25.66**

The total above ground forest volume type- wise in each sample plot (tree and shrub) is given as under (Appendix 1).

6.8. Aboveground biomass

Sal Forest consisting of *Shorea robusta* occupying a mean biomass of 0.33 t (± 0.81 S.D.), rohini of 0.33 t (± 0.81 S.D.) with other associates like amaltas of 0.33 t (± 0.85 S.D.), asna of 0.34 t (± 0.82 S.D.), chilla of 0.32 t (± 0.82 S.D.) respectively in a 400 m^2 sample plot size which accounts to a mean biomass of 275.70 t/ ha (± 163.78 S.D.) with a total biomass of 7.77 Mt in this forest. ***Sal Mixed Forest*** alone contribute 360.54t/ha (± 243.51 S.D.) with the total of 1.42 Mt biomass from this forest. ***Eucalyptus Plantation*** consisting of the eucalyptus tree species comprising of 0.33 t mean biomass (± 0.81S.D.) in a plot leading to mean biomass of 214.51t/ha (± 100.78 S.D.) with a total biomass of this plantation (0.19 Mt). ***Barringtonia Swamp Forest*** consiting of rohini contributes a mean biomass of 0.33 t (± 0.81 S.D.) followed by gular (*Ficus racemosa*) of 0.38 t (± 0.79 S.D.), gutel of 0.35 t (± 0.76 S.D.), and kari (*Miluisa spp.*) of 0.33 t (±0.80 S.D.) with a mean biomass 125.05t/ha (± 18.87 S.D.) leading to 0.13 Mt as total biomass along with ***Gulchaman Plantation*** consisting of gulchaman around 0.10 t biomass (± 0.09 S.D.) with rohini contributing around 0.05 t (± 0.09 S.D.) and jamun of 0.04 t (± 0.08 S.D.).

Syzygium Swamp Low Forest consisting of jamun alone contributing around a mean biomass of 0.34 t (± 0.81 S.D.) followed by gutel of 0.35 t (± 0.76 S.D.), haldu of 0.03 t (± 0.03 S.D.), kachnar of 0.22 t (± 0.56 S.D.), semal of 0.26 t (± 0.24 S.D.) which comes to 227.25 t/ha (± 132.31 S.D.) leading to 0.43 Mt as the total biomass from this forest. ***Sissoo Plantation*** consisting of sisham alone contributes around a mean biomass of 0.34 t (± 0.82 S.D.) followed by jamun of 0.33 t (± 0.83 S.D.), khair of 0.33 t (± 0.83 S.D.) with a mean 209.67t/ha (± 192.47 S.D.) and leading to total biomass of 0.19 Mt of sisham plantation. ***Moist Mixed Deciduous Forest*** consisiting of rohini contributing around 0.31 t mean biomass (± 0.71 S.D.) followed by sisham of 0.25 t (± 0.36 S.D.), kari of 0.26 t (± 0.65 S.D.), jamun of 0.31 t (± 0.71 S.D.) and *Putranjeva roxburghii* of 0.30 t (±0.38 S.D.) with 146.56 t/ha (± 33.96 S.D.) leading to the total biomass of this forest with 0.67 Mt. ***Khair- Sissoo Forest*** consisiting of sisham contributing 0.44 t mean biomass (± 0.21 S.D.) followed by rohini of 0.31 t (± 0.73 S.D.), jamun of 0.32 t (± 0.72 S.D.) and kari of 0.02 t (± 0.01 S.D.) with khair of 0.27 t (± 0.12 S.D.) and having a mean

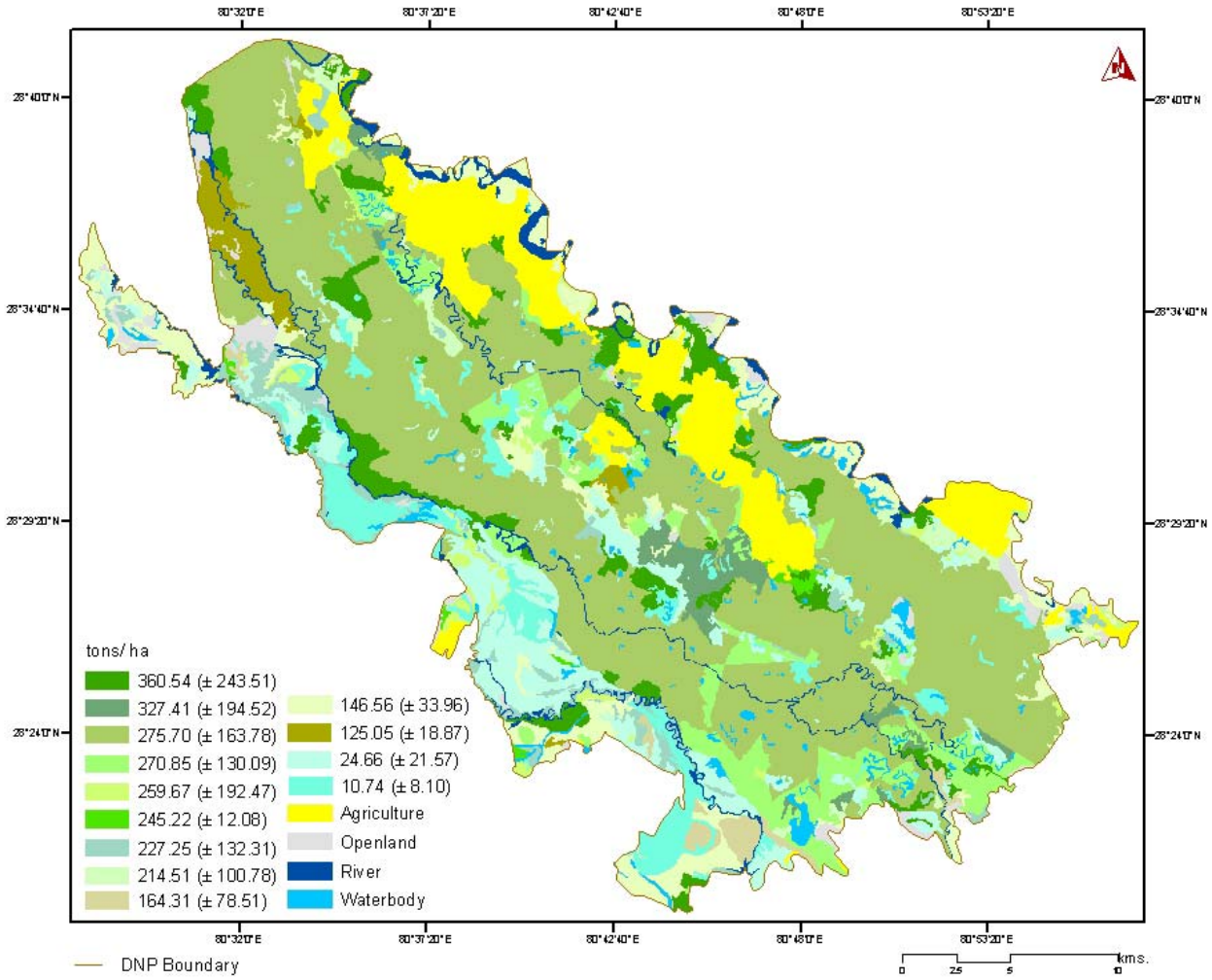

Fig. 6.6: Mean Biomass map of DNP

biomass of 245.22 t/ha (± 12.08 S.D.) leading to the total biomass of this forest type as 0.04 Mt. Both ***Teak- Sissoo*** and ***Teak- Eucalyptus Plantation*** consisting of teak contributing around 0.34 t mean biomass (± 0.83 S.D.) and sisham of 0.34 t (± 0.81 S.D.) on a sample plot with a mean biomass of 327.41 t/ha (± 194.52 S.D.) leading to the total biomass of 0.45 Mt. ***Tropical Semi- Evergreen Forest*** consisting of Arjun contributing around 2.03 t mean Biomass (±1.57 S.D.), followed by gutel of 0.21 t (± 0.15 S.D.) and *Morus indica* (mulberry) of 1.65 t mean biomass (±1.60 S.D.) with a mean biomass of 164.31 t/ha (± 78.51 S.D.) leading to the mean biomass of this forest 0.11 Mt. ***Teak Plantation*** consisting of teak alone contributes around 0.33 t mean biomass (±0.81 S.D.) with a mean biomass of 270.85 t/ha (± 130.09 S.D.) leading to the mean biomass of teak plantation as 1.16 Mt. ***Lowland Grassland*** contributes around 24.66 t mean biomass at (± 21.57 S.D.) with a total biomass of 0.12 Mt whereas ***Upland Grassland*** contributes around 10.74 t mean biomass (± 8.10 S.D.) with a total biomass of 0.03 Mt during peak season. Hence, values of mean biomass were nearly 2.5 times higher in the lowland grassland than the upland grassland (Kumar *et al*., 2002).

Table. 6.4. Mean Biomass

Sl. No.	Land Cover category	Mean Biomass (t/ ha)	Area (ha)	Total Biomass (Mt)
1	Sal Forest	275.70 (± 163.78)	28186.92	7.77
2	River	River	2052.20	-
3	Eucalyptus Plantation	214.51(± 100.78)	916.42	0.19
4	*Syzygium* Swamp Low Forest	227.25 (± 132.31)	1909.60	0.43
5	Openland	-	1330.12	-
6	Waterbody	-	1386.18	-
7	Lowland Grassland	24.66 (± 21.57)	4875.84	0.12
8	Sissoo Plantation	209.67 (± 192.47)	929.12	0.19
9	Moist Mixed Deciduous Forest	146.56 (± 33.96)	4594.41	0.67
10	Upland Grassland	10.74 (± 8.10)	3427.37	0.03
11	Khair- Sissoo Forest	245.22 (± 12.08)	202.50	0.04
12	Agriculture	-	6880.99	-
13	Teak- Sissoo and Teak- Eucalyptus Plantation	327.41 (± 194.52)	1390.80	0.45
14	*Barringtonia* Swamp Forest and Gulchaman Plantation	125.05 (± 18.87)	1091.82	0.13
15	Sal Mixed Forest	360.54 (± 243.51)	3954.95	1.42
16	Tropical Semi- Evergreen Forest	164.31 (± 78.51)	695.98	0.11
17	Teak Plantation	270.85 (± 130.09)	4285.35	1.16
		Total	**68110.58**	

The type- wise biomass in each sample plot (tree) is given in Appendix 2.

6.4. Relationships of volume with optical, NDVI and backscatter coefficients

The optical, NDVI (DN) values and calculated backscatter coefficient (like and cross polarizations) were extracted from the digital images (ETM and backscattering images) for all the sample plot locations (Appendix 3).

The following figures show the observed variations of all these digital responses with above ground forest volume. A logarithm function was used to derive the overall behavior of all the sample plots.

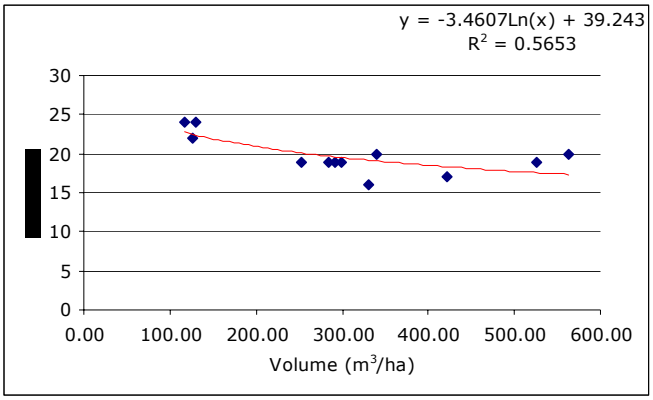

(a)

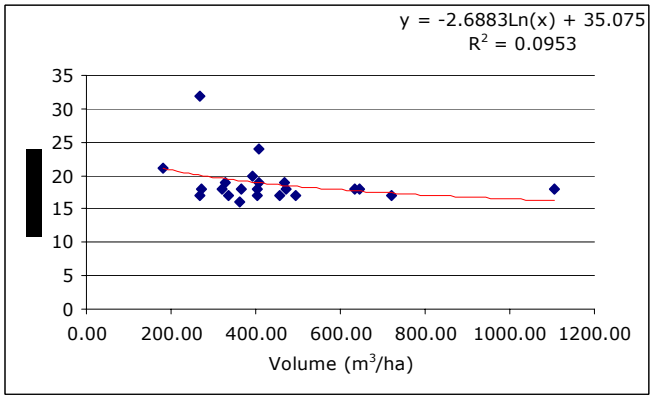

(d)

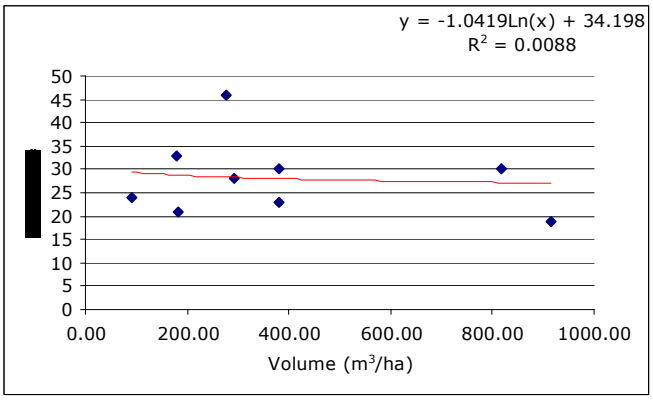

(b)

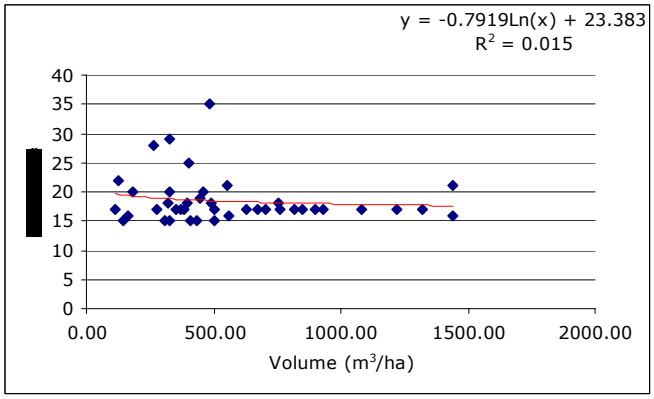

(e)

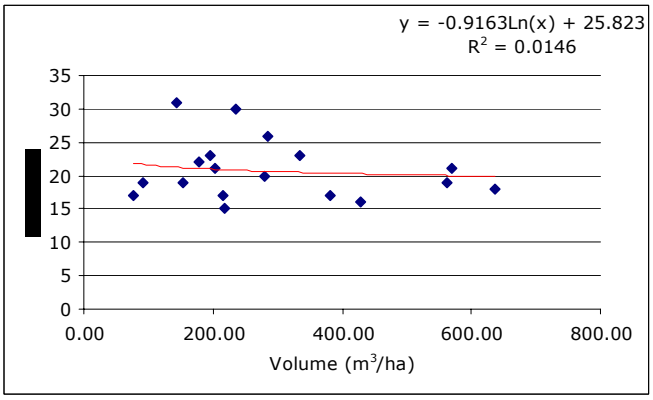

(c)

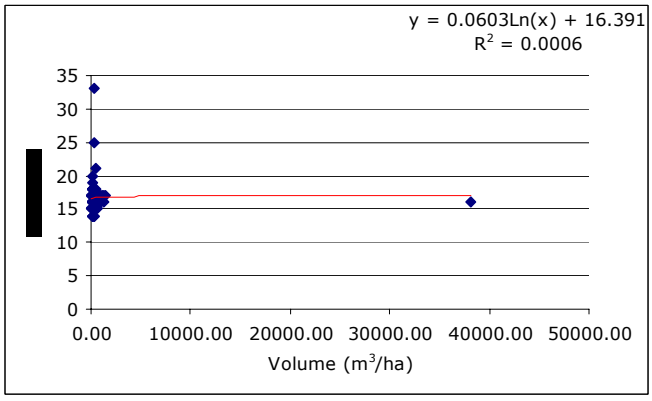

(f)

Fig. 6.7. Relationships between reflectance in red wavelength and volume for (a) eucalyptus (b) sisham (c) jamun (d) teak (e) sal mixed (f) sal

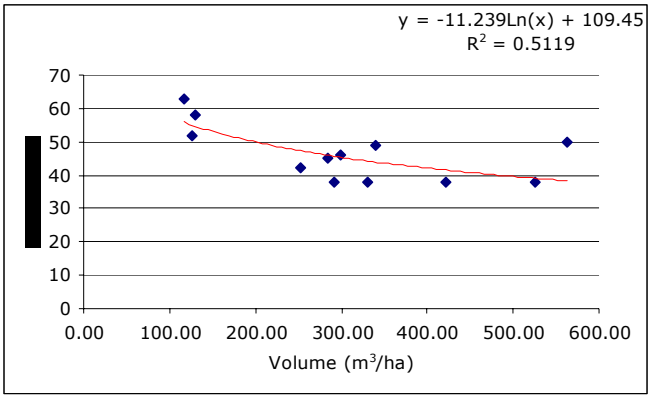

(a)

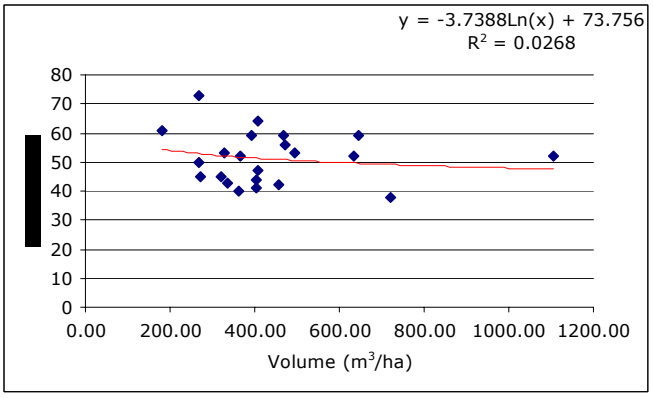

(d)

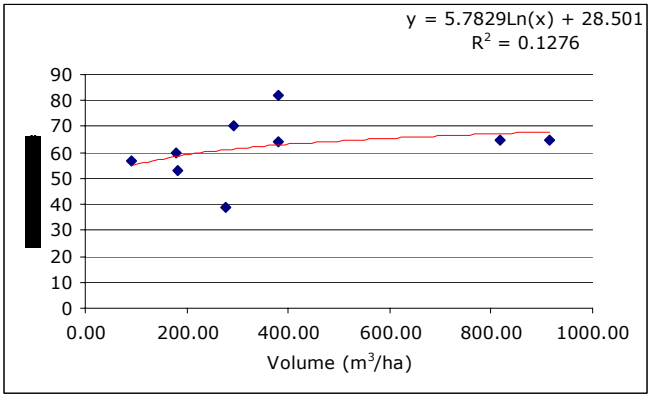

(b)

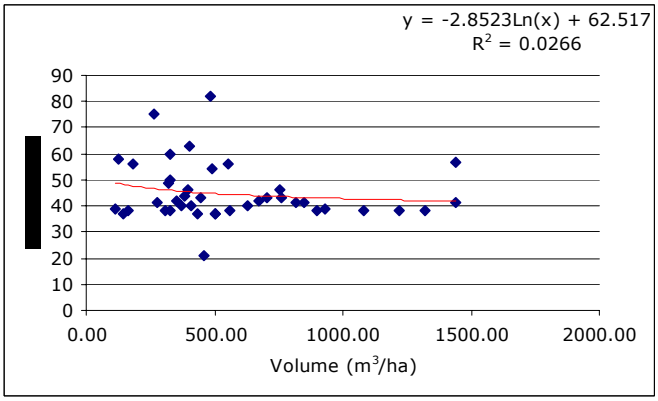

(e)

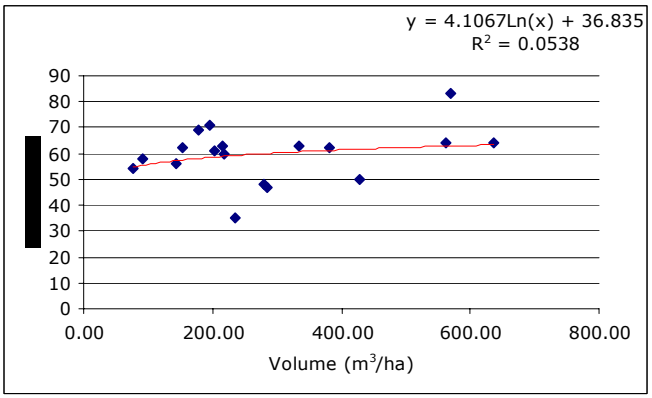

(c)

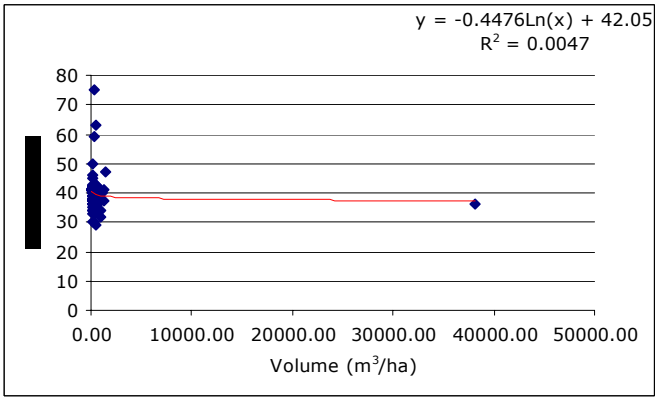

(f)

Fig. 6.8. Relationships between reflectance in infra red wavelength and volume for (a) eucalyptus (b) sisham (c) jamun (d) teak (e) sal mixed (f) sal

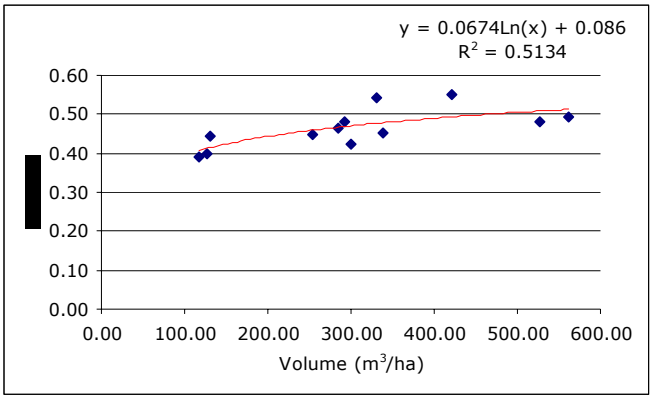

(a)

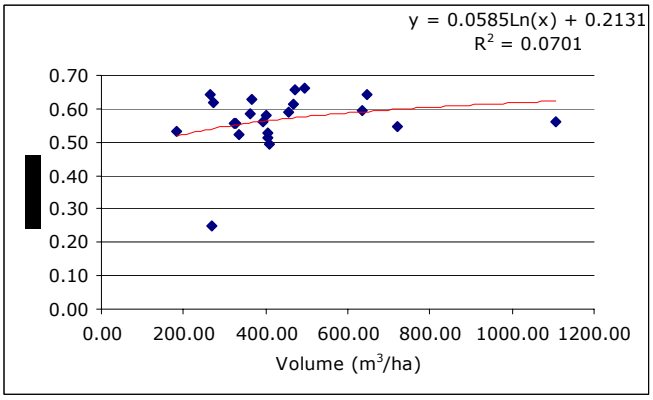

(d)

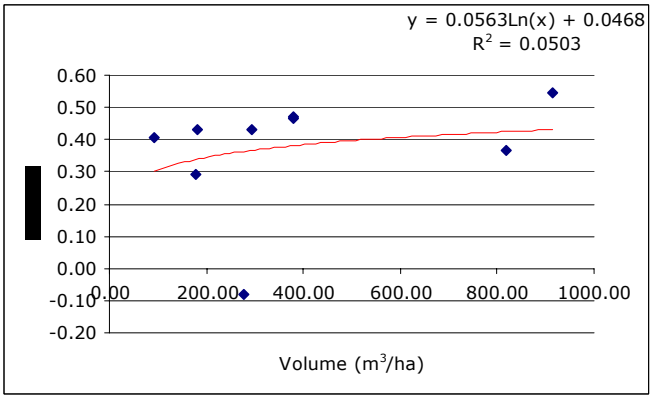

(b)

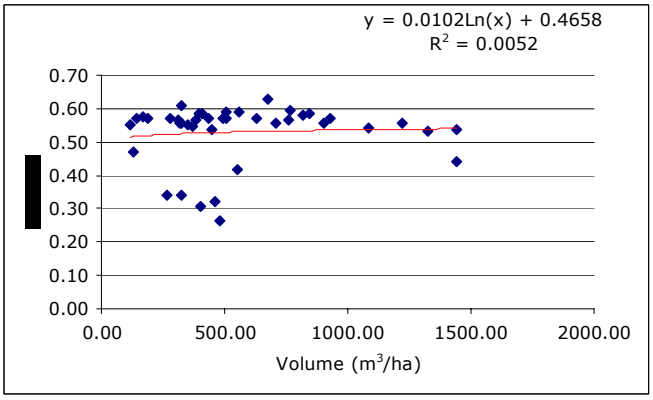

(e)

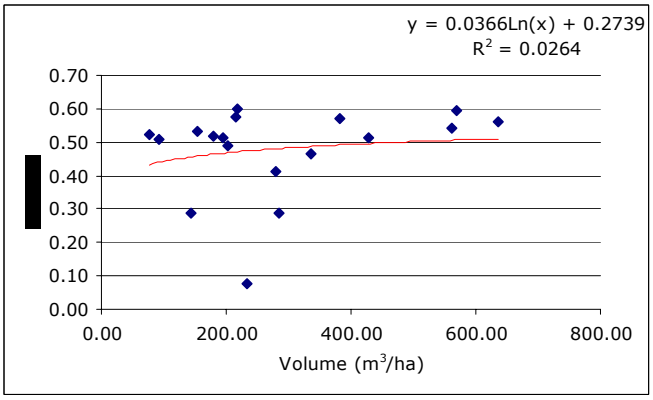

(c)

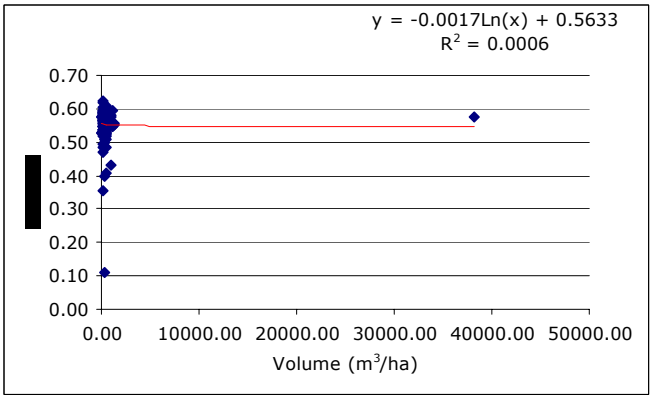

(f)

Fig. 6.9. Relationships between NDVI and volume for (a) eucalyptus (b) sisham (c) jamun (d) teak (e) sal mixed (f) sal

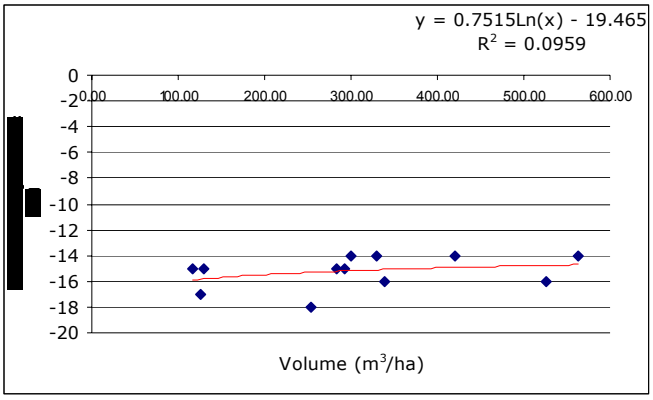

(a)

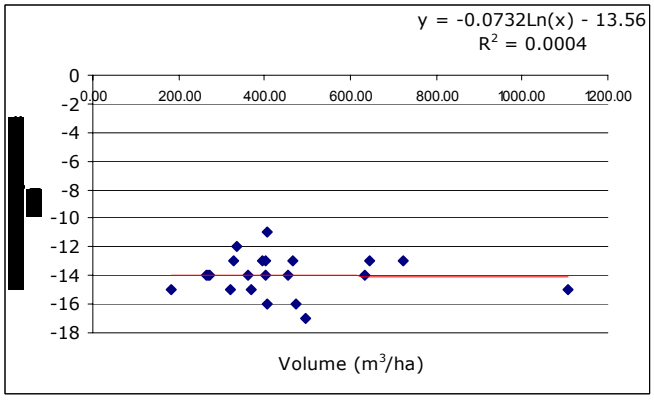

(d)

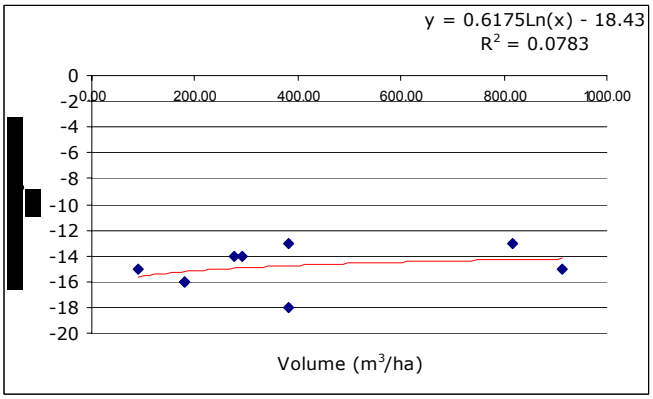

(b)

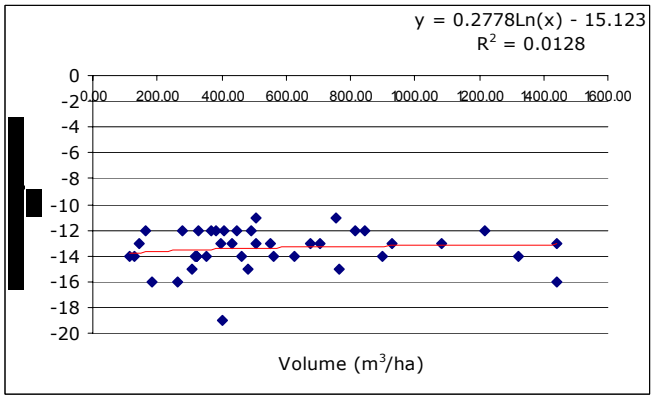

(e)

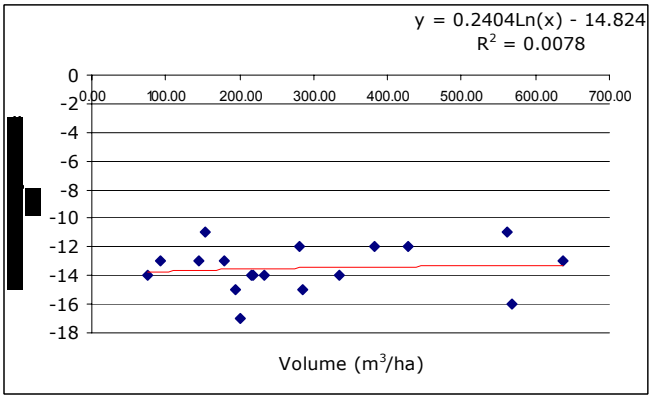

(c)

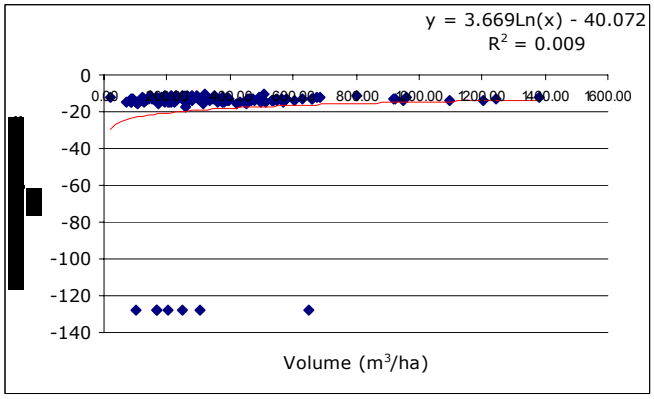

(f)

Fig. 6.10. Relationships between backscatter (like polarization) and volume for (a) eucalyptus (b) sisham (c) jamun (d) teak (e) sal mixed (f) sal

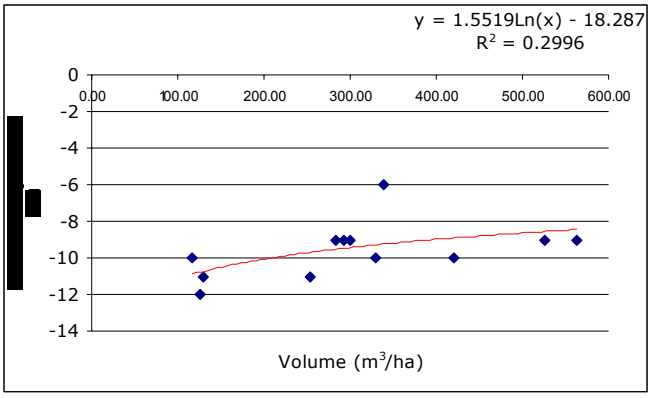

(a)

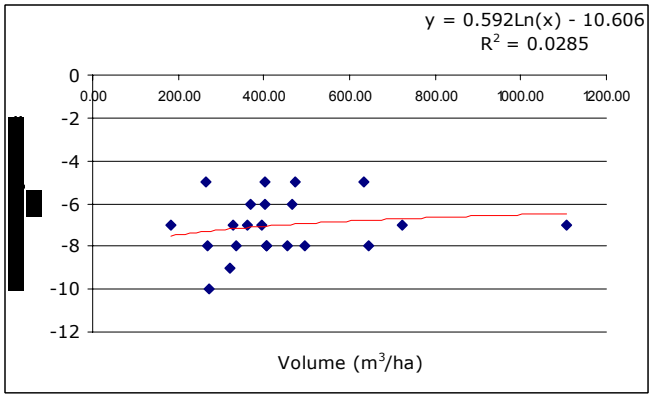

(d)

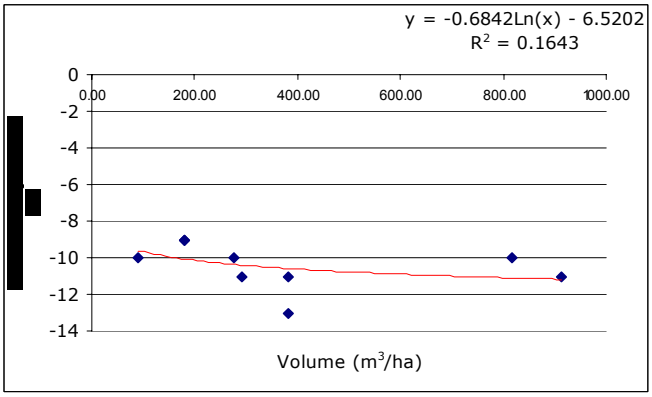

(b)

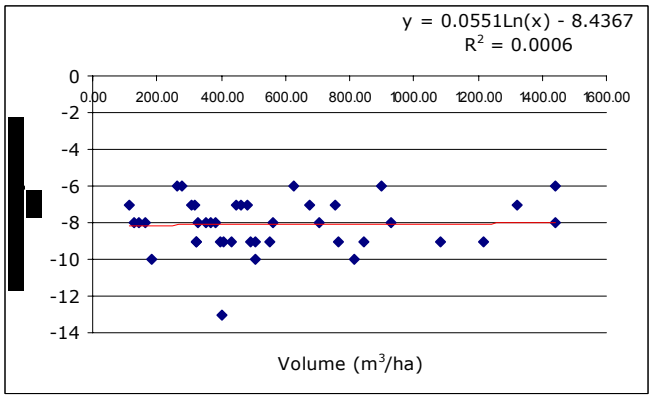

(e)

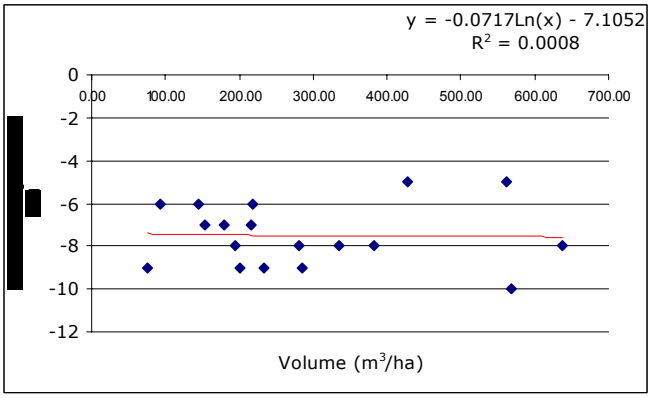

(c)

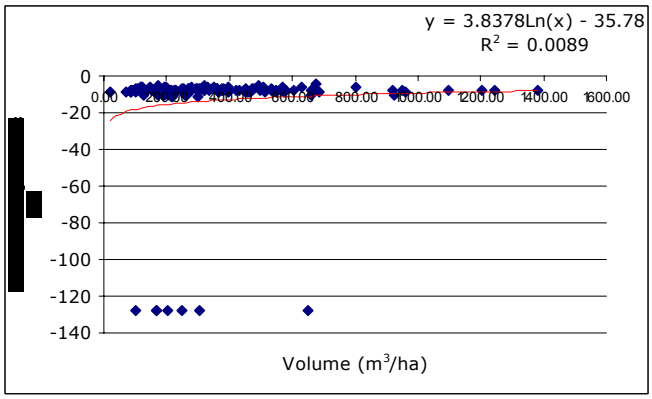

(f)

Fig. 6.11. Relationships between backscatter (cross polarization) and volume for (a) eucalyptus (b) sisham (c) jamun (d) teak (e) sal mixed (f) sal

From the above observation it is drawn that degree of correlation between red wavelength reflectance and volume gradually increases from sal forest through sal mixed forest and attained maximum at eucalyptus plantation. Red reflectance has highest correlation with volume (r^2 = 0.583) with eucalyptus plantation. The same trend is also seen in the case of Infra red reflectance with eucalyptus plantation achieving a correlation (r^2 = 0.54).

The degree of correlation between Normalized Difference Vegetation Index (NDVI) and volume gradually increases from sal forest, sal mixed forest, teak plantation, teak- eucalyptus plantation and attains a maximum with eucalyptus plantation. NDVI has highest correlation with volume (r^2 = 0.493) for eucalyptus plantation.

Similarly, the above observation draws that the relationship between backscattering coefficient (HH and HV) and volume gradually increases from sal forest, sal mixed forest, teak plantation and attains a maximum with eucalyptus plantation with HV Polarization. HV Polarization has highest correlation with volume (r^2 = 0.299) with eucalyptus plantation and r^2 = 0.095 (HH Polarization).

Table. 6.5. Relationships of forest volume with reflectance in red, Infra red, NDVI and backscattering coefficients

S. No.	Class	r^2				
		Red (DN)	Infra- red (DN)	NDVI (DN)	C- HH (dB)	C- HV (dB)
1	Eucalyptus Plantation	0.565	0.511	0.513	0.095	0.299
2	Sissoo Plantation	0.008	0.127	0.05	0.078	0.164
3	*Syzygium* Swamp Low Forest	0.014	0.053	0.026	0.007	0
4	Teak- Eucalyptus Plantation	0.285	0.350	0.124	0.008	0.007
5	Teak Plantation	0.095	0.026	0.070	0	0.028
6	Sal Mixed Forest	0.015	0.026	0.002	0.005	0
7	Sal Forest	0	0.004	0	0.008	0.008

6.5. Relationships of biomass with optical, NDVI and backscatter coefficients

The optical, NDVI (DN) values and calculated backscatter coefficient (like and cross polarizations) were extracted from the digital images (ETM and backscattering images) for all the sample plot locations. (Appendices- 3 and 4).

The following figures show the observed variations of all these digital responses with biomass. A logarithm function was used to derive the overall behavior of all the sample plots.

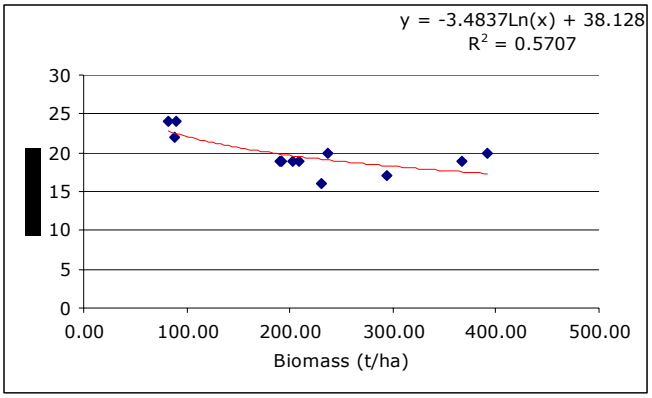

(a)

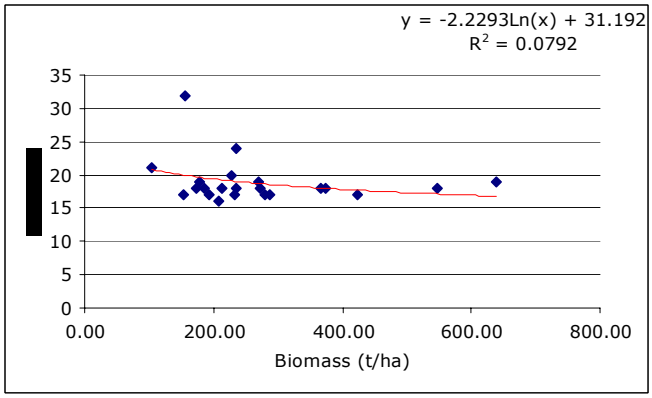

(d)

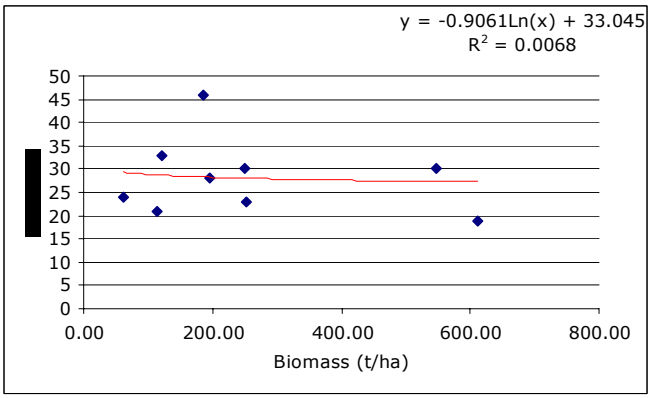

(b)

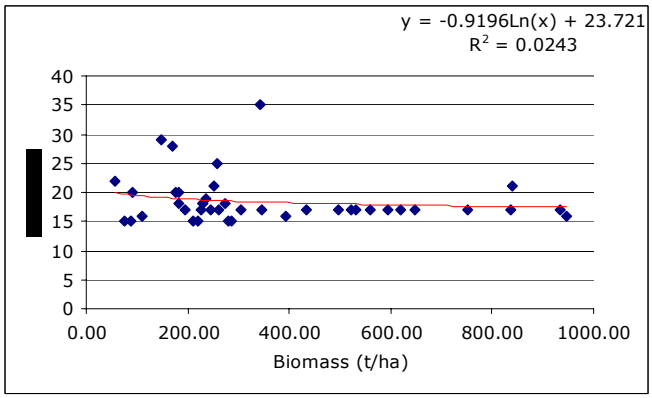

(e)

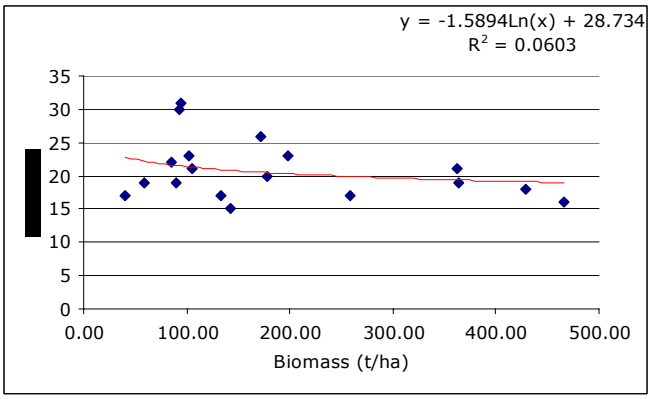

(c)

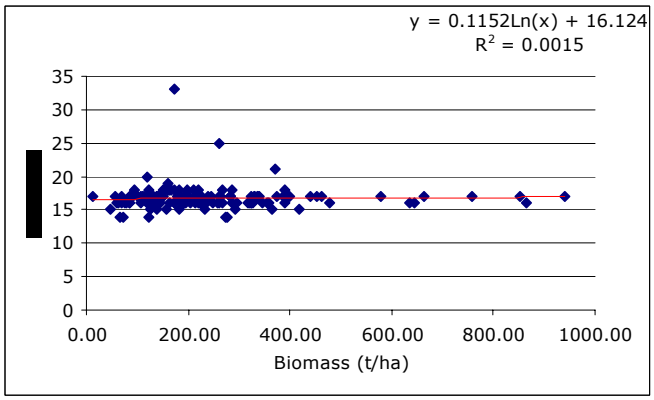

(f)

Fig. 6.12. Relationships between reflectance in red wavelength and biomass for (a) eucalyptus (b) sisham (c) jamun (d) teak (e) sal mixed (f) sal

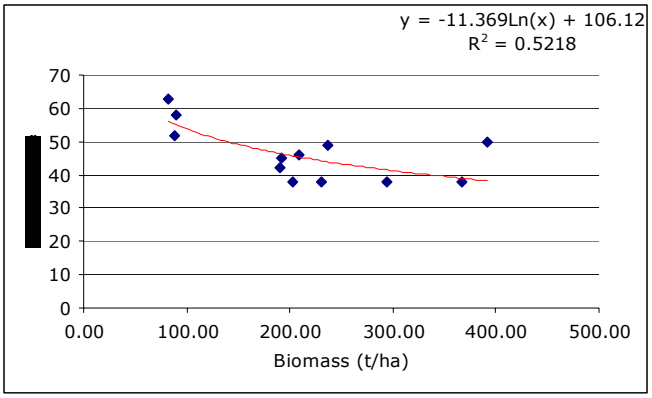

(a)

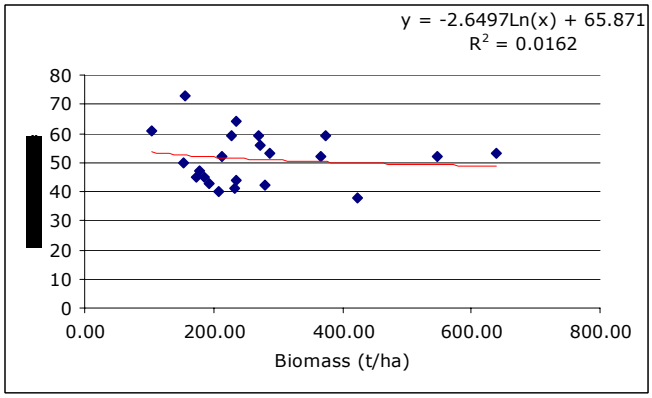

(d)

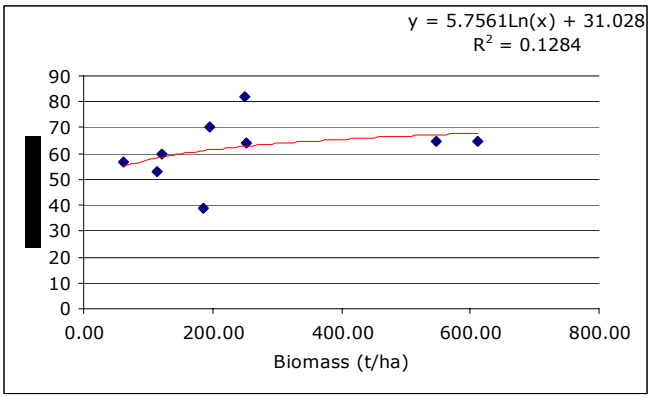

(b)

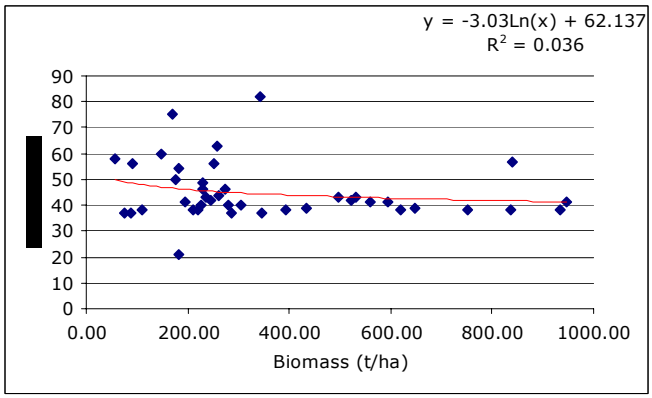

(e)

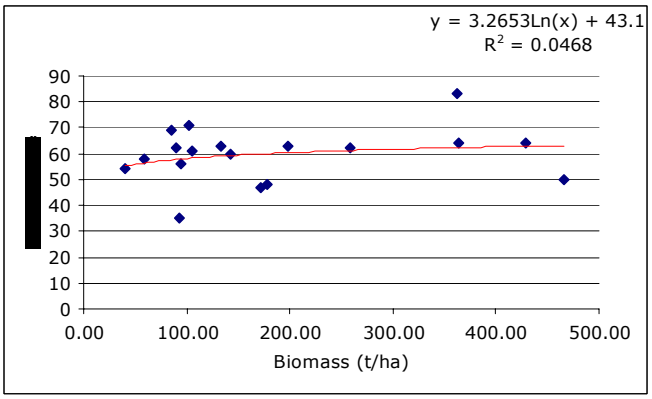

(c)

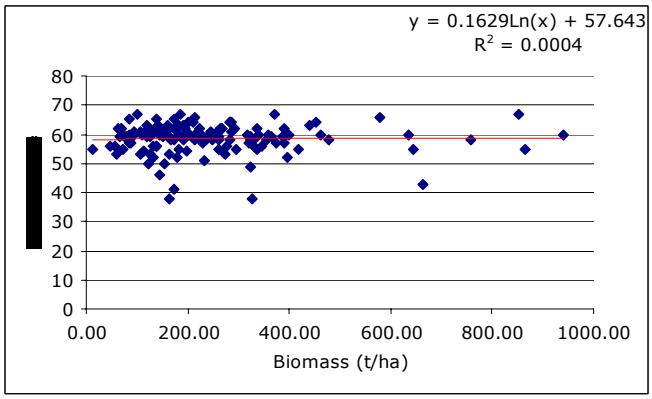

(f)

Fig. 6.13. Relationships between reflectance in infra red wavelength and biomass for (a) eucalyptus (b) sisham (c) jamun (d) teak (e) sal mixed (f) sal

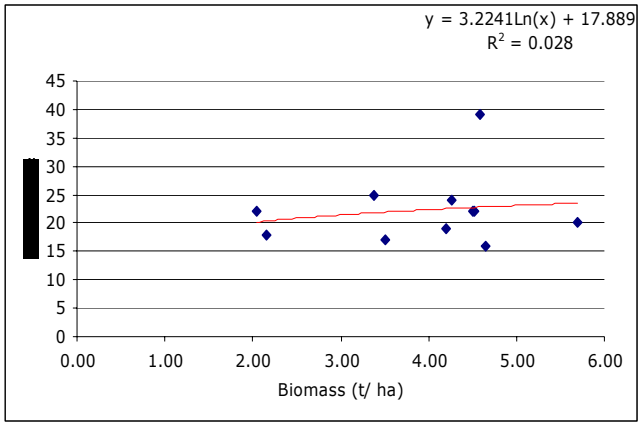

(g)

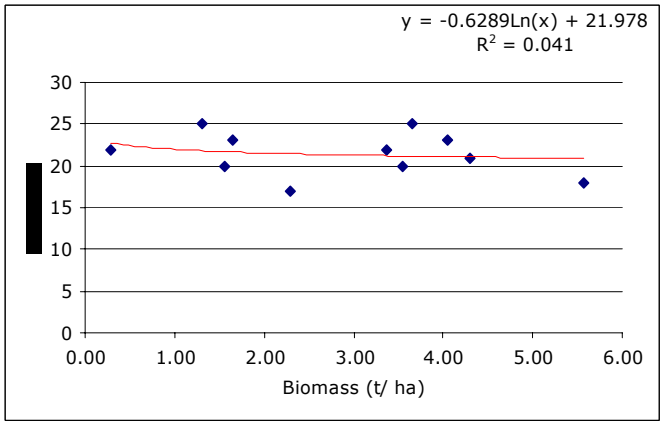

(h)

Fig. 6.14. Relationships between reflectance in red wavelength and biomass for (g) upland grass (h) lowland grass

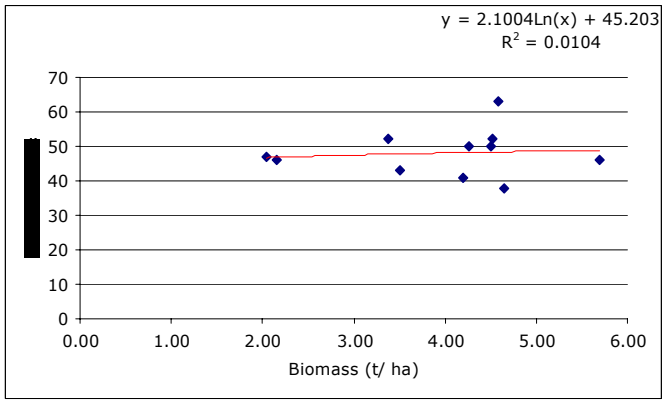

(g)

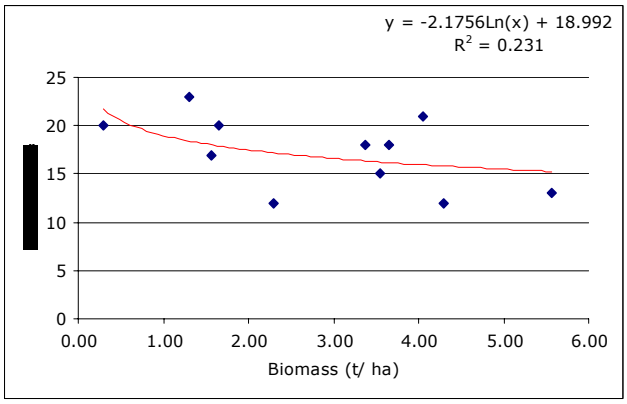

(h)

Fig. 6.15. Relationships between reflectance in infra red wavelength and biomass for (g) upland grass (h) lowland grass

From the above observation it is drawn that degree of correlation between red reflectance and biomass gradually increases from Sal forest through Sal mixed forest and attained maximum at eucalyptus plantation. Red reflectance has highest correlation with biomass ($r^2 = 0.57$) with eucalyptus plantation. The same trend is also seen with the case of Infra red reflectance with eucalyptus plantation achieving a correlation ($r^2 = 0.521$). And the relationship of Upland grass with red reflectance ($r^2 = 0.02$) and for lowland grass ($r^2 = 0.231$) with infra red reflectance.

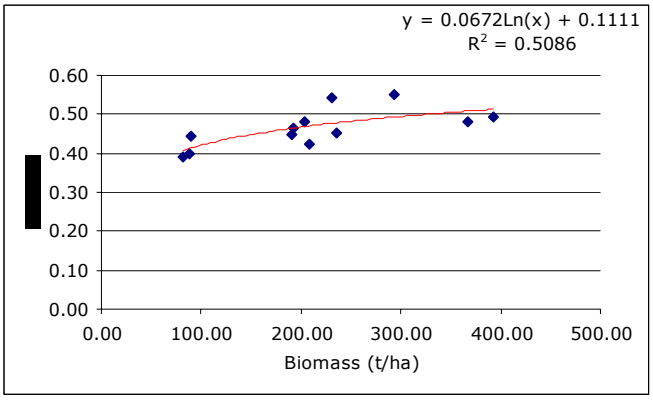

(a)

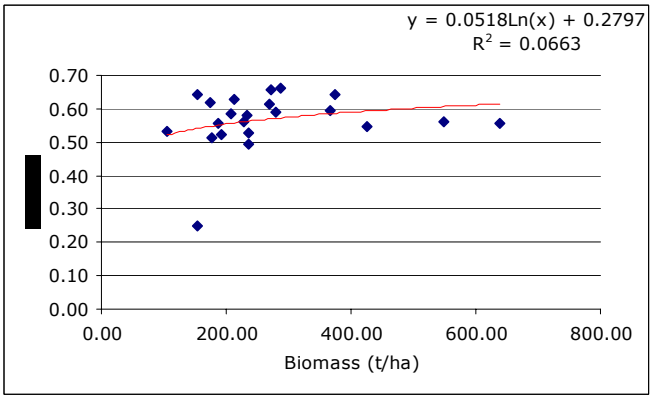

(d)

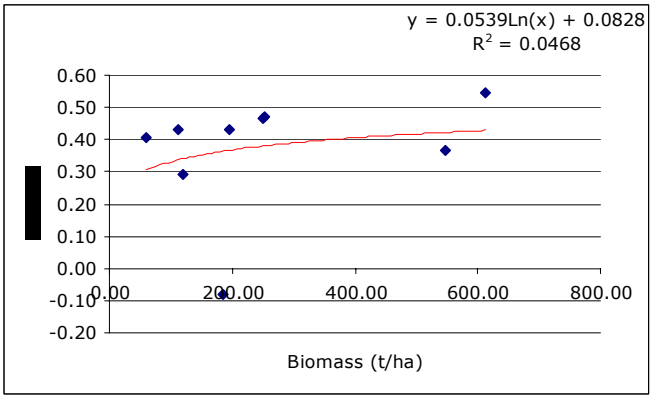

(b)

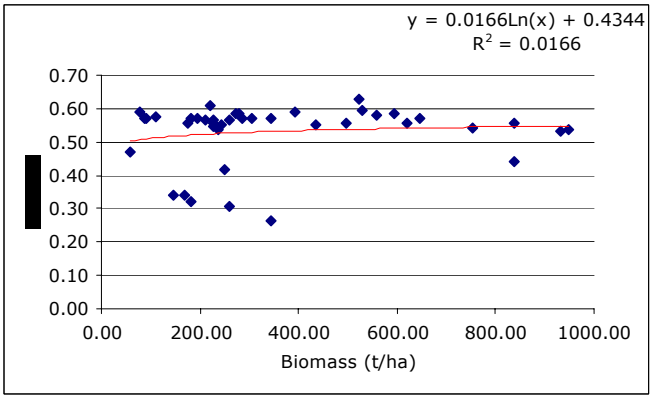

(e)

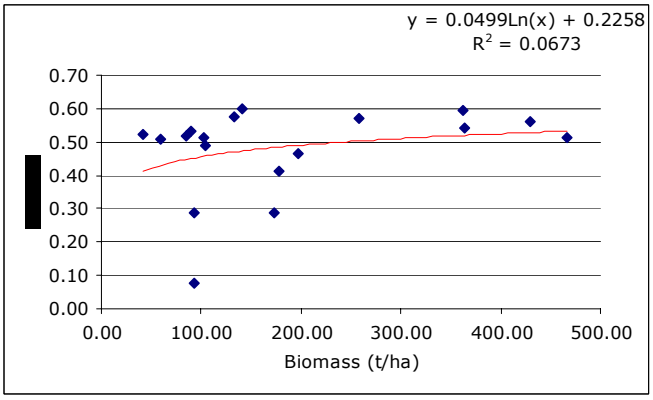

(c)

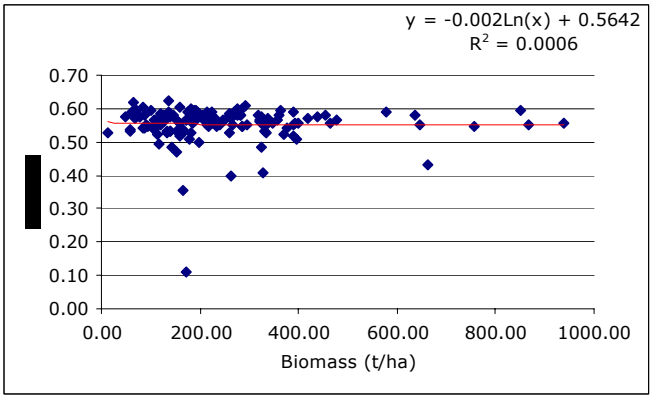

(f)

Fig. 6.16. Relationships between NDVI and biomass for (a) eucalyptus (b) sisham (c) jamun (d) teak (e) sal mixed (f) sal

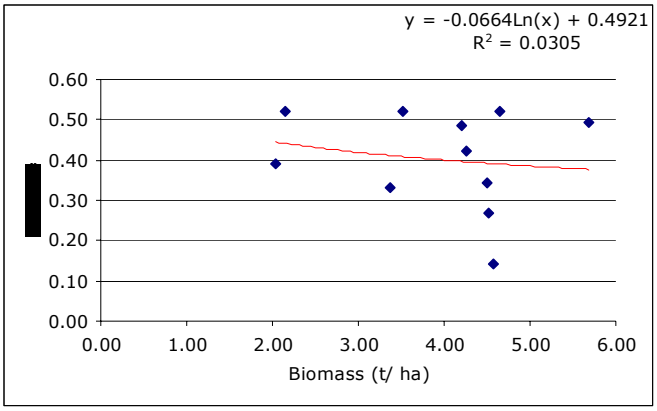

(g)

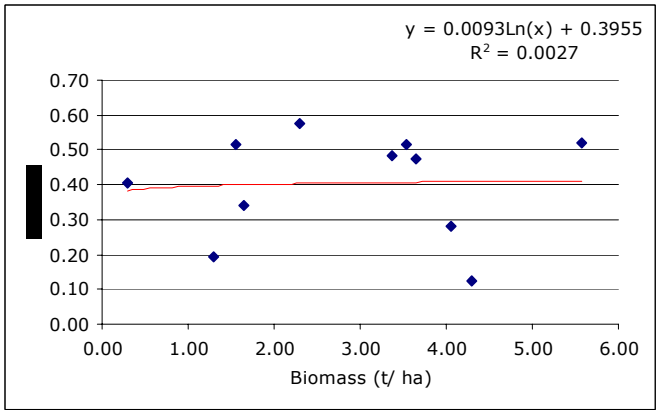

(h)

Fig. 6.17. Relationships between NDVI and biomass for (g) upland grass (h) lowland grass

From the above observation it is drawn that degree of correlation between Normalized Difference Vegetation Index (NDVI) and biomass gradually increases from Sal forest, Sal mixed forest, teak plantation, teak- eucalyptus plantation and attains a maximum with eucalyptus plantation. NDVI has highest correlation with biomass (r^2 = 0.508) for eucalyptus plantation.

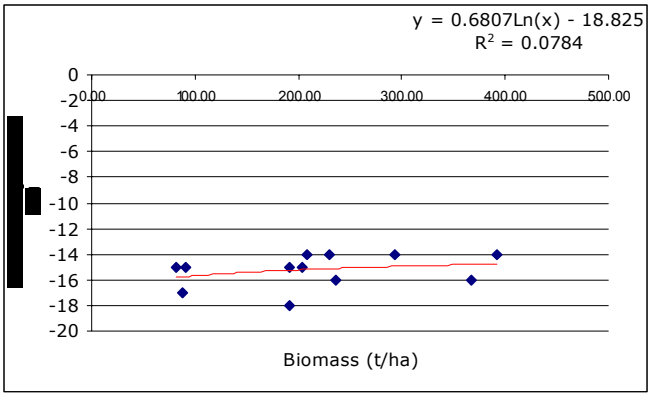

(a)

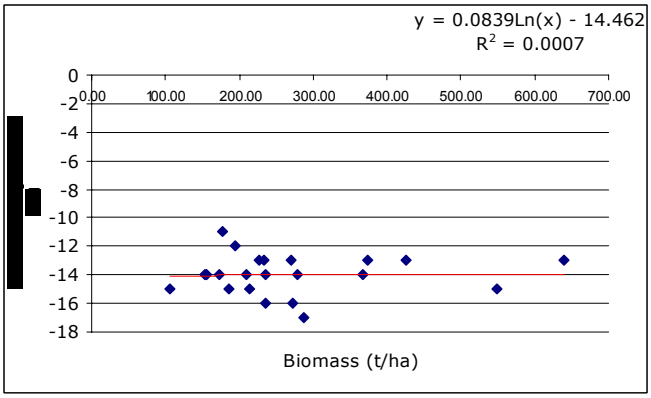

(d)

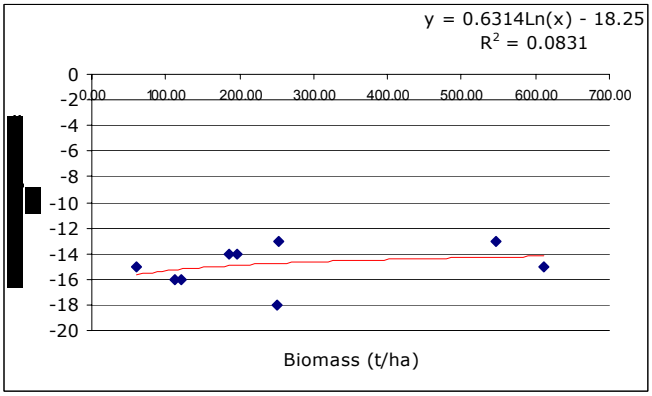

(b)

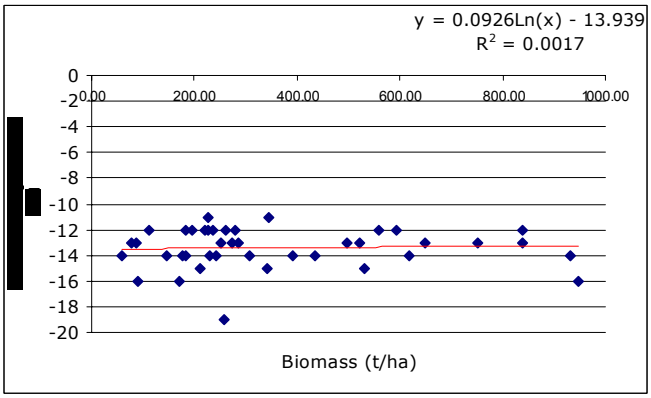

(e)

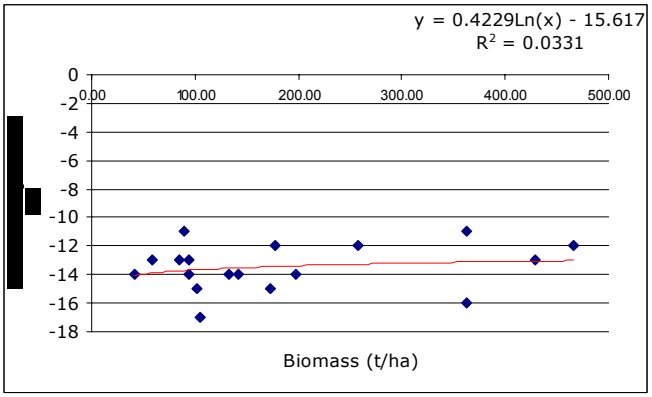

(c)

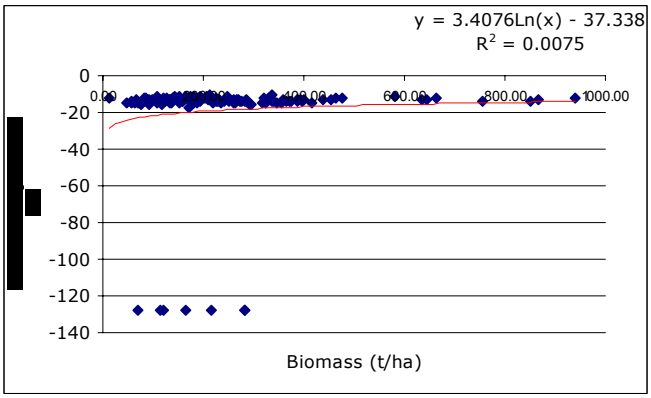

(f)

Fig. 6.18. Relationships between backscatter (like polarization) and biomass for (a) eucalyptus (b) sisham (c) jamun (d) teak (e) sal mixed (f) sal

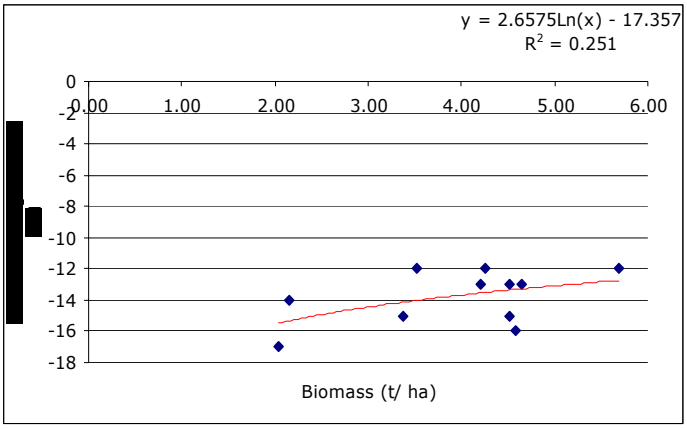

(g)

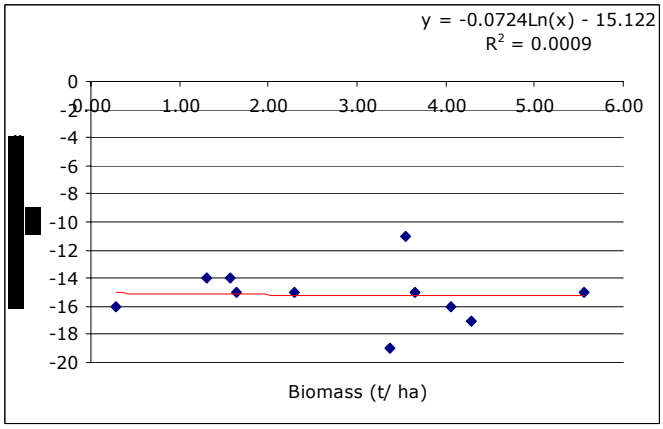

(h)

Fig. 6.19. Relationships between backscatter (like polarization) and biomass for (g) upland grass (h) lowland grass

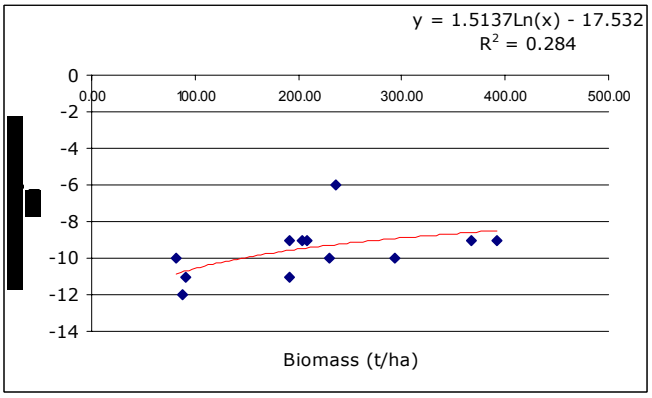

(a)

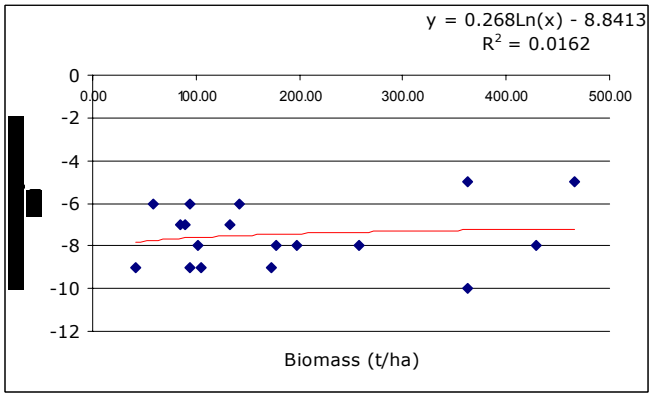

(c)

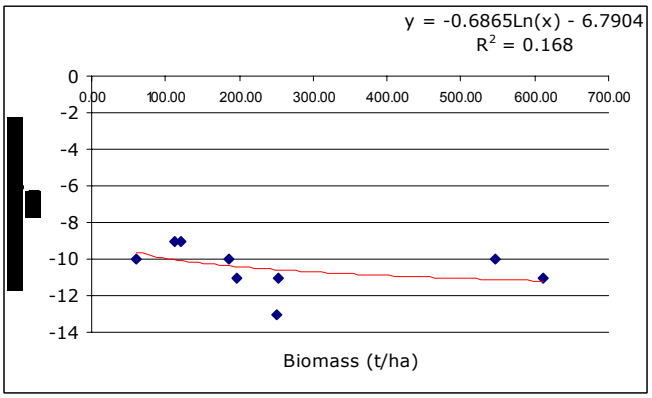

(b)

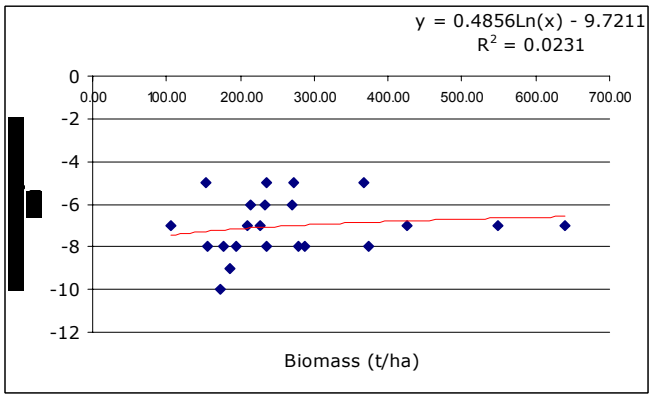

(d)

Fig. 6.20. Relationships between backscatter (cross polarization) and biomass for (a) eucalyptus (b) sisham (c) jamun (d) teak

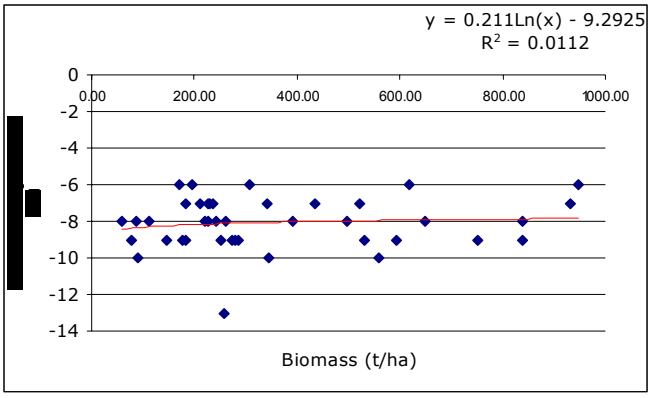

(e)

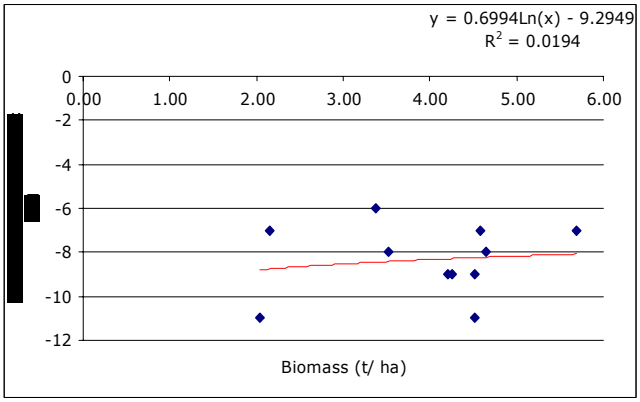

(g)

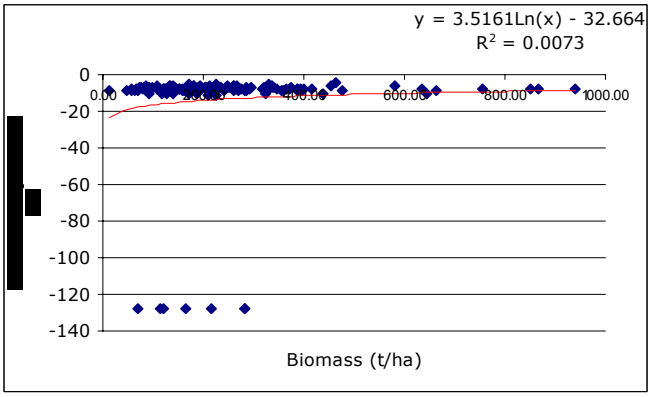

(f)

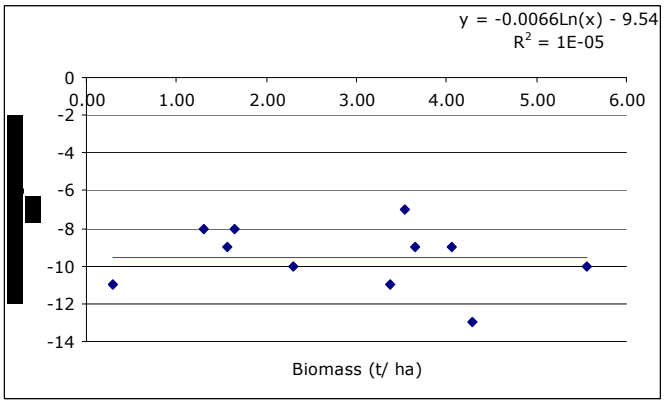

(h)

Fig. 6.21. Relationships between backscatter (cross polarization) and biomass for (e) sal mixed (f) sal (g) upland grass (h) lowland grass

From the above observation it is drawn that degree of correlation between backscattering coefficient (HH and HV) and biomass gradually increases from sal forest, sal mixed forest, teak plantation and attains a maximum with eucalyptus plantation with HV Polarization. HV Polarization has highest correlation with biomass ($r^2 = 0.284$) with eucalyptus plantation and sissoo plantation ($r^2 = 0.16$) with teak- eucalyptus plantation having ($r^2 = 0.134$) using HV Polarization whereas using HH ($r^2 = 0.137$) Polarization. For Upland grass being HH polarization ($r^2 = 0.251$).

Table. 6.6. Relationships of forest biomass with reflectance in red, Infra red, NDVI and backscattering coefficients

S. No.	Class	r^2				
		Red (DN)	Infra red (DN)	NDVI (DN)	C- HH (dB)	C- HV (dB)
1	Eucalyptus Plantation	0.57	0.521	0.508	0.078	0.284
2	Sissoo Plantation	0.006	0.128	0.046	0.083	0.168
3	*Syzygium* Swamp Low Forest	0.06	0.046	0.067	0.033	0.0162
4	Teak- Eucalyptus Plantation	0.353	0.165	0.128	0.137	0.134
5	Teak Plantation	0.079	0.016	0.066	0	0.023
6	Sal Mixed Forest	0.024	0.036	0.016	0.001	0.011
7	Sal Forest	0.001	0	0	0.007	0.007
8	Upland Grassland	0.028	0.01	0.03	0.251	0.019
9	Lowland Grassland	0.041	0.231	0.002	0	0.036

6.6. Classification Accuracy

To assess the classification accuracy, independent ground samples collected from the field work, fine resolution images and derived land cover (forest type and density) maps have been used. The cover type information of these locations (GPS points) was compared with classified maps. The field sample locations were overlaid on classified maps (Forest type and density) to assess corresponding classes. Two confusion matrix approach was followed for accuracy, Table 6.8 and Table 6.9 indicate the same. In this study, overall accuracy was 91.62 % and Khat coefficient was 0.89 using optical satellite data whereas 73.54 % and 0.71 overall accuracy and Khat coefficient respectively using ASAR data.

The user's accuracy in some of the classes viz., Tropical Semi- Evergreen Forest, Sissoo Plantation and Upland Grassland etc. is found relatively low using optical satellite data whereas Gulchaman Plantation, Grassland gets mixed up showing a very low with ASAR data. This is attributed to intermixing in the classes in different species composition. Some of the classes like Sal Forest, Sal Mixed Forest and Lowland Grassland (with optical) and Teak and Teak- Eucalyptus Plantations, *Syzygium* Swamp Low Forest, Eucalyptus Plantation (ASAR) showed a very good agreement. The non-forest categories showed a good agreement with optical data as comparative to ASAR derived classified maps. Some of the other classes viz., Eucalyptus Plantation, *Syzygium* Swamp Low Forest, Moist Mixed Deciduous Forest, Sal Forest, Teak Plantation and Khair- Sissoo Forest showed almost 100% accuracy with optical data and similar trend is also seen with Sissoo Plantation and Teak- Sissoo Plantation using ASAR data.

Table. 6.7. Confusion matrix (optical)

	Classes																							
Classes	DSF	R	EP	SSLF	Op	Wb	LG	SP	MMDF	UG	OSF	KSF	Ag	TSP	BSF	MSMF	TEP	TSEF	OSMF	DSMF	MSF	GP	TP	Total	User's accuracy (%)
DSF	67	0	0	0	0	0	0	0	0	0	0	0	0	0	0	0	0	0	0	0	0	1	68	98.53
R	0	5	0	0	0	0	0	0	0	1	0	0	0	0	0	0	0	0	0	0	0	0	6	83.33
EP	0	0	24	0	0	0	0	0	0	0	0	0	0	0	0	0	0	0	0	0	0	0	24	100.00
SSLF	0	0	0	36	0	0	0	0	0	0	0	0	0	0	0	0	0	0	0	0	0	0	36	100.00
Op	0	0	0	0	5	0	0	0	0	0	0	0	0	0	0	0	0	0	0	0	0	0	5	100.00
Wb	1		1	0	0	18	0	0	0	0	1	0	0	0	0	0	0	0	0	0	0	0	21	85.71
LG	0	0	0	0	0	0	29	0	0	1	0	0	0	0	0	0	0	0	0	0	0	0	30	96.67
SP	0	1	0	1	0	1	0	26	0	0	0	0	0	0	0	0	0	0	0	0	0	0	29	89.66
MMDF	0	0	0	0	0	0	0	0	15	0	0	0	0	0	0	0	0	0	0	0	0	0	15	100.00
UG	0	1	0	0	0	1	2	0	0	35	0	0	0	0	0	0	0	0	0	0	0	0	39	89.74
OSF	0	0	0	0	0	0	0	0	0	0	42	0	0	0	0	0	0	0	0	0	0	0	42	100.00
KSF	0	0	0	0	0	0	0	0	0	0	0	5	0	0	0	0	0	0	0	0	0	0	5	100.00
Ag	0	0	0	0	0	0	0	0	0	0	0	0	5	0	0	0	0	0	0	0	0	0	5	100.00
T- SP	0	0	0	0	0	0	0	0	0	0	0	0	0	2	0	0	0	0	0	0	0	0	2	100.00
BSF	0	0	0	0	0	0	0	0	0	0	0	0	0	0	1	0	0	0	0	0	0	0	1	0.00
MSMF	0	0	0	0	0	0	0	1	0	0	0	0	0	0	0	30	0	0	1	1	0	0	33	90.91
T- EP	0	0	0	0	0	0	0	0	0	1	0	0	0	0	0	0	10	0	0	0	0	0	11	90.91
TSEF	0	1	0	0	0	0	0	0	0	0	0	0	0	0	0	0	0	4	0	0	0	0	5	80.00
OSMF	0	0	0	0	0	0	0	0	0	0	0	0	0	0	0	0	0	0	5	0	0	0	5	100.00
DSMF	0	0	0	0	0	0	0	1	0	0	1	0	0	0	0	0	0	0	0	25	0	0	27	92.59
MSF	1	0	0	0	0	0	0	0	0	0	0	0	0	0	0	0	0	0	0	0	35	0	36	97.22
GP	0	0	0	0	0	0	0	0	0	0	0	0	0	0	0	0	0	0	0	0	0	1	1	100.00
TP	0	0	0	0	0	0	0	0	0	0	0	0	0	0	0		0	0	0	0	0	0	34	100.00
Total	69	8	25	37	5	20	31	28	15	38	44	5	5	2	1	30	10	4	6	26	35	1	35	480	
Producer's accuracy (%)	97.1	63	96	97.2	100	90	93.5	92.9	100	92.1	95.4	100	100	100	100	100	100	100	83.3	96.1	100	100	97.1		

Overall accuracy: 91.62

K_{hat} coefficient: 0.90

Table. 6.8. Confusion matrix (ASAR)

	Classes																
Classes	R	OSF	Ag	EP	TEP	Op	Wb	G	SP	TP	DSF	MSF	SSLF	TSEF	GP	Total	User's accuracy (%)
R	5	0	0	0	0	0	0	0	4	0	1	1	2	2	0	15	33.33
OSF	0	72	0	0	0	0	1	2	0	1	4	2	0	0	0	82	87.80
Ag	0	6	12	0	0	0	1	4	6	1	0	0	0	0	0	30	40
EP	0	1	0	28	0	1	2	1	1	1	1	1	2	0	0	39	71.79
TEP	0	1	0	1	12	0	0	1	0	1	0	0	0	0	0	16	75
Op	0	0	0	0	0	1	0	0	1	0	0	0	0	0	0	2	50
Wb	0	0	0	0	0	1	6	5	0	0	1	0	0	0	0	13	46.15
G	0	1	0	0	0	0	6	35	10	1	3	1	7	1	0	65	53.84
SP	0	0	0	0	0	0	0	0	1	0	0	0	0	0	0	1	100
TP	0	0	0	1	1	0	0	0	1	37	0	0	0	0	0	40	92.5
DSF	0	2	0	0	0	1	0	6	1		79	3	2	0	0	94	84.04
MSF	0	2	0	0	0	0	1	2	1	1	2	47	1	0	0	57	82.45
SSLF	2	0	0	0	0	0	0	0	0	0	0	0	10	0	0	12	83.33
TSEF	0	0	0	0	0	0	0	0	0	0	0	0	0	7	0	7	100
GP	0	0	0	2	0	0	0	2	0	0	0	1	1	0	1	7	14.28
Total	7	85	12	32	13	4	17	58	26	43	91	56	25	10	1	480	
Producer's accuracy (%)	71.32	84.71	100	88	92.31	25	35	60	3.82	86	86.81	83.90	40	70	100		

Overall accuracy: 73.54

K_{hat} coefficient: 0.71

DSF - Dense Sal Forest, EP - Eucalyptus Plantation, SSLF -*Syzygium* Swamp Low Forest, , Wb – Waterbody, LG - Lowland Grassland, SP - Sissoo Plantation, MMDF - Moist Mixed Deciduous Forest, UG - Upland Grassland, OSF - Open Sal Forest, K-SF - Khair- Sissoo Forest, Ag – Agriculture, T- SP - Teak- Sissoo Plantation, BSF - *Barringtonia* Swamp Forest, MSMF - Moderately Closed Sal Mixed Forest, T- EP - Teak- Eucalyptus Plantation, TSEF - Tropical Semi- Evergreen Forest, TP - Teak Plantation, OSMF - Low Sal Mixed Forest, DSMF - Dense Sal Mixed Forest, MSF - Moderately Closed Sal Forest, GP - Gulchaman Plantation, R - River,Op - Openland.

CHAPTER- 7

DISCUSSSION, CONCLUSIONS AND RECOMMENDATION

7.1. Discussion

Color composite images using combinations of the two SAR data configurations (C_{HV}, C_{HH}, C_{HH}) and optical remote sensing data were used to access the potential for estimating the forest stand volume and woody biomass. Using optical satellite data and visual interpretation, 15 forest types against 19 forest crown density/ cover classes have been classified very closed to the forest types as stated by Champion and Seth with 91.62 percent overall accuracy and Khat coefficient: 0.90 as compare to 73.54 percent overall accuracy and 0.71 Khat coefficient respectively using ASAR data. This shows that optical remote sensing data (Enhanced Thematic Mapper) onboard Earth Resources Satellite 'Landsat' can provide accurately forest type/ crown density classifications as compare to ASAR microwave data. But, the forest stands or vegetation classes like teak and Teak- Eucalyptus plantations were easily identifiable using the ASAR Gamma Filtered data (red mixed) against the gray background of the Sal forest than the optical satellite data. The number of classes reduces in the case of ASAR due to the intermixing of some of the major classes, e.g., sal forest merged with sal mixed forest due to similar trend of tone, texture and other associates, whereas sal forest can be sub- divided into three crown density classes: Dense Sal Forest (> 60%), Moderately Closed Sal Forest (40- 60%) and Open Sal Forest (< 40%) respectively from the optical data. Again, due to the spectral and texture mixing up of two grassland (both Upland and Lowland) in the ASAR data, so these are grouped as one class (grassland).

Sal forest being, the native and primary vegetative type in this terai region, alone contributes around a maximum mean volume of 631.86 m^3/ha. (± 352.42 S.D.) whereas a minimum of 212.47 m^3/ha. (± 24.12 S.D.) from both *Barringtonia* swamp forest and gulchaman plantation. The total volume estimated ranges from 91.38 m^3/ha (sisham plantation) up to 1442.71 m^3/ha (sal mixed forest). However, a total volume of 17.81 Mm^3 (sal forest) and a minimum of 0.07 Mm^3 (in the case of Khair- Sissoo Forest) is

observed with a total volume of 25.66 Mm^3. in the study area. As sal covers the top canopy having an old age, almost hugh girth and height, depicts the maximum mean volume.

From the aboveground woody biomass perspective, sal mixed forest contributing around a mean biomass of 360.54 t/ ha (± 243.51S.D.) and a minimum of 125.05 t/ ha (± 18.87 S.D.) from both *Barringtonia s*wamp forest and gulchaman plantation. The total biomass estimated ranges from 61.14 t/ha (sisham plantation) up to 947.98 t/ha (sal mixed forest).However, a total biomass of 1.42 Mt (sal mixed forest) and a minimum of 0.05 Mt (Khair- Shisham forest) with a total of 11.75 Mt is estimated from the study area.

In the case of grasslands, lowland grass contributes a mean biomass around 24.66 t/ ha (±21.57 S.D.) which depicts the water- logging condition and other conditions like anthropogenic activities e.g., forest fire, cutting and grazing. This grassland covers a total of 0.12 Mt as compared to 0.03 Mt in the upland grassland having a mean biomass approximately 10.74 t/ ha (± 8.10 S.D.). Hence, approximately 2.5 times higher in the lowland grassland than the upland grassland in mean biomass estimation (Kumar *et al*., 2002). Field data were collected in late march (cool season) depicting very low growth and productivity (total living biomass) than as expected during summer season with 24.66 t/ha against 3.95 t/ha in lowland grass. Thus, it is too early for measurements to reach its normal peak biomass.

In the block level analysis, tribal habitation/ agriculture occupying 69.74 km^2 (10.24 %) as largest area out of 681.11 km^2 and 2.60 km^2 (0.38 %) with Laudiria block (the least). The maximum total volume is found in Masankhamb block having 1.77 Mm^3 with maximum contribution of 1.29 Mm^3 from sal forest whereas Laudiria block having the least volume of 0.08 Mm^3 with highest contribution from teak plantation (0.06 Mm^3). Similar trend is also observed from the analysis that Masankhamb block contributes the highest total biomass of 0.79 Mt with significant contribution by sal forest with 0.50 Mt. Subsequently, Laudiria block contributes the least total biomass of 0.04 Mt with significant contribution from teak plantation (0.03 Mt).

From the remote sensing data responses and interaction with the field derived volume and woody biomass, the eucalyptus plantation has got the highest correlation with reflectance in red wavelength region (r^2 = 0.565) against r^2 = 0.511 with Infra red region and this class also give a good agreement with NDVI value (r^2 = 0.513) as compared to other forest type. Whereas, cross polarization ASAR data gives a weak correlation of r^2 = 0.299 as compare to r^2 = 0.09 for like polarization. This confirms the poor significant relationship with both optical and backscattering coefficients.

For biomass, eucalyptus plantation had r^2 = 0.57 with reflectance in red wavelength region and r^2 = 0.521 (infra red region). With NDVI value (r^2 = 0.508) as compared to other forest type. Whereas, with cross ASAR data, it achieved a weak correlation of r^2 = 0.284 against r^2 = 0.078 for like polarization. In the case of grassland, the Upland Grassland and like polarization having r^2 = 0.251; and Lowland Grass (r^2 = 0.231) with infra red wavelength region.

So, no significant relationships was noticed between the reflectance in red and infra red wavelengths region, NDVI and SAR responses with forest volume and biomass; the highest correlation coefficient derived (r^2 = 0.299) was with the cross polarization (volume) for eucalyptus plantation while r^2 = 0.95 (like polarization). Only weak relationships were observed in all the cases.

7.2. Conclusions and Recommendations

It has been demonstrated that remote sensing data can provide accurately forest classifications to the species level better than 90 % (optical satellite data) and up to 70 % (ASAR) overall accuracy. EnviSat C- Band ASAR and optical data were related to the above ground volume and dry biomass of North Indian Moist Deciduous Forest type in India. The teak and teak- Eucalyptus plantations at the test site were easily identifiable visually indicating red mixed. No significant correlations were observed for C- Band ASAR data in the conventional radar polarization configurations of HV and HH.

The stand chosen were around 1 ha and situated at 25.8 º - 31.2 º incidence angles from the SAR viewing angle. The values of the red, Infra- red and backscattering coefficients (σ^o) for eucalyptus, shisham, teak- eucalyptus plantation, teak plantation, sal mixed forest and sal forest stands were plotted against their mean volume and woody biomass in all the cases with respect to tropical forest. If stands of different are mixed, the correlation co- efficient and the sensitivities exhibit significantly lower values, however which indicates that bole volume is limited to a species level in the study area. Thus, at C- band, most of the backscattered energy originates from the upper canopy/ crown layer. Since, the signal becomes saturated at small bole volumes, the sensitivity and the correlation with these bole volumes and biomass are negligible. Moreover, the crown layers are very similar in the forest that has been analysed, all exhibiting approximately the same σ º (-5 to -13).

The results indicated that radar backscatter may be insensitive to variations in above ground volume and biomass at levels beyond some quoted backscatter saturation levels. We obtained poor results from ASAR for aboveground forest volume and biomass estimates using dual polarizations. This results show that a longer wavelength than C-band is recommended in order to retrieve both these bio- physical parameters and with the present ASAR dataset, a high incidence angle of 30.8º to 42.7º (SI 4- 6 Beam product) should be utilized for such studies.

The capability of microwave energy to penetrate forest vegetation makes possible the extraction of information on both the foliar and woody components from radar data. Depth of penetration, and hence the type of derivable information, is dependent upon parameters relating to both radar sensor and the target such as the wavelength, polarizations and incidence angle used, as well as the geometric and dielectric properties of the leaves, twigs and small branches. At C- Band, the backscattered energy is correlated mainly with the crown constituents such as leaves, twigs and small branches. Information on the other components beneath the canopy can be sensed through the use of bands with longer with longer wavelengths such as the L- or P- band. The sensitivity of co- polarized and cross- polarized waves to the shapes and orientation of the different tree constituents provide an added advantage in the information extraction procedure.
It has been found from the above study that the C- HV polarization shows the highest correlation for the all the cases. Given the relatively greater degree of penetration by horizontally polarized waves and the strong interaction of the vertically polarized energy with the vertically oriented canopy parts, different wavelength – polarization combinations can be used to suit the purpose of the study.

Thus the study indicated poor relationship between backscattering coefficients, forest volume and biomass. Microwave data with higher incidence angle, longer wavelength and cross polarizations could have given better results.

REFERENCES

Alves, D. S, and Skole, D. L., 1996. Characterizing land cover dynamics using multitemporal imagery. *International Journal of Remote Sensing*, 17, 835–839.

Anonymous, 1983. Nationwide mapping of forest and non-forest areas using Landsat False Color Composite for the period 1972–75 and 1980–82, National Remote Sensing Agency, Hyderabad, Technical Report, 1, 1–36.

Anonymous, 2001. Management Plan of Dudwa Tiger Reserve: 2001- 2001 to 2009- 2010, Uttar Pradesh, 407.

Ardo, J., 1992. Volume quantification of coniferous forest compartments using spectral radiance record by Landsat Thematic Mapper. *International Journal of Remote Sensing*, 13, 1779–1786.

Aronoff, S., 1989. Geographic Information Systems: A Management Perspective, WDL Publications, Ottawa, Canada.

Baccini, A., Friedl, M.A., Woodcock, C.E. and Warbington, R., 2004. Forest biomass estimation over regional scales using multisource data. *Geophysical Research Letters*, 31, L10501, doi: 10.1029.

Barbosa, P.M., Stroppiana, D. and Gregoire, J., 1999. An assessment of vegetation fire in Africa 1981–1991: burned areas, burned biomass, and atmospheric emissions. *Global Biogeochemical Cycles*, 13, 933–950.

Beaudoin, A., Le Toan, T., Goze, S., Nezry, E., Lopes, A., Mougin, E., Hsu, C.C., Han, H.C., Kong, J.A. and Shin, R.T., 1994. Retrieval of forest biomass from SAR data. *International Journal of Remote Sensing*, 15, 2777–2796.

Bell, D.J., Oliver, W.L.R., 1992. Northern Indian tall grasslands: management and species conservation with special reference to fire. In: Singh, K.P., Singh, J.S. (Eds.), Tropical Ecosystems: Ecology and Management. Wiley Eastern, New Delhi, pp. 109-123.

Blanchard, B. J., and Chang, A.T.C., 1983. Estimation of soil moisture from Seasat SAR data. *Water Resources Bulletin*, American Water Resources Association, 19 (5), 803-810.

Botkin, D. B., Estes, J. E., Mcdonald, R. M. and Wilson, M.V., 1984. Studying the Earth's vegetation from space; *BioScience*, 34, 508.

Boyd, D.S., Foody, G.M. and Curran, P.J., 1999. The relationship between the biomass of Cameroonian tropical forests and radiation reflected in middle infrared wavelengths (3.0–5.0 *m*m). *International Journal of Remote Sensing*, 20, 1017–1023.

Browden, L.W., and Pruitt, E.L., 1983.Manual of Remote Sensing, American Remote Sensing Agency, USA.

Brown, S. and Gaston, G., 1995. Use of forest inventories and geographic information systems to estimate biomass density of tropical forests: application to tropical Africa. *Environmental Monitoring and Assessment*, 38, 157–168.

Brown, S. and Iverson, L.R., 1992. Biomass estimation for tropical forests. World Resource Review, 4, 366–384.

Brown, S., 2002. Measuring carbon in forests: current status and future challenges. *Environmental Pollution*, 116, 363–372.

Brown, S., Gillespie, A.J.R. and Lugo, A.E., 1989. Biomass estimation methods for tropical forests with applications to forest inventory data. *Forest Science*, 35, 881–902.

Burrough, P.A., and Mc Donnell, R. 1998. Principles of geographical information systems, Oxford University Press, U.K.

Calva˜,O, T. and Palmeirim, J.M., 2004. Mapping Mediterranean scrub with satellite imagery: biomass estimation and spectral behaviour. *International Journal of Remote Sensing*, 25, 3113–3126.

Castel, T., Guerra, F., Caraglio, Y. and Houllier, F., 2002. Retrieval biomass of a large Venezuelan pine plantation using JERS-1 SAR data: analysis of forest structure impact on radar signature. *Remote Sensing of Environment*, 79, 30–41.

Champion, H. G. and Seth, S. K., 1968. *A Revised Survey of Forest Types of India,* New Delhi: Government of India Publication.

Chauhan, N. R., Lang, R. H., and Ranson, K. J., 1991. Radar modeling of a boreal forest. *IEEE Transactions on Geoscience and Remote Sensing*, 29, 627-638.

Curran, P. J., and Franquin, P., 1980. Multispectral remote sensing of vegetation amount. *Progress in Physics of Geography*, 4, 315-341.

Davis, B.E., 2001. GIS: Avisual approach, Delmar Thomson Learning, Albany.

De Jong, S.M., Pebesma, E.J. and Lacaze, B., 2003. Above ground biomass assessment of Mediterranean forests using airborne imaging spectrometry: the DAIS Peyne experiment. *International Journal of Remote Sensing*, 24, 1505–1520.

Dobson, M. C., Ulaby, F. T., and Pierce, L. E., 1995a. Land-cover classification and estimation of terrain attributes using synthetic aperture radar. *Remote Sensing of Environment*, 51 (1), 199-214.

Dobson, M. C., Pierce, L. E., Sarabandi, K., Ulaby, F.T., and Sharik, T.L., 1992a. Preliminary analysis of ERS-1 SAR for forest ecosystem studies. *IEEE Transactions on Geoscience and Remote Sensing*, 30 (2), 203-211.

Dobson, M. C., Ulaby, F. T., Le Toan, T., Beaudoin, A., Kasischke, E.S., and Christensen, N.L., 1992, Dependence of radar backscatter on coniferous forest biomass. *IEEE Transactions on Geoscience and Remote Sensing*, 30, 412- 414.

Dobson, M.C., Ulaby, F.T., Pierce, L.E., Sharik, T.L., Bergen, K.M., Kellndorfer, J., Kendra, J.R., Li, E., Lin, Y.C., Nashashibi, A., Sarabandi, K.L. and Siqueira, P., 1995b. Estimation of forest biomass characteristics in northern Michigan with SIR-C/ XSAR data. *IEEE Transactions on Geoscience and Remote Sensing*, 33, 877–894.

Dong, J., Kaufmann, R.K., Myneni, R.B., Tucker, C.J., Kauppi, P.E., Liski, J., Buermann, W., Alexeyev, V. and Hughes, M.K., 2003. Remote sensing estimates of boreal and temperate forest woody biomass: carbon pools, sources, and sinks. *Remote Sensing of Environment*, 84, 393–410.

Durden, S. L., Van Zyl, J. J., and Zebker, H. A., 1989. Modeling and observation of the radar polarization signature of forested areas. *IEEE Transactions on Geoscience and Remote Sensing*, 27, 290-301.

FAO, 1999, State of the World's Forests 1999. FAO report (Rome, Italy: FAO).

Fazakas, Z., Nilsson, M., and Olsson, H., 1999. Regional forest biomass and wood volume estimation using satellite data and ancillary data. *Agricultural and Forest Meteorology*, 417–425.

Fearnside, P. M., and Guimara~ es, W. M., 1996, Carbon uptake by secondary forests in Brazilian Amazonia. *Forest Ecology and Management*, 80, 35–46.

Fisher, P., 1997. The pixel: a snare and a delusion. *International Journal of Remote Sensing*, 18, 679–685.

Foody, G.M., Boyd, D.S. and Cutler, M.E.J., 2003. Predictive relations of tropical forest biomass from Landsat TM data and their transferability between regions. *Remote Sensing of Environment*, 85, 463–474.

Foody, G.M., Cutler, M.E., Mcmorrow, J., Pelz, D., Tangki, H., Boyd, D.S. and Douglas, I., 2001. Mapping the biomass of Bornean tropical rain forest from remotely sensed data. *Global Ecology and Biogeography*, 10, 379–387.

Franco-Lopez, H., Ek, A.R. and Bauer, M.E., 2001. Estimation and mapping of forest stand density, volume, and cover type using k-nearest neighbors method. *Remote Sensing of Environment*, 77, 251–274.

Franklin, J. and Hiernaux, P.Y.H., 1991. Estimating foliage and woody biomass in Sahelian and Sudanian woodlands using a remote sensing model. *International Journal of Remote Sensing*, 12, 1387–1404.

Fransson, J.E.S., and Israelsson, H., 1999, Estimation of stem volume in boreal forests using ERS-1 C- and JERS-1 L- band SAR data. *International Journal of Remote Sensing*, 20, 123- 137.

Fraser, R.H. and Li, Z., 2002. Estimating fire-related parameters in boreal forest using SPOT VEGETATION. *Remote Sensing of Environment*, 82, 95–110.

FSI, 1996. Volume Equations for Forests of India, Nepal and Bhutan – Forest Survey of India, Dehradun, pp, 6-45.

Gautam, B.R., 2005. Forest land use Planning a precursor to Decision Support System, Project report, CSSTEAP, Dehradun, India.

Halme, M. and Tomppo, E., 2001. Improving the accuracy of multisource forest inventory estimates by reducing plot location error—a multicriteria approach. *Remote Sensing of Environment*, 78, 321–327.

Harrell, P.A., Kasischke, E.S., Bourgeau-Chavez, L.L., Haney, E.M. and Christensen, N.L. J.R., 1997, Evaluation of approaches to estimating aboveground biomass in southern pine forests using SIR-C data. *Remote Sensing of Environment*, 59, 223–233.

Hatfield, J. L., 1983. Remote sensing estimates of potential and actual crop yield. *Remote Sensing of Environment*, 13, 301-311.

Henderson, F.M. and Lewis, A.J., (Eds). 1998. Principles and Applications of Imaging Radar: Manual of Remote Sensing (3 Ed.), John Wiley and Sons, New York.

Holben, B. N., & Fraser, R. S., 1984. Red and near infrared response to offnadir viewing. *International Journal of Remote Sensing*, 5, 145-160.

Honza´, K, M., Lucas, R.M., Do Amaral, I., Curran, P.J., Foody, G.M. and Amaral, S., 1996. Estimation of the leaf area index and total biomass of tropical regenerating forests: comparison of methodologies. In Amazonian Deforestation and Climate, J.H.C. Gash, C.A. Nobre, J.M. Roberts and R.L. Victora (Eds), Chichester: John Wiley, 365–381.

Houghton, R. A. and Woodwell G. M., 1981. Biotic contributions to the global carbon cycle: the role of remote sensing; *Proc Seventh International Symposium on Machine Processing of Remote Sensed Data*, West Lafayette, Indiana, 593–602.

Houghton, R.A., Lawrence, K.T., Hackler, J.L. and Brown, S., 2001. The spatial distribution of forest biomass in the Brazilian Amazon: a comparison of estimates. *Global Change Biology*, 7, 731–746.

Hussin, Y. A., Reich R. M., and Hoffer R. M., 1991. Estimating slash pine biomass using radar backscatter. *IEEE Transactions on Geoscience and Remote Sensing*, 29, 427-431.

Imhoff, M.L., Johnson, P., Holford, W., Hyer, J., May, L., Lawrence, W. and Harcombe, P., 2000, BioSar (TM): an inexpensive airborne VHF multiband SAR system for vegetation biomass measurement. *IEEE Transactions on Geoscience and Remote Sensing*, 38, 1458–1462.

Imhoff, M. L., 1995, Radar backscatter and biomass saturation: ramifications for global biomass inventory. *IEEE Ttransactions on Geoscience and Remote Sensing*, 33, 511–518.

IPCC, 2003. Good Practice Guidance for Land Use, Land-Use Change and Forestry. IPCC National Greenhouse Gas Inventories Programme, Hayama, Japan, 295.

Israelsson, H., Askne, J., Sylvander, R., 1994. Potential of SAR for forest bole volume estimation, *International Journal of Remote Sensing*, 15 (14), 2809- 2826.

IUCN, 1993. Nature reserves of the Himalaya and the mountains of Central Asia. Prepared by the World Conservation Monitoring Centre. Gland, Switzerland: Oxford Univ. Press.

Jackson, R. D., Slater, P. N., and Pinter, P. J., 1983. Discrimination of growth and water stress in wheat by various vegetation indices through clear and turbid atmospheres. *Remote Sensing of Environment*, 15, 187-208.

Javed, S., 1996. Studies on Bird Community Structure on *Terai* Forest in Dudwa National Park. Ph.D. Thesis, Centre for Wildlife and Ornithology, Aligarh Muslim University, Aligarh (India): 149 pp.

Justice, C. O., Townshend, J. R.D., Holben, B.N., and Tucker, C. J., 1985. Analysis of the phenology of global vegetation using meteorological satellite data. *International Journal of Remote Sensing*, 6, 1271-1381.

Kachhawaha, T.S., 1990-'Large Scale Forest / Vegetation Mapping in Rajaji National Park, Uttar Pradesh using Landsat TM and IRS 1A LISS II Satellite data'. Project Report RSAC-UP, Lucknow.

Kasischke, E.S., Goetz, S., Hansen, M.C., Ustin, S.L., Ozdogan, M., Woodcock, C.E. and Rogan, J., 2004, Temperate and boreal forests. In: *Remote Sensing for Natural Resource Management and Environmental Monitoring*, S.L. Ustin (Ed.), Hoboken, NJ: John Wiley and Sons, pp. 147–238.

Kasischke, E.S., Melack, J.M. and Dobson, M.C., 1997. The use of imaging radars for ecological applications—a review. *Remote Sensing of Environment*, 59, 141–156.

Krankina, O.N., Harmon, M.E., Cohen, W.B., Oetter, D.R., Zyrina, O., and Duane, M.V., 2004. Carbon stores, sinks and sources in forests North western Russia: Can we reconcile forest inventories with remote sensing results? *Climatic Change*, 67, 257-272.

Kumar, H., Mathur, P.K., Lehmkuhl, J.F., Khati, D.S., De, R., and Longwah, W., 2002. Terai Conservation Area (TCA), Vol. 6, Report, Wildlife Institute of India, Dehradun, 37-84.

Kuplich, T.M., Curran. P.J., and Atkinson, P.M., 2005. Relating SAR image texture to the biomass of regenerating tropical forests. *International Journal of Remote Sensing*, 26, 21, 4829- 4854.

Kuplich, T.M., Salvatori, V. and Curran, P.J., 2000. JERS-1/SAR backscatter and its relationship with biomass of regenerating forests. *International Journal of Remote Sensing*, 21, 2513–2518.

Lang, R. H., Chauhan, N. S., Ranson, J. K., and Kilic, O., 1994. Modeling P-band SAR returns from a red pine stand. *Remote Sensing of Environment*, 47, 132-141.

Le Toan, T., Beaudoin, A., Riom, J., and Guyon, D., 1992. Relating forest biomass to SAR data. *IEEE Transactions on Geoscience and Remote Sensing*, 30, 403–411.

Leblon, B., Granberg, H., Ansseau, C. and Royer, A., 1993. A semi-empirical model to estimate the biomass production of forest canopies from spectral variables, part 1: relationship between spectral variables and light interception efficiency. *Remote Sensing Reviews*, 7, 109–125.

Leckie, D.G., 1998. Forestry applications using imaging radar: Principles and applications of Imaging Radar, In: Manual of Remote Sensing (3rd Edn), Vol. 2, F.M. Henderson and A.J. Lewis (Eds), Chichester: John Wiley and Sons, 437–509.

Lefsky, M.A., Cohen, W.B. and Spies, T.A., 2001. An evaluation of alternate remote sensing products for forest inventory, monitoring, and mapping of Douglas fir forests in western Oregon. *Canadian Journal of Forest Research*, 31, 78–87.

Lehtonen, A., Mäkipää, R., Heikkinen, J., Sievänen, R. and Liski, J. 2004. Biomass expansion factors (BEFs) for Scots pine, Norway spruce and birch according to stand age for boreal forests. *Forest Ecology and Management*, 188, 211-224.

Lehmkuhl, J.F., 1994. A classification of subtropical riverine grassland and forest in Chitwan National Park, Nepal. Vegetatio, 111, 29- 43.

Lillesand, T.M., and Kiefer, R.W., 1999. Remote Sensing and Image interpretation. New York: John Willy and Sons.

Limaye, V.D., and Sen, B.R., 1956. *Indian Forest Records*: *Timber Mechanics*. Manager of Publications, Delhi.

Lu, D., 2005. Aboveground biomass estimation using Landsat TM data in the Brazilian Amazon Basin. *International Journal of Remote Sensing*, 26, 2509–2525.

Lucas, R.M., Curran, P.J., Honzak, M., Foody, G.M., Do Amaral, I. and Amaral, S., 1998. The contribution of remotely sensed data in the assessment of the floristic composition, total biomass and structure of Amazonian tropical secondary forests. In: *Regenerac¸ao˜ Florestal: Pesquisas na Amazonia*, (C. Gascon and P. Moutinho Eds), Manaus: INPA Press, 61–82.

Lucas, R.M., Held, A.A., Phinn, S.R. and Saatchi, S., 2004. Tropical forests. In Remote Sensing for Natural Resource Management and Environmental Monitoring, S.L. Ustin (Ed.), Hoboken, NJ: John Wiley and Sons, 239–315.

Luckman, A., Baker, J., Honzak, M. and Lucas, R., 1998. Tropical forest biomass density estimation using JERS-1 SAR: seasonal variation, confidence limits, and application to image mosaics. *Remote Sensing of Environment*, 63, 126–139.

Luckman, A., Baker, J.R., Kuplich, T.M., Yanasse, C.C.F. and Frery, A.C., 1997. A study of the relationship between radar backscatter and regenerating forest biomass for space borne SAR instrument. *Remote Sensing of Environment*, 60, 1–13.

Maheshwaran, G., 1998. Ecology of Black- Necked Stork in Dudwa National Park. Ph.D. Thesis. Centre for Wildlife and Ornithology, Aligarh Muslim University, Aligarh (India).

Malingreau,J. P., 1991. Remote sensing for tropical forest monitoring: an overview; In *Remote Sensing and Geographic Information Systems for Resource Management in Developing Countries* (Eds) A. S. Belward and C. R. Valenzuela (Dordrecht: Kluwer), 253–278.

Maslekar, A. R., 1974. Remote Sensing and its scope in Indian forestry; *Indian Forester*, 100, 192–201.

Mc Donald, K. C. and Ulaby, F. T., 1993. Radiative transfer modeling of discontinuous tree canopies at microwave frequencies. *International Journal of Remote Sensing*, 14 (11), 2097-2128.

Mc Donald, K. C., Dobson, M. C., and Ulaby, F. T., 1990. Using MIMICS to model L-band multiangle and multitemporal backscatter for a walnut orchard. *IEEE Transactions on Geoscience and Remote Sensing*, 28, 477-491.

Mickler, R.A., Earnhardt, T.S. and Moore, J.A., 2002. Regional estimation of current and future forest biomass. *Environmental Pollution,* 116, S7–S16.

Moghaddan, Durden, M., S. and Zebker, H., 1994. Radar measurements of forested areas during OTTER. *Remote Sensing of Environment*, 47, 154-166.

Nelson, R., Jimenez, J., Schnell, C.E., Hartshorn, G.S., Gregoire, T.G. and Oderwald, R., 2000b. Canopy height models and airborne lasers to estimate forest biomass: two problems. *International Journal of Remote Sensing*, 21, 2153–2162.

Nelson, R., Krabill, W. and Tonelli, J., 1988. Estimating forest biomass and volume using airborne laser data. *Remote Sensing of Environment*, 24, 247–267.

Nelson, R.F., Kimes, D.S., Salas, W.A. and Routhier, M., 2000a. Secondary forest age and tropical forest biomass estimation using Thematic Mapper imagery. *Bioscience*, 50, 419–431.

Pairman, D., Mcneill, S., Scott, N. and Belliss, S., 1999. Vegetation identification and biomass estimation using AIRSAR data. *Geocarto International*, 14, 69–77.

Phua, M. and Saito, H., 2003. Estimation of biomass of a mountainous tropical forest using Landsat TM data. *Canadian Journal of Remote Sensing*, 29, 429–440.

Popescu, S.C., Wynne, R.H. and Nelson, R.F., 2003. Measuring individual tree crown diameter with lidar and assessing its influence on estimating forest volume and biomass. *Canadian Journal of Remote Sensing*, 29, 564–577.

Porwal, M. C., Dabral, S. L. and Roy, P. S., 1994. Revision and updating of stock maps using remote sensing and Geographic Information System (GIS); *Proc. ISRS Silver Jubilee Symposium*, Dehradun, 334–342.

Potter, C.S., 1999. Terrestrial biomass and the effects of deforestation on the global carbon cycle: results from a model of primary production using satellite observations. *BioScienc*e, 49, 769–778.

Qureshi, Q., Sawarkar, V.B and Mathur, P.K., 1991. Swamp Deer Population Structure, Patterns of Habitat Utilization and Some Management Needs in Dudwa National Park. Wildlife Institute of India, Dehradun.

Rahmani, A.R., Narayan, G., Rosalind, L. and Sankaran, R., 1990. Status of Bengal Florican: In: *Status and Ecology of Lesser and Bengal Florican*. Final Report. Bombay Natural History Society, Bombay: 55- 78.

Rajput, S.S.., Shukla, N.K., Gupta, V.K., and Jain, J.D., 1996. Timber Mechanics: Strength Classification and Grading of timber. *ICFRE Publication- 38*, ICFRE, Dehradun, 103.

Ranson, J. K. and Sun, G., 1994. Northern forest classification using temporal multifrequency and multipolarimetric SAR images. *Remote Sensing of Environment*, 47, 142-153.

Ranson, K. J. and Sun, G., 1994. Mapping biomass of a northern forest using multifrequency SAR data. *IEEE Transactions on Geoscience and Remote Sensing*, 32, 388-396.

Rauste, Y., Hame, T., Pullainen, J., Heiska, K., and Hallikainen, M., 1994, Radar- based forest biomass estimation. *International Journal of Remote Sensing*, 15, 3- 16.

Richards, J. A., Sun, G-Q., and. Simonett, D. S., 1987. L-band radar backscatter modeling of forest stands. *IEEE Transactions on Geoscience and Remote Sensing*, 25, 487-498.

Rignot, E. and Way, J. B., 1994. Monitoring freeze-thaw cycles along north-south Alaskan transects using ERS-1 SAR. *Remote Sensing of Environment*, 49, 131-137.

Rodgers, W.A. and Panwar, H.S., 1988. Planning wildlife protected network in India, Vol.1-2: Report, Wildlife Institute of India, Dehradun.

Rouse, J. W., Haas, R. H., Schell, J. A., and Deering, D. W., 1973. Monitoring vegetation systems in the Great Plains with ERTS. Proceedings of the 3rd ERTS Symposium NASA SP-351, 1, 48–62.

Roy, P. S., 1993. Remote Sensing for forest ecosystem analysis and management: In *Environmental Studies In India* (Eds.) M Balakrishnan, New Delhi: Oxford and IBH, pp. 335–363.

Roy, P. S., and Ravan, S. A., 1994. Habitat management for biodiversity maintenance using aerospace remote sensing; In: *Tropical Ecosystems: A Synthesis of Tropical Ecology and Conservation* (Eds.) M Balakrislman, R Borgstrom and S W Bie, New Delhi: Oxford and IBH, pp. 309–345.

Roy, P. S., Diwakar, P. G., Vohra, T. P. S. and Shan, S. K., 1990. Forest Resource Management using Indian Remote Sensing Satellite data; *Asian-Pacific Remote Sensing J., 3*, 11–22.

Roy, P. S., Kaul, R. N., Sharma, M. R., and Garbyal, S. G., 1985. Forest type stratification and delineation of shifting cultivation areas in eastern part of Arunachal Pradesh using Landsat MSS data; *International Journal of Remote Sensing*, 6, 411–418.

Roy, P.S. and Ravan, S.A., 1996. Biomass estimation using satellite remote sensing data—an investigation on possible approaches for natural forest. *Journal of Bioscience*, 21, 535–561.

Saatchi, S.S. and Moghaddam, M., 1995. Biomass distribution in boreal forest using SAR imagery. SPIE, 2314, 437–448.

Sader, S.A., Waide, R.B., Lawrence, W.T. and Joyce, A.T., 1989. Tropical forest biomass and successional age class relationships to a vegetation index derived from Landsat TM data. *Remote Sensing of Environment*, 28, 143–156.

Sale, J.B., and Singh, S., 1987. Reintroduction of Greater Indian *Rhinoceros* into Dudwa National Park. *Oryx.* Vol. 21, No.2: 81-84.

Sankaran, R. and Rahmani, A.R., 1991. The Bengal Florican in Dudwa National Park. In: *Status and Ecology of Lesser and Bengal Florican*. Final Report. Bombay Natural History Society, Bombay: 45- 54.

Santos, J.R., Freitas, C.C., Araujo, L.S., Dutra, L.V., Mura, J.C., Gama, F.F., Soler, L.S. and Sant' Anna, S.J.S., 2003. Airborne P-band SAR applied to the aboveground biomass studies in the Brazilian tropical rainforest. *Remote Sensing of Environment*, 87, 482–493.

Schroeder, P., Brown, S., Mo, J., Birdsey, R. and Cieszewski, C., 1997. Biomass estimation for temperate broadleaf forests of the US using inventory data. *Forest Science*, 43, 424–434.

Singh, R.L., 1985. Management of Reintroduced Indian *Rhinoceros*- A Pioneer Experiment, Unpublished Report, Dudwa National Park, Uttar Pradesh.

Singh, V.P., 1984. Bio- ecological Studies on Swamp Deer in Dudwa National Park. Ph.D. Dissertation. Kanpur University, Kanpur.

Sinha, S.P., and Sawarkar, V.B., 1991. Management of the Reintroduced Indian Great One-Horned *Rhinoceros* in Dudwa National Park, Uttar Pradesh. Project Report, Wildlife Institute of India, Dehradun.

Steininger, M.K., 2000. Satellite estimation of tropical secondary forest aboveground biomass data from Brazil and Bolivia. *International Journal of Remote Sensing*, 21, 1139–1157.

Sun, G. and Simonet, D. S., 1988. Simulation of L-band HH microwave backscattering from coniferous forest stands: a comparison with SIR-B data. *International Journal of Remote Sensing*, 9, 907-925.

Sun, G., Ranson, K.J. and Kharuk, V.I., 2002. Radiometric slope correction for forest biomass estimation from SAR data in the western Sayani Mountains, Siberia. *Remote Sensing of Environment*, 79, 279–287.

Tiwari, K. P., 1978. A comparative evaluation of landuse and forest type classification and mapping with aerial photograph vis a vis conventional ground stock mapping—a case study in Tehri Garhwal; *Indian Forester,* 104, 747–767.

Tiwari, K.A., 1994. Mapping forest biomass through digital processing of IRS-1A data. *International Journal of Remote Sensing*, 15, 1849–1866.

Tomar, M. S., 1976. Use of aerial photographs in working plans; *Indian Forester,* 102, 98–108.

Tomppo, E., Nilsson, M., Rosengren, M., Aalto, P. and Kennedy, P., 2002. Simultaneous use of Landsat-TM and IRS-1C WiFS data in estimating large area tree stem volume and aboveground biomass. *Remote Sensing of Environment*, 82, 156–171.

Treuhaft, R.N., Law, B.E. and Asner, G.P., 2004. Forest attributes from Radar interferometric structure and its fusion with optical remote sensing. *Bioscience*, 54, 561–571.

Trotter, C.M., Dymond, J.R. and Goulding, C.J., 1997. Estimation of timber volume in a coniferous plantation forest using Landsat TM. *International Journal of Remote Sensing*, 18, 2209–2223.

Tucker, C. J., Holben, B. N., ElginJr., J. H., and McMurtrey, J. E. , 1981. Remote sensing of total dry matter accumulation in winter wheat. *Remote Sensing of Environment*, 11, 171-189.

Uhl, C., Buschbacher, R., and Serra~ o, E. A. S., 1988, Abandoned pastures in eastern Amazonia. I. Patterns of plant succession. *Journal of Ecology*, 76, 663–681.

Ulaby, F. T., Sarabandi, K., Mcdonald, K., Whitt, M., and Dobson, M. C., 1990. Michigan microwave canopy scattering model. *International Journal of Remote Sensing*, 11, 1223-1253.

Wang, Y., Kasischke, E. S., Davis, F. W., Melack, J. M, and Christensen, N. L., Jr., 1994b. The effects of changes in loblolly pine biomass and soil moisture variations on ERS-1 SAR backscatter--a comparison of observations with theory. *Remote Sensing of Environment*, 49, 1, 25-31.

Wang, Y., Davis, F. W., and Melack, J. M., 1993a. Simulated and observed backscatter at P-, L-, and C-bands from ponderosa pine stands. *IEEE Transactions on Geoscience and Remote Sensing*, 31, 4, 871-879.

Wang, Y., Day, J. L., Davis, F. W., and Melack, J. M., 1993b. Modeling L-band radar backscatter from Alaskan boreal forest. *IEEE Transactions on Geoscience and Remote Sensing*, 31, 1146-1154.

Way, J. B., Rignot, E. J. M., Mcdonald, K. C., Oren, R., Kwok, R., Bonan, G., Dobson, M. C., Viereck, L. A., and Roth, J. A., 1994. Evaluating the type and state of Alaska taiga forests with imaging radar for use in ecosystem models. *IEEE Transactions on Geoscience and Remote Sensing*, 32, 353-370.

Woodcock, C.E., Collins, J.B., Jakabhazy, V.D., Li, X.,Macomber, S. And Wu, Y., 1997. Inversion of the Li-Strahler canopy reflectance model for mapping forest structure. *IEEE Transactions on Geoscience and Remote Sensing*, 35, 405–414.

Wu, Y. and Strahler, A.H., 1994. Remote estimation of crown size, stand density, and biomass on the Oregon transect. *Ecological Applications*, 42, 299–312.

Wylie, B.K., Meyer, D.J., Tieszer, L.L. and Mannel, S., 2002. Satellite mapping of surface biophysical parameters at the biome scale over the North American grasslands, a case study. *Remote Sensing of Environment*, 79, 266–278.

Zheng, D., Rademacher, J., Chen, J., Crow, T., Bresee, M., Le Moine, J. and Ryu, S., 2004. Estimating aboveground biomass using Landsat 7 ETM+ data across a managed landscape in northern Wisconsin, USA. *Remote Sensing of Environment*, 93, 402–411.

APPENDICES

Appendix 1. The forest volume type- wise in each sample plot (tree).

Plot No.	Vegetation Class (Type)	Volume (m^3 /ha)
1	Sal Forest	187.08
2	Sal Forest	446.15
4	Sal Forest	127.19
5	Sal Forest	464.47
15	Sal Forest	279.59
24	Sal Forest	454.34
35	Sal Forest	171.03
36	Sal Forest	262.17
37	Sal Forest	191.80
38	Sal Forest	169.06
39	Sal Forest	470.40
40	Sal Forest	498.60
41	Sal Forest	107.07
42	Sal Forest	391.42
43	Sal Forest	92.67
44	Sal Forest	182.15
45	Sal Forest	123.84
47	Sal Forest	460.06
48	Sal Forest	505.62
52	Sal Forest	605.09
53	Sal Forest	532.85
54	Sal Forest	334.12
55	Sal Forest	395.92
57	Sal Forest	382.96
58	Sal Forest	567.96
59	Sal Forest	256.37
60	Sal Forest	315.84
61	Sal Forest	127.55
62	Sal Forest	156.99
63	Sal Forest	328.38
66	Sal Forest	114.48
67	Sal Forest	378.28
68	Sal Forest	119.68
69	Sal Forest	360.19
70	Sal Forest	396.47
71	Sal Forest	129.56
72	Sal Forest	406.78
74	Sal Forest	196.73
75	Sal Forest	252.29
76	Sal Forest	86.55
77	Sal Forest	310.00
78	Sal Forest	253.03
80	Sal Forest	220.77
81	Sal Forest	319.12
82	Sal Forest	253.40

83	Sal Forest	278.98
84	Sal Forest	204.93
86	Sal Forest	169.06
87	Sal Forest	248.59
88	Sal Forest	166.95
89	Sal Forest	307.14
90	Sal Forest	101.37
91	Sal Forest	400.22
93	Sal Forest	392.55
94	Sal Forest	200.89
98	Sal Forest	213.18
102	Sal Forest	373.39
103	Sal Forest	627.56
104	Sal Forest	802.23
105	Sal Forest	201.10
108	Sal Forest	86.37
109	Sal Forest	184.73
110	Sal Forest	478.49
111	Sal Forest	367.39
112	Sal Forest	19.59
117	Sal Forest	168.35
120	Sal Forest	295.94
121	Sal Forest	178.65
122	Sal Forest	1097.88
123	Sal Forest	1244.57
124	Sal Forest	193.52
125	Sal Forest	215.17
126	Sal Forest	531.55
127	Sal Forest	365.73
128	Sal Forest	549.44
129	Sal Forest	320.34
130	Sal Forest	250.37
131	Sal Forest	467.99
132	Sal Forest	263.13
133	Sal Forest	675.72
134	Sal Forest	359.99
135	Sal Forest	451.72
136	Sal Forest	550.86
137	Sal Forest	508.21
138	Sal Forest	330.87
139	Sal Forest	293.19
141	Sal Forest	960.29
142	Sal Forest	255.15
143	Sal Forest	278.36
144	Sal Forest	223.73
145	Sal Forest	537.72
149	Sal Forest	165.83
150	Sal Forest	253.32
151	Sal Forest	320.53
152	Sal Forest	490.56
153	Sal Forest	563.87
154	Sal Forest	398.24

158	Sal Forest	458.27
160	Sal Forest	578.59
164	Sal Forest	274.28
165	Sal Forest	271.28
166	Sal Forest	171.11
167	Sal Forest	659.27
169	Sal Forest	349.48
170	Sal Forest	360.12
176	Sal Forest	319.70
177	Sal Forest	181.92
178	Sal Forest	684.92
182	Sal Forest	378.90
183	Sal Forest	422.75
184	Sal Forest	662.38
185	Sal Forest	300.23
186	Sal Forest	573.69
187	Sal Forest	303.58
190	Sal Forest	1383.02
191	Sal Forest	923.03
192	Sal Forest	256.86
195	Sal Forest	128.84
197	Sal Forest	918.57
198	Sal Forest	86.41
199	Sal Forest	1202.00
206	Sal Forest	193.68
207	Sal Forest	230.55
216	Sal Forest	146.09
217	Sal Forest	229.36
240	Sal Forest	344.92
247	Sal Forest	100.62
253	Sal Forest	101.50
259	Sal Forest	173.95
262	Sal Forest	72.64
263	Sal Forest	142.59
265	Sal Forest	215.60
269	Sal Forest	226.25
270	Sal Forest	193.35
272	Sal Forest	229.10
279	Sal Forest	512.84
8	Sal Mixed Forest	276.34
13	Sal Mixed Forest	846.66
14	Sal Mixed Forest	928.69
16	Sal Mixed Forest	432.99
17	Sal Mixed Forest	326.58
18	Sal Mixed Forest	901.54
19	Sal Mixed Forest	309.52
20	Sal Mixed Forest	166.00
21	Sal Mixed Forest	561.23
22	Sal Mixed Forest	324.38
25	Sal Mixed Forest	352.14
26	Sal Mixed Forest	492.40
27	Sal Mixed Forest	398.34

28	Sal Mixed Forest	1440.32
29	Sal Mixed Forest	1323.37
32	Sal Mixed Forest	1081.72
34	Sal Mixed Forest	763.61
49	Sal Mixed Forest	115.56
50	Sal Mixed Forest	626.91
51	Sal Mixed Forest	430.30
106	Sal Mixed Forest	756.53
157	Sal Mixed Forest	815.10
168	Sal Mixed Forest	505.98
171	Sal Mixed Forest	409.25
174	Sal Mixed Forest	384.24
188	Sal Mixed Forest	1219.78
193	Sal Mixed Forest	707.39
208	Sal Mixed Forest	483.37
211	Sal Mixed Forest	550.35
215	Sal Mixed Forest	264.38
218	Sal Mixed Forest	128.64
220	Sal Mixed Forest	446.80
222	Sal Mixed Forest	323.98
223	Sal Mixed Forest	460.24
232	Sal Mixed Forest	402.03
239	Sal Mixed Forest	143.96
242	Sal Mixed Forest	1442.71
264	Sal Mixed Forest	368.17
271	Sal Mixed Forest	674.17
281	Sal Mixed Forest	185.52
287	Sal Mixed Forest	318.65
9	Sissoo Plantation	292.39
181	Sissoo Plantation	380.65
226	Sissoo Plantation	277.46
244	Sissoo Plantation	179.75
249	Sissoo Plantation	180.87
252	Sissoo Plantation	817.43
261	Sissoo Plantation	91.38
268	Sissoo Plantation	914.09
283	Sissoo Plantation	380.80
30	*Eucalyptus* Plantation	562.33
31	*Eucalyptus* Plantation	420.94
79	*Eucalyptus* Plantation	321.91
148	*Eucalyptus* Plantation	339.12
209	*Eucalyptus* Plantation	117.46
212	*Eucalyptus* Plantation	126.51
224	*Eucalyptus* Plantation	292.15
225	*Eucalyptus* Plantation	129.84
248	*Eucalyptus* Plantation	330.03
255	*Eucalyptus* Plantation	299.86
266	*Eucalyptus* Plantation	284.13
280	*Eucalyptus* Plantation	526.30
46	Gulchaman Plantation	209.70
140	Gulchaman Plantation	237.87
179	Gulchaman Plantation	189.87

156	Khair- Sissoo Forest	334.86
163	Khair- Sissoo Forest	395.24
175	Khair- Sissoo Forest	424.55
3	Moist Mixed Deciduous Forest	232.93
6	Moist Mixed Deciduous Forest	150.35
95	Moist Mixed Deciduous Forest	271.35
230	Moist Mixed Deciduous Forest	295.59
278	Moist Mixed Deciduous Forest	291.61
107	*Syzygium* Swamp Low Forest	427.79
114	*Syzygium* Swamp Low Forest	561.23
172	*Syzygium* Swamp Low Forest	382.27
173	*Syzygium* Swamp Low Forest	216.17
194	*Syzygium* Swamp Low Forest	636.86
200	*Syzygium* Swamp Low Forest	75.70
201	*Syzygium* Swamp Low Forest	568.83
229	*Syzygium* Swamp Low Forest	280.30
233	*Syzygium* Swamp Low Forest	179.20
234	*Syzygium* Swamp Low Forest	234.25
235	*Syzygium* Swamp Low Forest	202.00
237	*Syzygium* Swamp Low Forest	195.30
238	*Syzygium* Swamp Low Forest	154.04
245	*Syzygium* Swamp Low Forest	144.87
246	*Syzygium* Swamp Low Forest	219.00
274	*Syzygium* Swamp Low Forest	335.11
275	*Syzygium* Swamp Low Forest	92.62
276	*Syzygium* Swamp Low Forest	285.77
92	Teak - Eucalyptus Plantation	648.09
118	Teak - Eucalyptus Plantation	1098.83
119	Teak - Eucalyptus Plantation	129.67
155	Teak - Eucalyptus Plantation	573.15
159	Teak - Eucalyptus Plantation	450.20
231	Teak - Eucalyptus Plantation	196.92
241	Teak - Eucalyptus Plantation	347.15
285	Teak - Eucalyptus Plantation	797.24
7	Teak Plantation	646.12
10	Teak Plantation	472.09
11	Teak Plantation	495.96
12	Teak Plantation	367.71
64	Teak Plantation	1106.49
65	Teak Plantation	948.41
73	Teak Plantation	298.28
96	Teak Plantation	288.17
97	Teak Plantation	721.22
99	Teak Plantation	455.65
147	Teak Plantation	466.52
213	Teak Plantation	407.21
214	Teak Plantation	322.19
227	Teak Plantation	266.15
228	Teak Plantation	268.21
250	Teak Plantation	393.68
251	Teak Plantation	633.95
254	Teak Plantation	181.86

256	Teak Plantation	360.78
257	Teak Plantation	402.62
258	Teak Plantation	334.62
277	Teak Plantation	404.21
101	Tropical Semi- Evergreen Forest	536.44
180	Tropical Semi- Evergreen Forest	232.31
219	Tropical Semi- Evergreen Forest	259.24
236	Tropical Semi- Evergreen Forest	368.11

Appendix 2. The biomass type- wise in each sample plot (tree).

Plot No.	Vegetation Class (Type)	Aboveground biomass (t /ha)
1	Sal Forest	127.13
2	Sal Forest	318.54
4	Sal Forest	85.58
5	Sal Forest	321.90
15	Sal Forest	192.83
24	Sal Forest	323.13
35	Sal Forest	120.49
36	Sal Forest	180.85
37	Sal Forest	134.77
38	Sal Forest	121.26
39	Sal Forest	329.92
40	Sal Forest	346.74
41	Sal Forest	76.41
42	Sal Forest	276.93
43	Sal Forest	66.26
44	Sal Forest	324.60
45	Sal Forest	86.41
47	Sal Forest	322.46
48	Sal Forest	359.58
52	Sal Forest	417.43
53	Sal Forest	364.06
54	Sal Forest	229.16
55	Sal Forest	274.49
57	Sal Forest	266.28
58	Sal Forest	375.75
59	Sal Forest	180.98
60	Sal Forest	225.50
61	Sal Forest	90.81
62	Sal Forest	108.99
63	Sal Forest	227.13
66	Sal Forest	78.18
67	Sal Forest	259.74
68	Sal Forest	83.56
69	Sal Forest	259.22
70	Sal Forest	285.82
71	Sal Forest	87.08

72	Sal Forest	284.82
74	Sal Forest	131.78
75	Sal Forest	138.80
76	Sal Forest	57.90
77	Sal Forest	221.07
78	Sal Forest	174.08
80	Sal Forest	158.32
81	Sal Forest	225.33
82	Sal Forest	180.19
83	Sal Forest	190.25
84	Sal Forest	144.87
86	Sal Forest	113.63
87	Sal Forest	163.98
88	Sal Forest	119.60
89	Sal Forest	214.61
90	Sal Forest	69.16
91	Sal Forest	284.12
93	Sal Forest	283.67
94	Sal Forest	140.33
98	Sal Forest	152.26
102	Sal Forest	264.55
103	Sal Forest	453.11
104	Sal Forest	579.41
105	Sal Forest	137.39
108	Sal Forest	58.24
109	Sal Forest	124.08
110	Sal Forest	335.26
111	Sal Forest	260.93
112	Sal Forest	13.43
117	Sal Forest	108.35
120	Sal Forest	201.78
121	Sal Forest	125.03
122	Sal Forest	756.55
123	Sal Forest	866.05
124	Sal Forest	139.79
125	Sal Forest	151.36
126	Sal Forest	338.51
127	Sal Forest	239.75
128	Sal Forest	388.83
129	Sal Forest	224.37
130	Sal Forest	173.19
131	Sal Forest	326.78
132	Sal Forest	186.78
133	Sal Forest	463.63
134	Sal Forest	235.07
135	Sal Forest	294.04
136	Sal Forest	388.51
137	Sal Forest	336.67

138	Sal Forest	133.59
139	Sal Forest	205.71
141	Sal Forest	662.35
142	Sal Forest	191.37
143	Sal Forest	193.47
144	Sal Forest	218.57
145	Sal Forest	370.07
149	Sal Forest	120.39
150	Sal Forest	180.77
151	Sal Forest	197.33
152	Sal Forest	331.61
153	Sal Forest	388.31
154	Sal Forest	282.19
158	Sal Forest	268.36
160	Sal Forest	399.10
164	Sal Forest	190.54
165	Sal Forest	183.89
166	Sal Forest	118.15
167	Sal Forest	439.17
169	Sal Forest	246.45
170	Sal Forest	249.68
176	Sal Forest	213.95
177	Sal Forest	126.01
178	Sal Forest	477.72
182	Sal Forest	261.57
183	Sal Forest	292.71
184	Sal Forest	393.24
185	Sal Forest	209.52
186	Sal Forest	397.02
187	Sal Forest	215.34
190	Sal Forest	939.85
191	Sal Forest	645.17
192	Sal Forest	171.58
195	Sal Forest	93.54
197	Sal Forest	635.98
198	Sal Forest	62.38
199	Sal Forest	850.66
206	Sal Forest	139.73
207	Sal Forest	160.53
216	Sal Forest	106.82
217	Sal Forest	165.95
240	Sal Forest	233.32
247	Sal Forest	69.61
253	Sal Forest	72.66
259	Sal Forest	171.41
262	Sal Forest	47.34
263	Sal Forest	99.59
265	Sal Forest	152.91

269	Sal Forest	159.67
270	Sal Forest	143.59
272	Sal Forest	164.44
279	Sal Forest	355.64
8	Sal Mixed Forest	195.71
13	Sal Mixed Forest	594.24
14	Sal Mixed Forest	647.59
16	Sal Mixed Forest	286.75
17	Sal Mixed Forest	219.71
18	Sal Mixed Forest	618.95
19	Sal Mixed Forest	210.82
20	Sal Mixed Forest	111.31
21	Sal Mixed Forest	391.72
22	Sal Mixed Forest	176.73
25	Sal Mixed Forest	243.72
26	Sal Mixed Forest	183.29
27	Sal Mixed Forest	272.69
28	Sal Mixed Forest	947.98
29	Sal Mixed Forest	932.47
32	Sal Mixed Forest	752.42
34	Sal Mixed Forest	530.15
49	Sal Mixed Forest	76.87
50	Sal Mixed Forest	435.39
51	Sal Mixed Forest	306.37
106	Sal Mixed Forest	228.23
157	Sal Mixed Forest	559.90
168	Sal Mixed Forest	344.47
171	Sal Mixed Forest	279.00
174	Sal Mixed Forest	259.81
188	Sal Mixed Forest	837.11
193	Sal Mixed Forest	496.20
208	Sal Mixed Forest	342.70
211	Sal Mixed Forest	251.08
215	Sal Mixed Forest	170.25
218	Sal Mixed Forest	58.13
220	Sal Mixed Forest	237.33
222	Sal Mixed Forest	146.70
223	Sal Mixed Forest	181.89
232	Sal Mixed Forest	258.40
239	Sal Mixed Forest	88.47
242	Sal Mixed Forest	838.69
264	Sal Mixed Forest	226.59
271	Sal Mixed Forest	522.85
281	Sal Mixed Forest	90.87
287	Sal Mixed Forest	228.74
9	Sissoo Plantation	195.61
181	Sissoo Plantation	252.04
226	Sissoo Plantation	185.62

244	Sissoo Plantation	120.26
249	Sissoo Plantation	113.00
252	Sissoo Plantation	546.86
261	Sissoo Plantation	61.14
268	Sissoo Plantation	611.53
283	Sissoo Plantation	251.06
30	*Eucalyptus* Plantation	391.94
31	*Eucalyptus* Plantation	293.40
79	*Eucalyptus* Plantation	190.67
148	*Eucalyptus* Plantation	236.36
209	*Eucalyptus* Plantation	81.87
212	*Eucalyptus* Plantation	88.39
224	*Eucalyptus* Plantation	203.30
225	*Eucalyptus* Plantation	90.50
248	*Eucalyptus* Plantation	230.03
255	*Eucalyptus* Plantation	209.00
266	*Eucalyptus* Plantation	191.85
280	*Eucalyptus* Plantation	366.83
46	Gulchaman Plantation	126.50
140	Gulchaman Plantation	143.16
179	Gulchaman Plantation	105.50
156	Khair- Sissoo Forest	262.91
163	Khair- Sissoo Forest	281.63
175	Khair- Sissoo Forest	282.56
3	Moist Mixed Deciduous Forest	135.13
6	Moist Mixed Deciduous Forest	94.57
95	Moist Mixed Deciduous Forest	154.35
230	Moist Mixed Deciduous Forest	183.61
278	Moist Mixed Deciduous Forest	165.18
17	*Syzygium* Swamp Low Forest	465.88
114	*Syzygium* Swamp Low Forest	363.02
172	*Syzygium* Swamp Low Forest	258.44
173	*Syzygium* Swamp Low Forest	132.89
194	*Syzygium* Swamp Low Forest	429.09
200	*Syzygium* Swamp Low Forest	40.99
201	*Syzygium* Swamp Low Forest	362.52
229	*Syzygium* Swamp Low Forest	178.07
233	*Syzygium* Swamp Low Forest	85.11
234	*Syzygium* Swamp Low Forest	93.50
235	*Syzygium* Swamp Low Forest	104.87
237	*Syzygium* Swamp Low Forest	101.84
238	*Syzygium* Swamp Low Forest	89.33
245	*Syzygium* Swamp Low Forest	93.73
246	*Syzygium* Swamp Low Forest	141.69
274	*Syzygium* Swamp Low Forest	197.66
275	*Syzygium* Swamp Low Forest	59.41
276	*Syzygium* Swamp Low Forest	172.50
92	Teak - Eucalyptus Plantation	412.49

118	Teak - Eucalyptus Plantation	635.29
119	Teak - Eucalyptus Plantation	89.32
155	Teak - Eucalyptus Plantation	358.29
159	Teak - Eucalyptus Plantation	262.91
231	Teak - Eucalyptus Plantation	122.73
241	Teak - Eucalyptus Plantation	202.31
285	Teak - Eucalyptus Plantation	535.96
7	Teak Plantation	373.46
10	Teak Plantation	272.87
11	Teak Plantation	286.67
12	Teak Plantation	212.84
64	Teak Plantation	639.55
65	Teak Plantation	548.18
73	Teak Plantation	178.13
96	Teak Plantation	173.24
97	Teak Plantation	424.68
99	Teak Plantation	279.48
147	Teak Plantation	269.65
213	Teak Plantation	235.37
214	Teak Plantation	186.23
227	Teak Plantation	153.83
228	Teak Plantation	155.02
250	Teak Plantation	227.55
251	Teak Plantation	366.45
254	Teak Plantation	105.21
256	Teak Plantation	208.53
257	Teak Plantation	232.72
258	Teak Plantation	193.41
277	Teak Plantation	235.84
101	Tropical Semi- Evergreen Forest	280.31
180	Tropical Semi- Evergreen Forest	109.95
219	Tropical Semi- Evergreen Forest	123.89
236	Tropical Semi- Evergreen Forest	143.09
288	Upland Grassland	0.29
289	Upland Grassland	1.30
290	Upland Grassland	4.06
291	Upland Grassland	3.65
292	Upland Grassland	3.37
293	Upland Grassland	1.56
294	Upland Grassland	3.55
295	Upland Grassland	5.57
296	Upland Grassland	4.29
297	Upland Grassland	2.30
298	Upland Grassland	1.65
304	Lowland Grassland	4.20
305	Lowland Grassland	4.51
306	Lowland Grassland	4.26
307	Lowland Grassland	4.52

308	Lowland Grassland	3.51
309	Lowland Grassland	2.15
310	Lowland Grassland	4.65
311	Lowland Grassland	2.04
312	Lowland Grassland	3.38
313	Lowland Grassland	4.58
314	Lowland Grassland	5.69

Appendix 3. Relationships between aboveground volume and biomass with optical, NDVI and backscattering.

Plot No.	Forest Type	Volume (m^3)	Volume (m^3/ha)	Biomass (t/ha)	B	G	R	IR	IR	T IR	IR	σ°_{HH}	σ°_{HV}	NDVI
Plot 1	Sal Forest	7.48	187.08	127.13	54	20	16	59	38	128	10	-13	-10	0.57
Plot 2	Sal Forest	17.85	446.15	318.54	53	20	16	60	37	128	11	-15	-8	0.58
Plot 3	Moist Mixed Deciduous Forest	20.43	232.93	135.13	51	20	16	56	35	128	10	-12	-8	0.56
Plot 4	Sal Forest	5.09	150.35	85.58	54	20	16	65	42	128	12	-13	-8	0.60
Plot 5	Sal Forest	18.58	271.35	321.90	50	20	16	57	37	127	9	-12	-7	0.56
Plot 6	Moist Mixed Deciduous Forest	2.52	150.35	94.57	51	20	16	58	42	127	11	-14	-8	0.57
Plot 7	Teak Plantation	25.84	646.12	373.46	55	24	18	83	59	131	18	-13	-8	0.64
Plot 8	Sal Mixed Forest	11.05	276.34	195.71	52	21	17	62	41	127	11	-12	-6	0.57
Plot 9	Sissoo Plantation	11.70	292.39	195.61	62	28	28	70	95	136	34	-14	-11	0.43
Plot 10	Teak Plantation	18.88	472.09	272.87	55	22	18	87	56	130	17	-16	-5	0.66
Plot 11	Teak Plantation	19.84	495.96	286.67	54	21	17	83	53	128	16	-17	-8	0.66
Plot 12	Teak Plantation	14.71	367.71	212.84	54	22	18	79	52	128	15	-15	-6	0.63
Plot 13	Sal Mixed Forest	33.87	846.66	594.24	53	20	17	65	41	127	12	-12	-9	0.59
Plot 14	Sal Mixed Forest	37.15	928.69	647.59	52	20	17	62	39	127	11	-13	-8	0.57
Plot 15	Sal Forest	11.18	279.59	192.83	54	19	16	63	41	128	11	-14	-7	0.59
Plot 16	Sal Mixed Forest	17.32	432.99	286.75	51	19	15	55	37	127	10	-13	-9	0.57
Plot 17	Sal Mixed Forest	13.06	326.58	219.71	53	20	15	62	38	127	10	-12	-8	0.61
Plot 18	Sal Mixed Forest	36.06	901.54	618.95	54	20	17	60	38	128	11	-14	-6	0.56
Plot 19	Sal Mixed Forest	12.38	309.52	210.82	52	19	15	54	38	128	13	-15	-7	0.57
Plot 20	Sal Mixed Forest	6.64	166.00	111.31	51	20	16	59	38	128	10	-12	-8	0.57
Plot 21	Sal Mixed Forest	22.45	561.23	391.72	52	21	16	62	38	128	11	-14	-8	0.59
Plot 22	Sal Mixed Forest	12.98	324.38	176.73	56	23	20	70	50	129	15	-14	-9	0.56
Plot 24	Sal Forest	18.17	454.34	323.13	53	21	17	49	34	128	11	-15	-9	0.48
Plot 25	Sal Mixed Forest	14.09	352.14	243.72	54	20	17	59	42	127	12	-14	-8	0.55
Plot 26	Sal Mixed Forest	19.70	492.40	183.29	55	22	18	66	54	131	18	-12	-9	0.57
Plot 27	Sal Mixed Forest	15.93	398.34	272.69	54	23	18	69	46	129	13	-13	-9	0.59
Plot 28	Sal Mixed Forest	57.61	1440.32	947.98	54	20	16	53	41	128	13	-16	-6	0.54

Plot 29	Sal Mixed Forest	52.93	1323.37	932.47	53	20	17	56	38	128	11	-14	-7	0.53
Plot 30	Eucalyptus Plantation	22.49	562.33	391.94	54	22	20	59	50	131	17	-14	-9	0.49
Plot 31	Eucalyptus Plantation	16.84	420.94	293.40	54	20	17	59	38	129	11	-14	-10	0.55
Plot 32	Sal Mixed Forest	43.27	1081.72	752.42	54	21	17	57	38	128	12	-13	-9	0.54
Plot 34	Sal Mixed Forest	30.54	763.61	530.15	55	21	17	67	43	131	13	-15	-9	0.60
Plot 35	Sal Forest	6.84	171.03	120.49	52	20	16	61	37	128	10	-13	-8	0.58
Plot 36	Sal Forest	10.49	262.17	180.85	54	20	15	60	37	128	10	-11	-9	0.60
Plot 37	Sal Forest	7.67	191.80	134.77	52	20	16	62	37	129	12	-15	-6	0.59
Plot 38	Sal Forest	6.76	169.06	121.26	55	21	18	62	42	128	13	-12	-8	0.55
Plot 39	Sal Forest	18.82	470.40	329.92	53	21	17	58	41	129	13	-13	-7	0.55
Plot 40	Sal Forest	19.94	498.60	346.74	52	21	16	56	38	128	12	-15	-8	0.56
Plot 41	Sal Forest	4.28	107.07	76.41	54	20	16	59	38	128	11	-16	-7	0.57
Plot 42	Sal Forest	15.66	391.42	276.93	52	19	14	56	34	128	11	-14	-8	0.60
Plot 43	Sal Forest	3.71	92.67	66.26	51	20	14	59	37	128	12	-13	-8	0.62
Plot 44	Sal Forest	27.29	182.15	324.60	52	19	16	59	36	129	10	-14	-9	0.57
Plot 45	Sal Forest	4.95	123.84	86.41	53	20	16	60	42	128	12	-12	-6	0.58
Plot 46	Gulchaman Plantation	37.20	209.70	126.50	53	21	17	58	41	129	10	-13	-8	0.55
Plot 47	Sal Forest	18.40	209.70	322.46	53	20	16	58	41	127	11	-15	-10	0.57
Plot 48	Sal Forest	20.22	460.06	359.58	52	20	16	60	37	129	12	-13	-9	0.58
Plot 49	Sal Mixed Forest	4.62	505.62	76.87	50	19	15	58	37	127	11	-13	-9	0.59
Plot 50	Sal Mixed Forest	25.08	115.56	435.39	54	20	17	59	39	128	11	-14	-7	0.55
Plot 51	Sal Mixed Forest	17.21	626.91	306.37	53	21	17	62	40	129	13	-14	-6	0.57
Plot 52	Sal Forest	24.20	430.30	417.43	52	19	15	55	39	128	10	-15	-8	0.57
Plot 53	Sal Forest	21.31	605.09	364.06	53	19	15	59	37	128	10	-14	-8	0.59
Plot 54	Sal Forest	13.36	532.85	229.16	51	20	16	57	36	128	10	-14	-8	0.56
Plot 55	Sal Forest	15.84	334.12	274.49	52	19	14	53	33	128	10	-14	-8	0.58
Plot 57	Sal Forest	15.32	395.92	266.28	52	20	18	62	41	128	13	-13	-6	0.55
plot 58	Sal Forest	22.72	382.96	375.75	54	21	17	57	41	128	13	-14	-7	0.54
Plot 59	Sal Forest	10.25	567.96	180.98	53	20	17	55	36	128	11	-15	-6	0.53
Plot 60	Sal Forest	12.63	256.37	225.50	53	20	17	60	38	128	10	-14	-8	0.56
Plot 61	Sal Forest	5.10	315.84	90.81	51	20	17	59	37	127	11	-16	-7	0.55
Plot 62	Sal Forest	6.28	127.55	108.99	52	20	17	60	40	129	13	-15	-8	0.56

Plot 63	Sal Forest	13.14	156.99	227.13	51	20	16	58	41	127	10	-13	-8	0.57
Plot 64	Teak Plantation	44.26	328.38	639.55	55	22	19	67	53	128	16	-13	-7	0.56
Plot 65	Teak Plantation	37.94	1106.49	548.18	55	23	18	64	52	128	18	-15	-7	0.56
Plot 66	Sal Forest	4.58	948.41	78.18	52	20	16	59	37	128	12	-14	-8	0.57
Plot 67	Sal Forest	15.13	114.48	259.74	52	21	16	59	41	128	13	-14	-6	0.57
Plot 68	Sal Forest	4.79	378.28	83.56	52	19	17	57	37	128	12	-12	-7	0.54
Plot 69	Sal Forest	14.41	119.68	259.22	52	20	16	61	40	128	11	-13	-6	0.58
Plot 70	Sal Forest	15.86	360.19	285.82	53	21	16	64	38	128	11	-13	-7	0.60
Plot 71	Sal Forest	5.18	396.47	87.08	52	21	17	57	40	127	12	-13	-9	0.54
Plot 72	Sal Forest	16.27	129.56	284.82	54	20	18	61	41	127	12	-14	-9	0.54
Plot 73	Teak Plantation	11.93	406.78	178.13	56	23	19	59	47	128	16	-11	-8	0.51
Plot 74	Sal Forest	7.87	298.28	131.78	51	20	17	56	40	128	13	-13	-7	0.53
Plot 75	Sal Forest	10.09	196.73	138.80	55	20	17	56	41	128	11	-12	-6	0.53
Plot 76	Sal Forest	3.46	252.29	57.90	53	21	17	56	40	128	12	-14	-8	0.53
Plot 77	Sal Forest	12.40	86.55	221.07	54	20	16	59	39	128	13	-13	-8	0.57
Plot 78	Sal Forest	10.12	310.00	174.08	52	21	16	62	39	128	10	-14	-7	0.59
Plot 79	Eucalyptus Plantation	12.88	253.03	190.67	54	22	19	50	42	131	13	-18	-11	0.45
Plot 80	Sal Forest	8.83	321.91	158.32	52	20	15	61	40	128	11	-14	-8	0.61
Plot 81	Sal Forest	12.76	220.77	225.33	52	20	16	60	39	128	12	-13	-11	0.58
Plot 82	Sal Forest	10.14	319.12	180.19	53	21	17	52	39	128	12	-13	-6	0.51
Plot 83	Sal Forest	11.16	253.40	190.25	52	21	16	59	39	128	12	-12	-7	0.57
Plot 84	Sal Forest	8.20	278.98	144.87	52	21	16	60	37	128	11	-12	-8	0.58
Plot 86	Sal Forest	6.76	204.93	113.63	54	21	17	54	35	128	11	-128	-128	0.52
Plot 87	Sal Forest	9.94	169.06	163.98	52	20	16	53	38	128	11	-128	-128	0.54
Plot 88	Sal Forest	6.68	248.59	119.60	52	20	16	60	35	128	9	-128	-128	0.58
Plot 89	Sal Forest	12.29	166.95	214.61	54	22	17	66	40	128	12	-128	-128	0.59
Plot 90	Sal Forest	4.05	307.14	69.16	54	21	17	62	39	129	12	-128	-128	0.57
Plot 91	Sal Forest	16.01	101.37	284.12	53	21	17	58	42	130	13	-128	-128	0.55
Plot 92	Teak- Eucalyptus Plantation	25.92	400.22	412.49	54	21	19	62	38	131	11	-128	-128	0.53
Plot 93	Sal Forest	15.70	648.09	283.67	52	20	17	64	38	128	11	-128	-128	0.58
Plot 94	Sal Forest	8.04	392.55	140.33	54	20	17	63	39	128	11	-12	-8	0.57
Plot 95	Moist Mixed Deciduous Forest	12.93	271.35	154.35	52	21	16	60	38	127	12	-13	-8	0.58

Plot 96	Teak Plantation	11.53	271.35	173.24	52	21	18	76	45	128	11	-14	-10	0.62
Plot 97	Teak Plantation	28.85	721.22	424.68	52	21	17	58	38	127	13	-13	-7	0.55
Plot 98	Sal Forest	8.53	213.18	152.26	55	21	18	59	42	128	13	-15	-8	0.53
Plot 99	Teak Plantation	18.23	455.65	279.48	54	21	17	66	42	128	13	-14	-8	0.59
Plot 101	Tropical Semi- Evergreen Forest	21.46	536.44	280.31	57	22	18	74	48	129	13	-18	-10	0.61
Plot 102	Sal Forest	14.94	373.39	264.55	53	20	17	62	42	128	11	-15	-8	0.57
Plot 103	Sal Forest	25.10	627.56	453.11	54	21	17	64	40	128	11	-13	-6	0.58
Plot 104	Sal Forest	32.09	802.23	579.41	52	20	17	66	40	129	12	-11	-6	0.59
Plot 105	Sal Forest	8.04	201.10	137.39	53	20	15	65	39	127	12	-15	-8	0.63
Plot106	Sal Mixed Forest	30.26	756.53	228.23	55	22	18	65	46	128	13	-11	-7	0.57
Plot 107	*Syzygium* Swamp Low Forest	17.11	427.79	465.88	52	19	16	50	35	127	12	-12	-5	0.52
Plot 108	Sal Forest	3.45	86.37	58.24	51	20	16	53	36	127	11	-15	-9	0.54
Plot 109	Sal Forest	7.39	184.73	124.08	53	20	14	50	33	128	9	-13	-8	0.56
Plot 110	Sal Forest	19.14	478.49	335.26	53	20	17	55	38	129	11	-14	-7	0.53
Plot 111	Sal Forest	14.70	367.39	260.93	52	21	17	55	38	128	11	-14	-9	0.53
Plot 112	Sal Forest	0.78	19.59	13.43	52	20	17	55	41	127	11	-12	-9	0.53
Plot 114	*Syzygium* Swamp Low Forest	22.45	561.23	363.02	54	22	19	64	40	128	12	-11	-5	0.54
Plot 117	Sal Forest	6.73	168.35	108.35	53	20	16	53	39	128	12	-14	-7	0.54
Plot 118	Teak- Eucalyptus Plantation	43.95	1098.83	635.29	55	22	19	68	49	129	16	-11	-8	0.56
Plot 119	Teak- Eucalyptus Plantation	5.19	129.67	89.32	53	22	18	61	42	128	13	-12	-8	0.54
Plot 120	Sal Forest	11.84	295.94	201.78	53	21	17	64	40	129	11	-12	-7	0.58
Plot 121	Sal Forest	7.15	178.65	125.03	52	21	15	53	36	128	10	-14	-8	0.56
Plot 122	Sal Forest	43.92	1097.88	756.55	51	21	17	58	40	128	11	-14	-8	0.55
Plot 123	Sal Forest	49.78	1244.57	866.05	52	21	16	55	37	128	12	-13	-8	0.55
Plot 124	Sal Forest	7.74	193.52	139.79	52	20	17	56	40	128	11	-13	-10	0.53
Plot 125	Sal Forest	8.61	215.17	151.36	52	21	17	61	36	128	11	-11	-8	0.56
Plot 126	Sal Forest	21.26	531.55	338.51	52	21	17	60	43	128	12	-14	-7	0.56
Plot 127	Sal Forest	14.63	365.73	239.75	52	20	17	59	38	128	11	-14	-9	0.55
Plot 128	Sal Forest	21.98	549.44	388.83	54	21	18	57	41	129	12	-14	-8	0.52
Plot 129	Sal Forest	12.81	320.34	224.37	53	21	16	62	39	128	11	-12	-5	0.59
Plot 130	Sal Forest	10.01	250.37	173.19	53	20	16	58	40	128	11	-11	-7	0.57
Plot 131	Sal Forest	18.72	467.99	326.78	51	19	16	38	29	132	10	-14	-9	0.41

Plot 132	Sal Forest	10.53	263.13	186.78	53	22	17	67	43	128	11	-15	-10	0.60
Plot 133	Sal Forest	27.03	675.72	463.63	51	20	17	60	39	129	12	-12	-4	0.56
Plot 134	Sal Forest	14.40	359.99	235.07	52	20	16	58	40	129	12	-15	-7	0.57
plot 135	Sal Forest	18.07	451.72	294.04	54	20	16	55	43	129	13	-16	-7	0.55
plot 136	Sal Forest	22.03	550.86	388.51	53	21	16	62	42	128	13	-13	-9	0.59
Plot 137	Sal Forest	20.33	508.21	336.67	53	21	17	62	39	129	11	-10	-6	0.57
Plot 138	Sal Forest	13.23	330.87	133.59	52	20	16	52	36	128	11	-13	-6	0.53
plot 139	Sal Forest	11.73	293.19	205.71	53	20	16	60	38	128	11	-11	-7	0.58
Plot 140	Gulchaman Plantation	9.51	237.87	143.16	54	23	18	61	45	129	14	-11	-8	0.54
Plot 141	Sal Forest	38.41	960.29	662.35	52	21	17	43	32	128	10	-12	-9	0.43
Plot 142	Sal Forest	10.21	255.15	191.37	53	21	17	63	43	127	12	-13	-9	0.57
Plot 143	Sal Forest	11.13	278.36	193.47	53	21	16	62	39	128	11	-11	-6	0.59
Plot 144	Sal Forest	8.95	223.73	218.57	53	20	18	61	40	128	13	-15	-8	0.54
Plot 145	Sal Forest	21.51	537.72	370.07	56	24	21	67	63	132	21	-14	-8	0.52
plot 147	Teak Plantation	18.66	466.52	269.65	55	24	19	79	59	129	17	-13	-6	0.61
plot 148	Eucalyptus Plantation	13.56	339.12	236.36	54	21	20	53	49	133	18	-16	-6	0.45
Plot149	Sal Forest	6.63	165.83	120.39	53	21	17	63	40	129	13	-14	-8	0.57
Plot 150	Sal Forest	10.13	253.32	180.77	52	19	17	62	40	128	12	-14	-9	0.57
Plot 151	Sal Forest	12.82	320.53	197.33	54	20	18	54	42	128	12	-12	-8	0.50
Plot152	Sal Forest	19.62	490.56	331.61	53	20	17	56	37	127	10	-12	-5	0.53
Plot 153	Sal Forest	22.55	563.87	388.31	54	20	17	59	37	128	12	-13	-8	0.55
Plot 154	Sal Forest	15.93	398.24	282.19	54	20	17	64	41	128	12	-14	-9	0.58
Plot 155	Teak- Eucalyptus Plantation	22.93	573.15	358.29	54	20	20	52	45	130	15	-14	-7	0.44
Plot 156	Khair- Sissoo Forest	42.96	334.86	262.91	54	21	17	63	43	129	12	-14	-6	0.57
Plot 157	Sal Mixed Forest	32.60	815.10	559.90	53	21	17	64	41	127	12	-12	-10	0.58
Plot 158	Sal Forest	18.33	458.27	268.36	52	21	16	62	42	128	12	-13	-9	0.59
Plot 159	Teak- Eucalyptus Plantation	18.01	450.20	262.91	53	21	18	60	45	129	14	-15	-8	0.54
Plot 160	Sal Forest	23.14	578.59	399.10	53	20	17	60	41	127	12	-13	-8	0.56
Plot 163	Khair- Sissoo Forest	15.81	395.24	281.63	60	26	26	62	77	134	27	-14	-8	0.41
Plot 164	Sal Forest	10.97	274.28	190.54	53	21	16	58	40	128	11	-13	-7	0.57
Plot 165	Sal Forest	10.85	271.28	183.89	54	21	18	63	39	128	11	-12	-7	0.56
Plot 166	Sal Forest	6.84	171.11	118.15	55	22	20	59	50	131	18	-16	-10	0.49

Plot 167	Sal Forest	26.37	659.27	439.17	53	21	17	63	40	129	11	-13	-10	0.57
Plot 168	Sal Mixed Forest	20.24	505.98	344.47	53	20	17	62	37	128	9	-11	-10	0.57
Plot 169	Sal Forest	13.98	349.48	246.45	53	21	17	61	42	129	12	-11	-6	0.56
Plot 170	Sal Forest	14.40	360.12	249.68	53	20	16	58	38	129	12	-14	-7	0.57
Plot 171	Sal Mixed Forest	16.37	409.25	279.00	53	21	15	57	40	127	12	-12	-9	0.58
Plot 172	*Syzygium* Swamp Low Forest	15.29	382.27	258.44	52	21	17	62	43	128	12	-12	-8	0.57
Plot 173	*Syzygium* Swamp Low Forest	8.65	216.17	132.89	53	21	17	63	38	129	11	-14	-7	0.57
Plot 174	Sal Mixed Forest	15.37	384.24	259.81	54	20	17	61	44	127	13	-12	-8	0.56
Plot 175	Khair- Sissoo Forest	18.92	424.55	282.56	55	21	17	59	38	128	10	-15	-10	0.55
Plot 176	Sal Forest	12.79	319.70	213.95	52	21	17	59	40	129	11	-10	-6	0.55
Plot 177	Sal Forest	7.28	181.92	126.01	52	20	16	60	38	128	12	-12	-8	0.58
Plot 178	Sal Forest	27.40	684.92	477.72	51	20	16	58	36	128	10	-12	-9	0.57
Plot 179	Gulchaman Plantation	20.12	189.87	105.50	51	21	16	61	39	128	10	-12	-8	0.58
Plot 180	Tropical Semi- Evergreen Forest	17.84	232.31	109.95	51	20	16	54	25	128	9	-13	-10	0.54
Plot 181	Sissoo Plantation	15.23	380.65	252.04	59	26	23	64	51	131	18	-13	-11	0.47
Plot 182	Sal Forest	15.16	378.90	261.57	60	26	25	58	59	131	20	-15	-8	0.40
Plot 183	Sal Forest	16.91	422.75	292.71	52	19	15	62	38	128	11	-16	-8	0.61
Plot 184	Sal Forest	26.50	662.38	393.24	53	20	17	60	38	128	9	-13	-8	0.56
Plot 185	Sal Forest	12.01	300.23	209.52	54	21	18	64	37	128	11	-13	-11	0.56
Plot 186	Sal Forest	22.95	573.69	397.02	54	21	17	52	38	128	11	-14	-9	0.51
Plot 187	Sal Forest	12.14	303.58	215.34	51	20	16	58	36	128	11	-13	-7	0.57
Plot 188	Sal Mixed Forest	48.79	1219.78	837.11	52	20	17	60	38	128	10	-12	-9	0.56
Plot 190	Sal Forest	55.32	1383.02	939.85	53	20	17	60	47	129	15	-12	-8	0.56
Plot 191	Sal Forest	36.92	923.03	645.17	51	21	16	55	34	128	10	-13	-10	0.55
Plot 192	Sal Forest	10.27	256.86	171.58	65	29	33	41	75	142	34	-17	-10	0.11
Plot 193	Sal Mixed Forest	28.30	707.39	496.20	54	21	17	60	43	130	13	-13	-8	0.56
Plot 194	*Syzygium* Swamp Low Forest	25.47	636.86	429.09	56	21	18	64	51	131	17	-13	-8	0.56
Plot 195	Sal Forest	5.15	128.84	93.54	53	22	18	61	46	130	14	-13	-10	0.54
Plot 197	Sal Forest	36.74	918.57	635.98	54	20	16	60	41	129	11	-13	-8	0.58
Plot 198	Sal Forest	3.46	86.41	62.38	53	21	16	62	42	129	12	-15	-9	0.59
Plot 199	Sal Forest	48.08	1202.00	850.66	53	21	17	67	41	128	12	-14	-8	0.60
Plot 200	*Syzygium* Swamp Low Forest	3.03	75.70	40.99	55	20	17	54	37	129	11	-14	-9	0.52

Plot 201	*Syzygium* Swamp Low Forest	22.75	568.83	362.52	57	25	21	83	63	132	20	-16	-10	0.60
Plot 206	Sal Forest	7.75	193.68	139.73	53	21	16	61	38	128	11	-13	-8	0.58
Plot207	Sal Forest	9.22	230.55	160.53	54	22	19	60	42	129	12	-13	-9	0.52
Plot208	Sal Mixed Forest	19.33	483.37	342.70	67	31	35	60	82	134	37	-15	-7	0.26
Plot209	Eucalyptus Plantation	4.70	117.46	81.87	58	25	24	55	63	132	22	-15	-10	0.39
Plot211	Sal Mixed Forest	22.01	550.35	251.08	55	25	21	51	56	132	20	-13	-9	0.42
Plot212	Eucalyptus Plantation	5.06	126.51	88.39	55	24	22	51	52	132	17	-17	-12	0.40
Plot213	Teak Plantation	16.29	407.21	235.37	59	26	24	71	64	131	21	-16	-8	0.49
Plot214	Teak Plantation	12.89	322.19	186.23	54	22	18	63	45	128	13	-15	-9	0.56
Plot215	Sal Mixed Forest	10.58	264.38	170.25	62	27	28	57	75	133	30	-16	-6	0.34
Plot216	Sal Forest	5.84	146.09	106.82	54	21	17	61	39	128	11	-11	-6	0.56
Plot217	Sal Forest	9.17	229.36	165.95	54	22	18	58	42	128	13	-12	-8	0.53
Plot218	Sal Mixed Forest	5.15	128.64	58.13	58	24	22	61	58	131	18	-14	-8	0.47
Plot219	Tropical Semi- Evergreen Forest	91.41	259.24	123.89	74	37	44	59	89	135	45	-128	-128	0.15
Plot220	Sal Mixed Forest	17.87	446.80	237.33	56	22	19	63	43	129	14	-12	-7	0.54
Plot222	Sal Mixed Forest	12.96	323.98	146.70	59	29	29	59	60	132	22	-14	-9	0.34
Plot223	Sal Mixed Forest	18.41	460.24	181.89	56	23	20	39	21	133	9	-14	-7	0.32
Plot224	Eucalyptus Plantation	11.69	292.15	203.30	55	21	19	54	38	131	13	-15	-9	0.48
Plot225	Eucalyptus Plantation	5.19	129.84	90.50	58	25	24	62	58	130	19	-15	-11	0.44
Plot226	Sissoo Plantation	11.10	277.46	185.62	81	38	46	39	53	134	28	-14	-10	-0.08
Plot227	Teak Plantation	10.65	266.15	153.83	54	21	17	78	50	128	13	-14	-5	0.64
Plot228	Teak Plantation	10.73	268.21	155.02	64	28	32	53	73	132	31	-14	-8	0.25
Plot229	*Syzygium* Swamp Low Forest	11.21	280.30	178.07	54	21	20	48	46	128	15	-12	-8	0.41
Plot230	Moist Mixed Deciduous Forest	11.82	295.59	183.61	55	22	18	61	45	128	13	-13	-9	0.54
Plot231	Teak- Eucalyptus Plantation	7.88	196.92	122.73	53	22	17	64	43	127	13	-16	-8	0.58
Plot232	Sal Mixed Forest	16.08	402.03	258.40	57	23	25	47	63	130	22	-19	-13	0.31
Plot233	*Syzygium* Swamp Low Forest	7.17	179.20	85.11	59	24	22	69	58	132	18	-13	-7	0.52
Plot234	*Syzygium* Swamp Low Forest	9.37	234.25	93.50	63	28	30	35	31	128	12	-14	-9	0.08
Plot235	*Syzygium* Swamp Low Forest	8.08	202.00	104.87	57	24	21	61	58	131	19	-17	-9	0.49
Plot236	Tropical Semi- Evergreen Forest	14.72	368.11	143.09	54	22	18	65	46	129	14	-15	-8	0.57
Plot237	*Syzygium* Swamp Low Forest	7.81	195.30	101.84	58	25	23	71	67	129	21	-15	-8	0.51
Plot238	*Syzygium* Swamp Low Forest	6.16	154.04	89.33	56	22	19	62	49	129	15	-11	-7	0.53

Plot239	Sal Mixed Forest	5.76	143.96	88.47	53	20	15	55	37	127	11	-13	-8	0.57
Plot240	Sal Forest	13.80	344.92	233.32	52	19	15	51	30	128	10	-13	-7	0.55
Plot241	Teak- Eucalyptus Plantation	13.89	347.15	202.31	53	20	15	55	42	128	13	-12	-9	0.57
Plot242	Sal Mixed Forest	57.71	1442.71	838.69	59	24	21	54	57	131	19	-13	-8	0.44
Plot244	Sissoo Plantation	7.19	179.75	120.26	69	33	33	60	72	134	36	-16	-9	0.29
Plot245	*Syzygium* Swamp Low Forest	5.79	144.87	93.73	65	29	31	56	64	134	26	-13	-6	0.29
Plot246	*Syzygium* Swamp Low Forest	8.76	219.00	141.69	51	20	15	60	36	128	9	-14	-6	0.60
Plot247	Sal Forest	4.02	100.62	69.61	52	19	16	62	38	128	10	-15	-9	0.59
Plot248	Eucalyptus Plantation	13.20	330.03	230.03	54	20	16	54	38	128	13	-14	-10	0.54
Plot249	Sissoo Plantation	7.23	180.87	113.00	60	24	21	53	48	130	18	-16	-9	0.43
Plot250	Teak Plantation	15.75	393.68	227.55	56	24	20	71	59	129	18	-13	-7	0.56
Plot251	Teak Plantation	25.36	633.95	366.45	57	22	18	71	52	129	16	-14	-5	0.60
Plot252	Sissoo Plantation	32.70	817.43	546.86	64	30	30	65	65	136	24	-13	-10	0.37
Plot253	Sal Forest	4.06	101.50	72.66	52	19	14	55	34	127	10	-15	-7	0.59
Plot254	Teak Plantation	7.27	181.86	105.21	60	26	21	69	61	132	20	-15	-7	0.53
Plot255	Eucalyptus Plantation	11.99	299.86	209.00	54	21	19	47	46	130	16	-14	-9	0.42
Plot256	Teak Plantation	14.43	360.78	208.53	53	22	16	61	40	128	12	-14	-7	0.58
Plot257	Teak Plantation	16.10	402.62	232.72	53	21	17	64	41	129	11	-13	-6	0.58
Plot258	Teak Plantation	13.38	334.62	193.41	53	21	17	54	43	128	13	-12	-8	0.52
Plot259	Sal Forest	6.96	173.95	171.41	53	21	18	65	41	129	11	-13	-5	0.57
Plot261	Sissoo Plantation	3.66	91.38	61.14	60	26	24	57	65	133	25	-15	-10	0.41
Plot262	Sal Forest	2.91	72.64	47.34	53	20	15	56	41	128	11	-15	-9	0.58
Plot263	Sal Forest	5.70	142.59	99.59	52	21	17	67	45	128	13	-13	-7	0.60
Plot264	Sal Mixed Forest	14.73	368.17	226.59	53	20	17	58	40	128	12	-12	-8	0.55
Plot265	Sal Forest	8.62	215.60	152.91	54	21	18	50	39	128	12	-13	-8	0.47
Plot266	Eucalyptus Plantation	11.37	284.13	191.85	54	21	19	52	45	130	14	-15	-9	0.46
Plot268	Sissoo Plantation	36.56	914.09	611.53	54	22	19	65	63	129	19	-15	-11	0.55
Plot269	Sal Forest	9.05	226.25	159.67	54	21	18	63	43	131	14	-14	-9	0.56
Plot270	Sal Forest	7.73	193.35	143.59	52	20	16	46	30	128	9	-11	-7	0.48
Plot271	Sal Mixed Forest	26.97	674.17	522.85	54	20	17	75	42	128	12	-13	-7	0.63
Plot272	Sal Forest	9.16	229.10	164.44	54	20	18	38	34	128	11	-11	-8	0.36
Plot274	*Syzygium* Swamp Low Forest	13.40	335.11	197.66	59	26	23	63	57	130	24	-14	-8	0.47

Plot275	*Syzygium* Swamp Low Forest	3.70	92.62	59.41	55	23	19	58	47	129	14	-13	-6	0.51
Plot276	*Syzygium* Swamp Low Forest	11.43	285.77	172.50	60	26	26	47	60	132	20	-15	-9	0.29
Plot277	Teak Plantation	16.17	404.21	235.84	54	22	18	58	44	129	16	-14	-5	0.53
Plot278	Moist Mixed Deciduous Forest	11.66	291.61	165.18	56	22	18	59	42	129	13	-12	-7	0.53
Plot279	Sal Forest	20.51	512.84	355.64	52	21	16	58	38	126	12	-15	-9	0.57
Plot280	Eucalyptus Plantation	21.05	526.30	366.83	54	21	19	54	38	130	12	-16	-9	0.48
Plot281	Sal Mixed Forest	7.42	185.52	90.87	58	25	20	73	56	129	18	-16	-10	0.57
Plot283	Sissoo Plantation	15.23	380.80	251.06	64	33	30	82	99	139	36	-18	-13	0.46
Plot285	Teak- Eucalyptus Plantation	31.89	797.24	535.96	56	23	20	71	48	129	17	-14	-9	0.56
Plot287	Sal Mixed Forest	12.75	318.65	228.74	53	21	18	63	49	128	14	-14	-7	0.56

Appendix 4. Relationships between aboveground biomass with optical, NDVI and backscattering (Grass).

Plot No.	Grassland Type	Biomass (t/ha)	B	G	R	IR	IR	T IR	IR	σ°_{HH}	σ°_{HV}	NVDI
1	Upland Grassland	0.29	57	22	22	52	56	129	20	-16	-11	0.41
2	Upland Grassland	1.30	61	24	25	37	52	131	23	-14	-8	0.19
3	Upland Grassland	4.06	53	22	23	41	55	130	21	-16	-9	0.28
4	Upland Grassland	3.65	60	30	25	70	57	132	18	-15	-9	0.47
5	Upland Grassland	3.37	57	26	22	63	55	132	18	-19	-11	0.48
6	Upland Grassland	1.56	58	23	20	63	48	130	17	-14	-9	0.52
7	Upland Grassland	3.55	54	22	20	63	53	128	15	-11	-7	0.52
8	Upland Grassland	5.57	52	20	18	57	46	128	13	-15	-10	0.52
9	Upland Grassland	4.29	59	22	21	27	33	134	12	-17	-13	0.13
10	Upland Grassland	2.30	54	20	17	63	42	129	12	-15	-10	0.57
11	Upland Grassland	1.65	58	24	23	47	56	131	20	-15	-8	0.34
12	Lowland Grassland	4.20	57	22	19	55	41	131	13	-13	-9	0.49
13	Lowland Grassland	4.51	58	25	22	45	50	131	17	-13	-9	0.34
14	Lowland Grassland	4.26	59	26	24	59	50	129	19	-12	-9	0.42
15	Lowland Grassland	4.52	59	23	22	38	52	131	20	-15	-11	0.27
16	Lowland Grassland	3.51	53	21	17	54	43	128	13	-12	-8	0.52
17	Lowland Grassland	2.15	56	22	18	57	46	129	14	-14	-7	0.52
18	Lowland Grassland	4.65	51	19	16	51	38	127	12	-13	-8	0.52
19	Lowland Grassland	2.04	55	23	22	50	47	130	17	-17	-11	0.39
20	Lowland Grassland	3.38	60	25	25	50	52	130	21	-15	-6	0.33
21	Lowland Grassland	4.58	68	35	39	52	63	130	27	-16	-7	0.14
22	Lowland Grassland	5.69	55	23	20	59	46	130	14	-12	-7	0.49